Molecular mechanisms of the apoptosis-promoting activity of FABP5 inhibitors in prostate cancer cells

THESIS SUBMITTED IN ACCORDANCE WITH THE REQUIRETMENTS OF

THE UNIVERSITY OF LIVERPOOL

FOR THE DEGREE OF DOCTOR IN PHILOSOPHY

By:

Jiacheng Zhang

February 2019

Department of Molecular and Clinical Cancer Medicine (Pathology)

Abstract

The increased level of FABP5 promotes tumourigenicity and metastasis partially by suppressing apoptosis of prostate cancer cells. Recent studies demonstrated that in castration-resistant prostate cancer cells, androgen-receptor related signaling pathway did not effectively affect the malignant progression, whereas FABP5-PPARγ-VEGF signaling axis had a dominant influence in promoting the malignant progression. Therefore, targeting FABP5 with its inhibitors to promote apoptosis could be a novel strategy for prostate cancer treatment. In this work, we first treated an androgen-responsive cell line 22Rv1 and a highly malignant androgen-independent cell line PC3 with a chemically synthesized FABP5 inhibitor SB-FI-26 and a bio-FABP5-inhibitor dmrFABP5, respectively, to prove their promoting effect on apoptosis of the cancer cells; then we investigated the molecular mechanisms involved in how FABP5 inhibitor promoted apoptosis. Results showed that SB-FI-26 produced significant increases in percentages of apoptotic cells in both 22Rv1 and PC3 by 18.80% (±4.08) and 4.60% (±1.13), respectively. DmrFABP5 produced significant increases in percentages of apoptotic cells by 23.13% (±2.41) and 15.76% (±3.01), respectively, in these two cell lines. Both FABP5 inhibitors significantly reduced the levels of the phosphorylated (presumably, biologically active form) nuclear fatty acid receptor PPARγ, indicating that these inhibitors promoted apoptosis of the cancer cells through suppressing the biological activity of PPARγ. Further studies showed that, as the reduction of the level of p-PPARγ, the levels of AKT and NFκB were coordinately altered. These changes eventually led to the increased levels of cleaved Caspase-9 and cleaved Caspase-3 and thus increased number of apoptotic cells. These results, together with some previous studies, suggested that FABP5

inhibitors promoted apoptosis in prostate cancer cells by suppressing the biological effect of FABP5, and FBAP5 may suppress apoptosis through increasing the biological activity of PPARγ, which, in turn, leads to a reduced apoptosis by interfering with the AKT and NFκB signaling pathway.

Acknowledgments

I would like to take this opportunity to show my great appreciation and thanks to my primary supervisor Professor Youqiang, Ke, an excellent supervisor for me. I would like to thank you for providing me the opportunity to undertake PhD studying in this university. Your patience, endless support, encouragement and priceless advices led me to grow as a researcher.

In addition to my supervisor, I would like to thank Dr. Waseem Al-Jameel, Dr. Majed Saad Al Fayi and Miss Asmaa Al-Bayati for their help and support throughout my PhD study.

I am very grateful to my family and friends for their encouraging and love. Endless thanks to my mother for her love, support, and all her sacrifices, which helped me during my difficult times.

Finally, I would like to express my gratitude to all staff members in the Department of Molecular and Clinical Cancer Medicine, University of Liverpool, for their help with my experimental skills needed in my study.

Declaration

This thesis is a product of my own work which has been carried out during my PhD study in the Department of Molecular and Clinical Cancer Medicine (Pathology), University of Liverpool, between March 2015 and September 2017. All experiments presented in the result chapters were performed by me under the supervision of my supervisor, Professor Youqiang Ke.

Table of Contents

List of Abbreviations

Abbreviation	Full name
ADT	Androgen deprivation therapy
AR	Androgen Receptor
AREs	Activates androgen response elements
AKT	Protein kinase B
BAX	BCL-2-like protein 4
BCL-2	B-cell lymphoma 2
BPH	Benign prostatic hyperplasia
Caspases	cysteine-aspartic proteases, cysteine aspartases or cysteine-dependent aspartate-directed proteases

cDNA	Complementary DNA
C-FABP	Cutaneous fatty acid binding protein
CK	Cytokeratin
CL	Cell lysate
CRPC	Castration-resistant prostate cancer
DBD	DNA-binding domain
DHT	5-alpha-Dihydrotestostron
dmrFABP5	Double mutant recombinant FABP5
DMSO	Dimethyl sulfoxide
dsDNA	double-stranded DNA
DTT	Dithiothreitol
E-coli	Escherichia coli
EGF	Epidermal growth factor

FABPs	Fatty acid binding proteins
FABP5	Fatty acid binding protein 5
FW	Flow-through
GS	Gleason scores
IPTG	Isopropylthiogalactoside
kDa	kilo Dalton
LB	Lysogeny broth
LBD	Ligand-binding domain
LCFAs	Long-chain fatty acids
LH	Luteinizing hormone
LUTS	Lower urinary tract symptoms
mRNA	Messenger RNA
NF-κB	Nuclear Factor-KappaB
p-AKT	Phosphorylated-AKT
PAP	Prostatic acid phosphate

PBS	Phosphate buffered saline
PI-3K	Phosphatidylinositol-3 Kinase
PIN	Prostatic Intraepithelial Neoplasia
PPAR	Peroxisome proliferator-activated receptors
p-PPARγ	Phosphorylated-PPARγ
PPRE	Peroxisome Proliferator Response Elements
PSA	Prostate-Specific Antigen
PTEN	Phosphatase and tensin homolog
SB-FI-26	α-truxillic acid 1-naphthyl mono-ester
SDS-PAGE	Sodium dodecyl sulphate polyacrylamide gel electrophoresis
siRNA	small interfering RNA
TBS-T	Tris Base Salt-Tween
TURP	Transurethral resection of the prostate

TZ	Transitional Zone
VEGF	Vascular endothelial growth factor
wtrFABP5	Wild type recombinant FABP5

Chapter One:

Introduction

1. Introduction

1.1 Epidemiology of cancer

1.1.1 Cancer incidence

Cancer has been and still is a serious worldwide health threat. According to the fifth version of GLOBOCAN, more than 14.1 million new cancer cases were diagnosed in the world in 2012 (7.4 million in men and 6.7 million in women) (1). Amongst all the male and female cancer cases, breast (15%), prostate (13%), lung (13%), and bowel (12%) cancers are most common types (2) **(Fig 1.1)**.

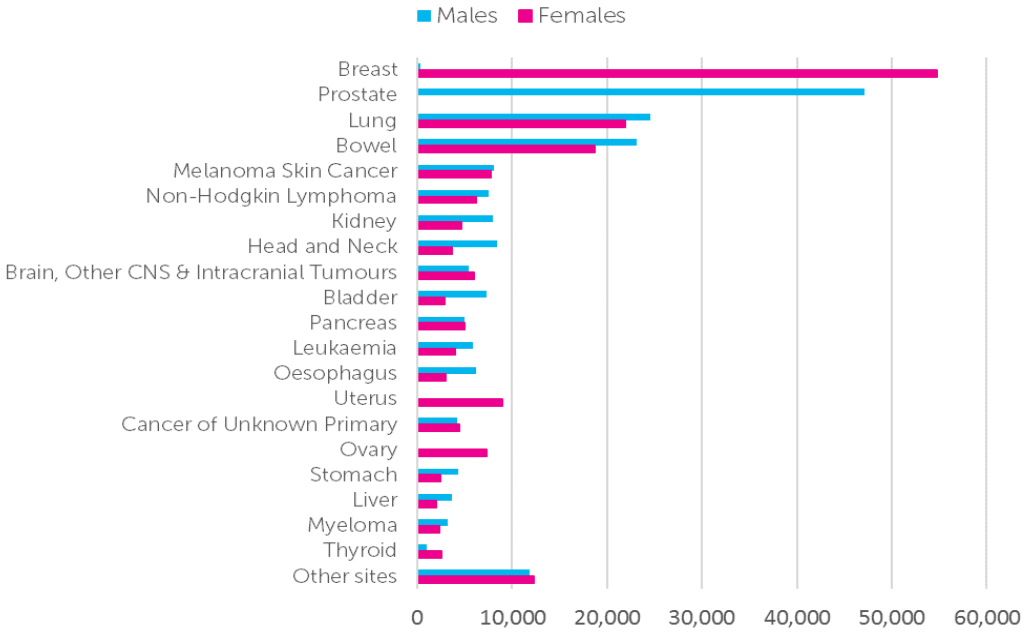

Figure 1.1. Twenty Most Common Cancers in the UK in 2015 (Cancer Research UK, 2015).

When cancer cases are grouped according to ages of the patients, the highest number

of cases is found in the 84 to 90 years old patient group. The number of cases diagnosed in the group aged up to 24 year old accounted for only 1.1% of the total cancer patients. However the number of cases diagnosed in the group aged at or over 65 accounted for more than 65% of the total cancer cases (2) **(Fig 1.2)**. While the black and white males have higher rates of cancer cases than Asian males, cancer incidence is more common in white females than that in Asian and black females (3).

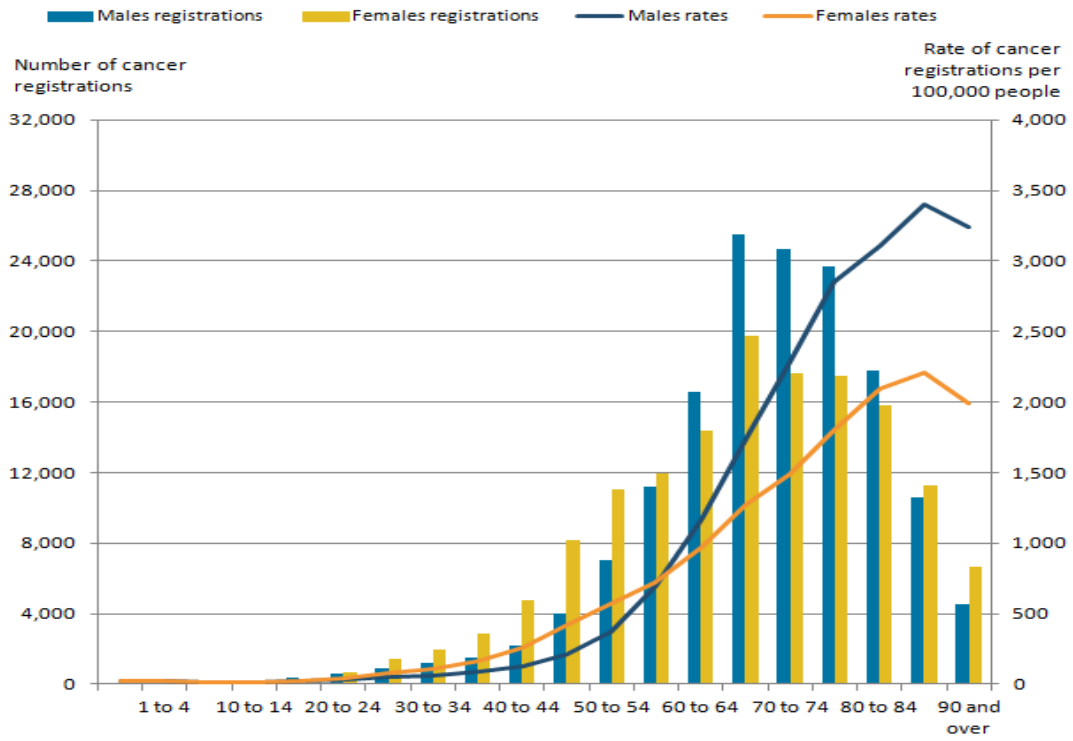

Figure 1.2. The number of cancer registrations and the age-specific rates (per 100,000 people) in the UK in 2015 (2).

1.2 Epidemiology of prostate cancer

1.2.1 Prostate cancer incidence

Prostate cancer is the most common cancer type in men and the second most common cancer in western countries (1) (4). Recently, incidence rates of prostate carcinoma raised were increased for all nations. Prostate cancer incidences are high in North America, Australia, France and Sweden, medium in Denmark, England, Italy, Spain and Israel; and low in Singapore, Japan, India, and China, respectively (5, 6). Around 417,000 additional prostate cancer patients were diagnosed each year in Europe (7); and also in the UK, it is common in male with the highest incidence rate, which is the 17th amongst the European countries (6). About 47,700 additional cases were diagnosed in the UK every year from 2013-2015. In recent ten years, prostate cancer incidence rate has increased by approximate 6% in males in the UK, this number is expected to increase by 12% between 2014 and 2035 (4).

Age is closely related to prostate cancer incidence. Older men have a higher incidence rate. In the UK, more than 35% additional prostate cancer cases were diagnosed in men aged 75 or over during the period of 2013-2015 (4). Age-specific incidence rate raised from around 50-54, reached the peak in 75-79, and slightly dropped from 80-84 before it increased steadily again. The highest rate was in 90 or over (8) **(Fig 1.3).**

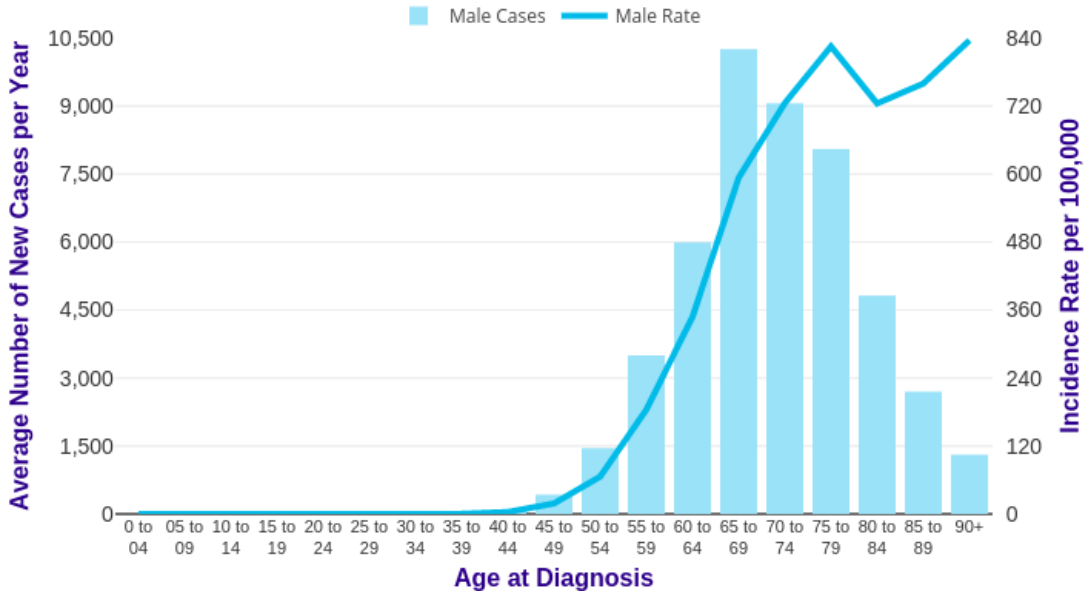

Figure 1.3. Average Number of prostate cancer new cases per year and age-specific incidence rates per 100,000 Population in males, UK, 2013-2015 (8)

1.2.2 Prostate cancer mortality

Prostate cancer is the 5th most common cause of cancer death for men in the world. The number raised more rapidly in developing countries including part of South America, Asia, sub-Sahara Africa and the Caribbean than in developed countries (1, 5, 6). In Europe, prostate cancer is the 6th most common cause of cancer death and the number of death in the UK ranked the 15th amongst the European countries (7).

In the UK, prostate cancer is the 2nd most common cause of cancer death. In 2016, about 11,600 (13%) deaths was caused by prostate cancer in the UK (9). Prostate cancer mortality was linked with the increased age (8, 9). Between 2014 and 2016, around 74% of prostate cancer death occurred in men aged 75 or over in the UK. Age-specific mortality rate started to raise from as low as age 55-59 to the highest rate in men aged 90 or more (9) **(Fig 1.4)**.

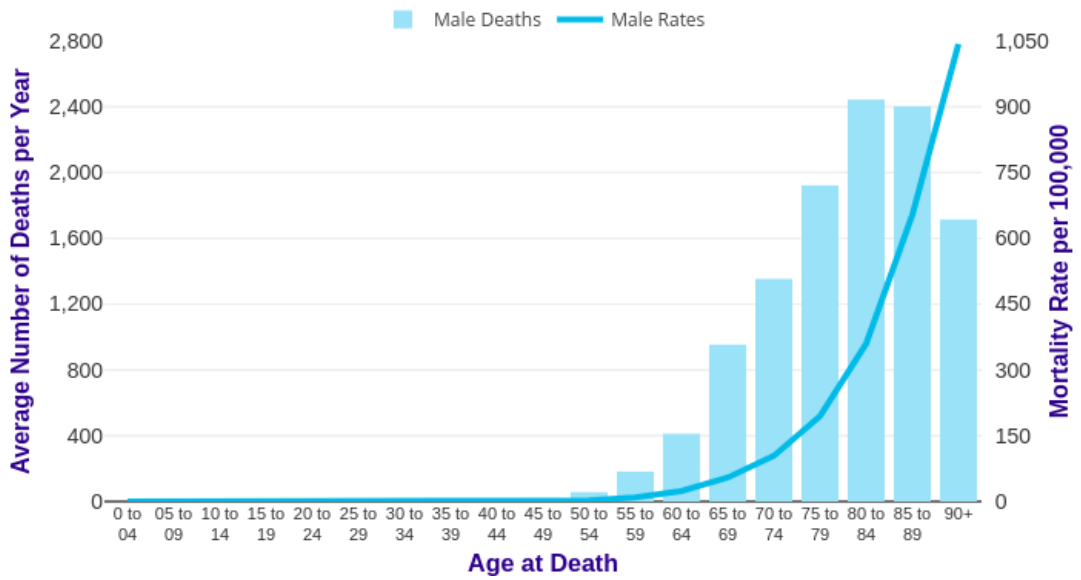

Figure 1.4. The average number of prostate cancer deaths each year and age specific mortality rates in Males in the UK in 2014-2016 (9).

1.2.3 Prostate cancer survival

Prostate cancer surviving rate increased between 1970 and 2012. In 1970s, around 2 in 10 men survived for a decade after their prostate cancer diagnosis. In 2012, more than 8 in 10 men survived. The increased survival rate may be caused by the development of prostate-specific antigen (PSA) test and transurethral resection of the prostate (TURP) which can provide better and earlier stage diagnosis (10, 11). Five-year survival rate of patients showed a relationship with age. Survival rates raised from 91% in men aged 15-49 and reached the peak at 94% in men aged 60-69, then rapidly fell to the bottom of 66% in men aged 80-99 diagnosed with prostate cancer in the UK during 2009 to 2013 (9) **(Fig 1.5)**.

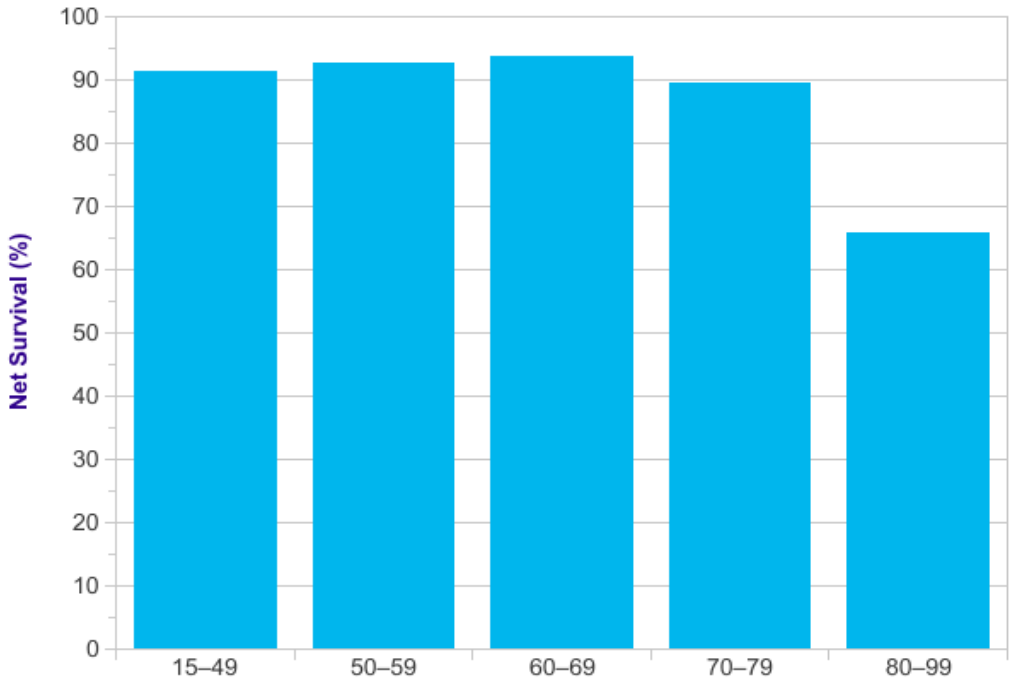

Figure 1.5. Prostate cancer relative ten-year survival rates in England (9).

1.2.4 Risk factors of prostate cancer

1.2.4.1 Age

Prostate cancer is rarely diagnosed in men before 40-year old, the incidence rises rapidly with the increasing age (5). The incidences were 13.7% for the age group of 60-79 year old, 2.2% for the age group of 40-59 year old and lower than 0.005% in the group younger than 39 years old (12). In addition, the rate of prostate cancer discovered during autopsies in deceased people was much higher: around 20% between the age of 50 and 60 and raised to 50% between 70 and 80 in men (13).

1.2.4.2 Race

It was reported that prostate cancer incidence and mortality rate are different amongst different races (14). People who had the highest prostate cancer risk were African American men, which had 275.3 prostate cases per 100,000 men; whereas whites had a rate of only 172.9 in 100,000, a reduction of 37.2% (15). Asian men had the lowest risk of prostate cancer, although it was reported that Asian men had a rapidly increasing trend in recent years (16).

1.2.4.3 Family history

It was recognized that family history was one of the key risk factors in men for prostate cancer (17). Men who have diagnosed prostate cancer family history are expected to have prostate cancer diagnosed 6 years earlier than those without family history (18). Hereditary factors were estimated in 5-10% of diagnosed cases, 40%

amongst those diagnosed patients were below the age of 55. Therefore, there was a strong relationship between family prostate cancer history and personal prostate cancer risk in men (19). Nevertheless, the clinical presentation of this disease with family history did not indicate cancer presenting at an early age, and there was no evidence to show any differences in the degree of malignancies between the hereditary-related cases and other cases (20-22). In addition, it was suggested that if one or more members of a family had a history with breast cancer, other family male members would have a significantly higher risk to develop prostate cancer (23).

1.2.4.4 Diet and lifestyle

It is reported that proper dietary habits and healthy lifestyle may be benefit for suppressing the risk of prostate cancer (24, 25). Men with high level consumption of fat and red meat has been proved to be associated with higher prostate cancer risk, whereas men with high level consumption of fatty fish represent lower risk (25, 26) In western countries, people consume high omega-6 polyunsaturated fatty acids (PUFA), whereas people in Asian countries with their high consumption of food containing a relatively high level of omega-3 PUFA, vegetables, complex carbohydrates, lean meats, and antioxidants have lower incidences of prostate cancer (27). The difference in diet between western countries and Asian countries may provide some clues into the relationship between fat level consumption and prostate cancer (28). Some factors, including circulating insulin-like growth factor 1 (IGF-1) and omega-6 PUFA family member linoleic acid (LA) were proved to be associated with increasing prostate cancer risk (24, 29, 30). Nevertheless, high-level intake of eicosapentaenoic acid (EPA), an omega-3 polyunsaturated fatty acid, is related to a declined risk of

prostate cancer (30).

1.2.4.5 Other factors

The statistical data showed that some factors, such as cigarette smoking, alcohol consumption, socioeconomic status, occupation, vasectomy, prostate gland inflammation and sexually transmitted infection, may have a link to the risk of prostate cancer (31).

1.3 The pathology of prostate cancer

1.3.1 Anatomy of the prostate gland

Prostate, as the largest male genital accessory gland, located at the neck of the urinary bladder, surrounding the proximal part of the urethra as an oval shaped gland (Fig 1.6) (32).

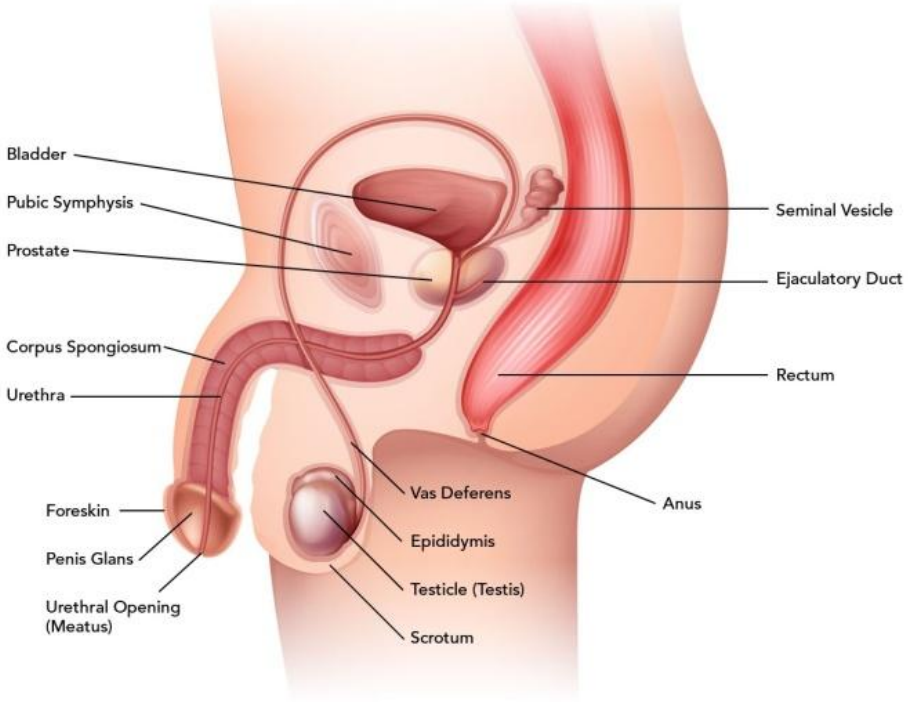

Figure 1.6: Schematic illustration of Male Reproductive system. (33)

The human prostate is divided to three zones: a peripheral zone, a central zone and a transitional zone (32). The peripheral zone is the largest zone of the prostate, it consists of approximately 70% of the total volume of the gland (32). The central zone makes up 25% of the total gland volume (32). The transitional zone makes up 5% of the total prostate tissue mass (Fig 1.7) (32). In these three zones, the peripheral zone is the most common location of inflammation and prostate tumour (64%) (34); the central zone accounts only 2.5% of prostate cancer occurrence (35); the transitional zone surrounding the urethra is the primary site of benign prostatic hyperplasia (BPH) (36).

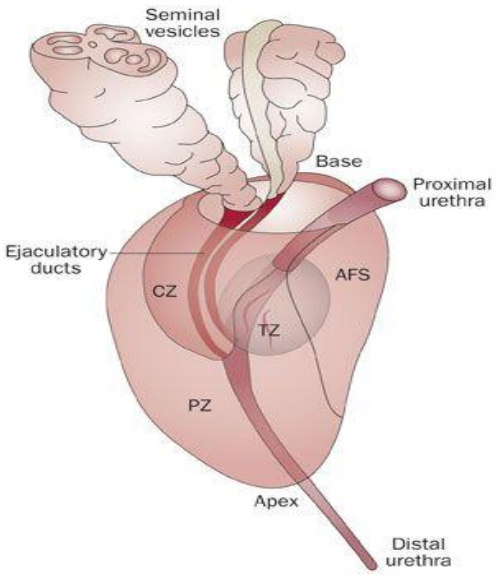

Figure 1.7. Anterior oblique view of the prostate and the urethra (37). The urethra originates proximally from the urinary bladder and follows a course distally through the prostate. The prostate is divided into three zones: central zone (CZ), transition zone (TZ) and peripheral zone (PZ). The ejaculatory ducts and seminal vesicles are situated at prostate base. The anterior fibromuscular stroma (AFS) is located

anteriorly.

1.3.2 Physiology of prostate

Prostate, known as a male sex accessory organ, plays a major role in reproductive process. Prostate gland produces a fluid that, together with sperm cells and fluids produced by the seminal vesicle, bulbourethral gland and other glands, makes up to semen. The fluid produced by prostate contains fructose, glucose, enzymes and PSA, and functions as diet for sperm to go through the female body during the reproduction process. Prostate fluid contains acidic minerals such as zinc and citrate, but other fluid in semen produced by seminal vesicles are alkaline which can neutralize the acidic vaginal secretions to help sperm surviving (38, 39)

1.3.3 Normal prostate cells

Prostate gland consists of epithelial and stromal cells. The prostate epithelial cells can be further divided into three main subtypes: luminal cells, basal cells and neuroendocrine cells (40).

Luminal cells are the most common type amongst prostate epithelial cells. They are part of the exocrine compartment of prostate, secreting protein such as PSA and prostatic acid phosphate (PAP) to the glandular lumina (41). Luminal cells are androgen depended cells, which express a high level of androgen receptor (AR). They also express cytokeratin (CK) 8, CK18 and the cell surface marker CD 57 (42).

Basal cells are the second largest epithelial cells in prostate gland. They are located above the basement membrane and are relatively undifferentiated with a limited

secretory ability. It is believed that basal cells form the main compartment of proliferation in prostate gland. Basal cells are androgen independent cells and they are unlikely to express AR and thus they do not response to androgen ablation treatment (43). These cells express high levels of CK 5 and 14 as well as CD44. In addition, they also express autocrine factors such as BCL-2 and p63 which have a protective function against DNA damage (44).

Neuroendocrine cells are located between the luminal and basal cells in prostate gland. They are not responsible to androgen and can be identified by expressing serotonin, a thyroid stimulating hormone, and chromogranin A. The clear function of neuroendocrine cells are not fully investigated, however, there are evidences suggest that they may support proliferation of luminal cells and development to the advanced stage of prostate carcinoma (45, 46).

1.3.4 Benign prostate hyperplasia and prostate cancer initiation

1.3.4.1 Benign prostate hyperplasia (BPH)

BPH is known as an enlargement in size of the gland, which is non-malignant and is widely observed in aged men. This phenomenon is diagnosed by over growth of the cellular elements of prostate and linked to age in almost all males (50% men with BPH are around age 60 and 90% men with BPH are by age 85). BPH is not caused by cancer or a precursor for cancer (47-49). BPH usually can be observed in prostate transition zone, a ring of tissue around the urethra and its growth is toward the centre side, constantly tightening around the urethra and are associated with lower urinary tract symptoms (LUTS) (50).

It is suggested that androgen plays a key role in BPH progress. Blockade of androgen or AR signaling path way is a major therapeutic method for BPH (50-52). However, the certain molecular mechanisms of how AR signaling affect BPH is still not fully investigated.

1.3.4.2 Prostatic intraepithelial neoplasia (PIN)

Prostatic Intraepithelial Neoplasia (PIN) is known as a sub stage, or a cancer precursor, of cellular transformation from a normal condition to a malignant prostatic epithelium. PIN indicates unusual proliferation of epithelial cells without invasion into surrounding stroma (53). PIN can be identified by a variety of architectural and cytological aspects so that it has minimal differences which could lead to indistinguishable from cancer (54).

PIN can be classified into low grade and high grade. Low grade PIN is a highly differentiated early invasive tumour with a major composition of basal cells (55). High grade PIN represents a poorly differentiated tumour with a secretory luminal cell population (43, 56). Four main forms of high grade PIN have been classified: Tufting (the most common type), cribriform, micropapillary and flat (57). It is shown that high grade PIN is an important marker and the only identified precursor of the prostatic carcinoma (58).

1.3.4.3 Gleason grading system

Dr. David Gleason established a histological grading method (Gleason score, GS) to evaluate the aggressiveness of prostate cancer in 1966 (59). The Gleason grade ranges from 1 – 5. It is a prostate cancer assessment system, which depends on subjective microscopic determination, represents the degree of loss of normal glandular tissue architecture. For example, grade 1 is the least aggressive pattern and Grade 5 is the most aggressive pattern (59) (Figure 1.8).

Because of the histological variation of different lesions within each tumour, two grades (primary and secondary) were recorded in each case. They can range from 2-10 by adding the two grade patterns together to form the so call Gleason scores (GS) or the combined GS (60). GS is a sum of primary grade, larger than 50% of total pattern seen, which shows the majority of tumour; and secondary grade, observed between 5% and 50% of total pattern, which shows the minority of tumour. This system has classified the scores into three groups: well differentiated (GS<6), moderately differentiated (GS 6-7) and poorly differentiated (GS 8-10) (61-63).

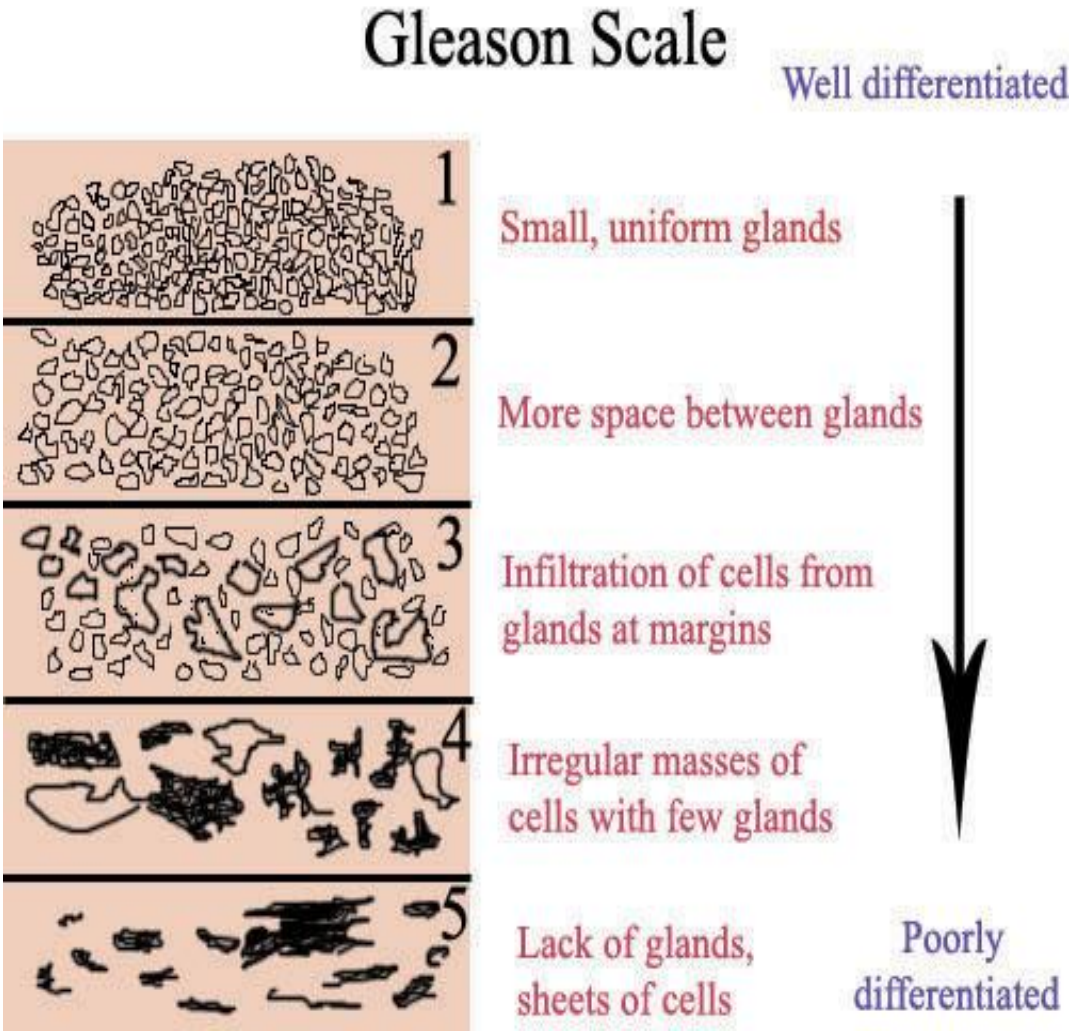

Figure 1.8. Gleason score grading system (61). Grade 1, well-differentiated and slight anaplasia. Grade 2, moderately-differentiated and moderate anaplasia. Grade 3-4 poorly-differentiated and marked anaplasia.

1.3.5 Diagnosis and treatment of prostate cancer

Most prostate cancer diagnosis decisions are firstly on the basis of elevated serum prostatic specific antigen (PSA) or digital rectal examination (DRE). Abnormal DRE is an indication for biopsy, however, the independent variable PSA is a better bio-marker of cancer than either DRE or transrectal ultrasound (TRUS). Definitive diagnosis depends on histopathologic grading (64). However, each procedure has its limitations leading to an over-biopsy for diagnosis, an over-treatment of low-risk patients and non-essential surgery (65).

In localized stage of prostate cancer, radical prostatectomy and external radiation are the common treatments (66).Since the recognition of the growth of prostate cancer cells depends on the presence of androgen, Androgen deprivation therapy (ADT) has been the main treatment for patients diagnosed with locally advanced and metastatic prostate cancer (67). The methods of ADT were classified as surgical castration (orchiectomy), chemical castration and anti-androgen therapy (68). The surgical castration consists of removing the testicles of the patient, The drugs used in chemical castration are LHRH agonists or antagonists, including leuprorelin, goserelin, triptorelin, histrlin, huserelin and degarelix (69, 70). Anti-androgens compete with endogenous androgens from binding with the ligand binding poket of AR. There are two general classes of anti-androgen therapy, steroidal (RU-486, cyproterone acetate, etc.) and non-steroidal (Flutamide, bicalutamide and Bicalutamide) (71).

However, patients with ADT frequently become resistance to castration. In this stage, prostate cancer developed to androgen-independent prostate cancer, or Castration-Resistant Prostate Cancer (CRPC). CRPC is the result of regrowth of prostate cancer

cells that have adapted to non-androgen or low-androgen environment. Recently, many studies reported the molecular mechanisms, such as AR-dependent and AR-independent pathways , influenced the CRPC development, but the clear mechanisms in this progression in still not fully understood (72, 73).

1.4 Prostate cancer cell lines

Prostate cancer researchers developed several cell models to help investigating the molecular pathogenesis, proliferation, apoptosis, tumorigenicity and metastasis. The most common prostate cancer cell lines widely used in laboratories are: PNT2, LNCaP, 22Rv1, DU-145, PC3 and PC3-M.

1.4.1 PNT2

PNT2 cell line is a normal human prostate cell line which was established from a 33 years old male's prostate epithelial cells by immortalization using transfection with a plasmid containing simian virus 40 genome (SV40) with a defective replication origin (74). Successful immortalisation was achieved only with SV40 expressing both large T and small t oncogenes, while attempts to immortalise with a vector expressing SV40 large T alone have given a few strains showing no extended lifespan and no cells which overcame the crisis (74).PNT2 cells also express PSA and PAP but negative with CK 14 (a marker of epithelial basal cells) (75).

1.4.2 LNCaP

LNCaP cells were obtained from a needle aspiration biopsy of a lymph node metastatic lesion of a 50 years old male with prostate adenocarcinoma in 1977 (76).

LNCaP cells are androgen sensitive, they express a high affinity nuclear androgen receptor (mutant T877A) which up-regulate cell growth by responding to androgens. *In vivo* studies showed that tumours occurred at the point of injection and were informed earlier in male than in female mice, indicating a probable androgen-sensitive characteristic. LNCaP cells express CK8 and 18, and express a wild type TP53 (77).

1.4.3 22Rv1

22Rv1 cell is derived from a human prostatic cancer xenograft (spread in mice after castration induced regression and relapse of the parental, androgen-responsible CWR22 xenograft) (78). 22Rv1 cell line is an androgen-sensitive, moderately malignant prostate epithelial cell line. This cell line express high level of PSA and AR, and has unique genotype and phenotype comparing to other prostate cell lines (78, 79).

1.4.4 DU-145

DU-145 was the first well established prostate cancer cell line. It was isolated from a moderately-differentiated brain metastasis of a 69 years old Caucasian male (76). DU-145 cell express extremely low level of PAP and negative with AR and PSA expression (76). They also express intermediate filament proteins and CK 7, 8, 9 and 19, but not CK 5 and 14 (80, 81). *In vivo* studies showed when DU-145 inoculated into SCID mice, metastases were found in liver, lung, spleen, adrenals, kidneys and lymph nodes (80).

1.4.5 PC3 and PC3-M

PC3 cell was isolated from a bone marrow metastasis of a GS 4 prostatic

adenocarcinoma from a 62 years old male (82). PC3 cells are androgen-independent and negative with PSA and AR expression. PC3-M is a metastatic subline of PC3. It was obtained from liver metastasis produced in nude mice by intra splenic injection of PC3 cells and it has similar properties with PC3 but with higher malignancy and more aggressive (83).

1.5 Androgens and prostate cancer

1.5.1 Androgens and prostate

Male androgens, also named as testoids, have a key impact on controlling the development, growth, function of prostate gland and on the maintenance of male characteristics by binding to AR (84). The main androgen in men is testosterone (more than 90%) which is primarily synthesized by the testes. Androgen is essential to the development of the basic function of prostate (85). The secretion of androgen in men is controlled by hypothalamus. As the androgen level (mainly testosterone) in peripheral blood is reduced, a pulse of luteinizing Hormone Releasing Hormone (LHRH) will be issued from hypothalamus and this pulse of LHRH can bind to the specific receptor in the pituitary gland, which triggers the release of luteinizing hormone (LH) (85). The released LH in peripheral blood leads to progress of steroidogenesis in leydig cells (86). Testosterone transformed to a more potent metabolite form: dihydrotestosterone (DHT) under the stimulation of 5-α-reductase enzyme in prostate gland. DHT binds to AR, a ligand controlling transcription factor in the nuclear hormone super family. In nucleus, DHT-AR bind to and activate androgen response elements (AREs) in promoter regions of downstream genes which could regulate cell growth, survival and differentiation of prostate cells (85-92).

In prostate cancer, in the localized stage radical prostatectomy and external radiation treatment are common therapeutic methods (66). For patients diagnosed as advanced or metastatic prostate cancer, suppression of androgen signaling is a key method for treatment, therefore androgen deprivation therapy (ADT) by medical, surgical castration, anti-androgens and combined androgen blockade becomes a common therapy (93). As the primarily effective treatment, ADT is able to induce primary response in 80% - 90% patients. Nevertheless, after 14 – 20 months, the duration of ADT response ends and patients experience progression to androgen-independent prostate cancer, which is no longer in response to androgen deprivation (94).

1.5.2 Androgen-independent prostate cancer

Androgen-independent prostate cancer, was also known as Castration Resistant Prostate Cancer (CRPC) (86). CRPC is a castration-insensitive stage of prostate cancer which has a worse prognosis and a shorter survival time from the beginning of progression (86). The identification of molecular mechanisms involved in the translation of prostate cancer cells from androgen-dependent to androgen-independent is a main issue for the prostate cancer research field and is one of the most important issues or prerequisite for the development of novel CRPC therapeutic strategy (73, 95, 96).

1.6 Progression to castration-resistance prostate cancer

The molecular mechanism on how androgen-dependent prostate cancer progresses to CRPC is an important research subject and it was investigated by many different

laboratories. Currently, ADT is the main therapy for prostate cancer (67). Nevertheless, most of the cases treated with ADT will relapse and progress to CRPC. Some CRPC cells express AR, some CRPC cells do not express AR. Whereas the AR-negative CRPC cells generally do not respond to ADT treatment, AR-positive CRPC cells are largely androgen responsive and express AR. But their further development and expansion does not depend on androgen stimulation anymore and thus ADT treatment is no longer effective to CRPC (73, 97). How exactly the prostate cancer cells become CRPC cells from androgen-dependent cells is not fully understood. There were several theories were brought about to explain the mechanism in this important transition (72). Every theory can only explain part of the question; and currently there is no single hypothesis can completely explain this transition satisfactorily.

1.6.1 AR-dependent signaling pathway in CRPC

AR is a member of the steroid hormone receptor family of ligand-dependent transcription factor. It consists of several functional domains: (1) ligand-binding domain (LBD); (2) DNA-binding domain (DBD); (3) hinge region; (4) large N-terminal domain (NTD) (98). It has been reported that a significant mechanism in CRPC growth is the continuous activation of AR (99). Although the ADT reduces the androgen level in peripheral blood, but it does not affect the DHT level. Thus the stimulation to AR can be continued by DHT (100). It was suggested that several molecular and cellular modifications may be linked to the development of CRPC, including AR amplifications, AR mutations, AR-ligand signaling, aberrant AR co-regulating factors and the AR splice- Biomarkers in prostate cancer (101, 102).

1.6.2 Other pathways

Many studies reported additional pathways related to CRPC progression. These including: inhibition of apoptosis by activation of anti-apoptotic BCL-2 gene which can lead to androgen independence (103, 104); it was reported that PI3K/AKT or mitogen activated protein kinase (MAPK) pathway can be stimulated by the activation of receptor tyrosine kinases and further causes phosphorylation of AR, which lead to produce a ligand independent AR (105, 106). Multiple pathways involve in prostate cancer cells survival in reduced level of androgens. Apart from the main theory that supported the AR sensitivity-amplification opinion, some new hypotheses were proposed in the recent years. One of the most important novel hypotheses was the FABP5-related signaling pathway theory, which suggested that it was this pathway, rather than the AR-related pathway, that played a key role in promoting the malignant progression of the CRPC cells (107).

1.7 Fatty acid binding proteins

1.7.1 Fatty acid binding protein family

Fatty acids are produced by hydrolysis of ester linkage in oil or fat, and have complicated functions on varies aspects of the cell metabolism in human body. Fatty acids functions as an energy source in cells (108). Recent study also demonstrated that fatty acids are signaling molecules and play important roles in intracellular signaling transduction in such cell metabolic processes as cell proliferation, gene regulation, and apoptosis (109-111). The most common major fatty acids in plant and animal are linoleic acids and arachidonic acids. Also, eicosapentaenoic acid (EPA) and docosahexaenoic acid (DHA) are considered to be major fatty acids in fish oil (112). Fatty acids are easy to penetrate cell membrane and get into cytoplasm after they are produced by adipocytes. Free fatty acids can also move to other cells either by passive diffusion or by transporters. After Fatty acids have entered into cytoplasm, they can either join metabolic pathways and serve as sources of nutrition or bind to intracellular fatty acid-binding proteins, which take them to different organelles (111).

Fatty acid binding proteins (FABPs), also known as intracellular lipid chaperones, belong to the super lipid-binding protein (LBP) family (113). Twelve members of FABPs have been identified since 1972, but 2 of them are restricted to fish (114, 115). FABP family members were first known or commonly located in different organs and were named after those organs (Table 1.1). However, the expression of FABPs is not limited to the named organs or cells. For example, FABP1 (liver FABP) expressed mainly in liver, and also in other organs or tissues like pancreas, intestine, lung, stomach, and kidney; FABP5 (epidermal FABP) is highly expressed in skin, tongue,

adipocyte, brain, intestine, macrophage, kidney, liver, lung, mammary gland, heart, skeletal muscle, testis, retina, lens and spleen (109, 115). Wherever fatty acids are expressed, they act as common materials for lipid biosynthesis and storage. Increased amount of FABP synthesis is usually accompanied by the increasing influx of fatty acids into the cells (116).

Table 1.1 Fatty acid-binding protein multigene family (117).

Protein	**Name**	**Alternative names**	**Tissue/cell expression**
FABP1	Liver FABP	L-FABP	Liver, intestine, pancreas, kidney, lung, stomach
FABP2	Intestinal FABP	I-FABP	Intestine, liver
FABP3	Heart/muscle FABP	H-FABP	Heart, skeletal muscle, brain, kidney, lung, stomach, testis, aorta, adrenal gland, mammary gland, placenta, ovary, brown adipose tissue
FABP4	Adipocyte FABP	A-FABP	Adipocyte, macrophage, dendritic cell
FABP5	Epidermal FABP	E-FABP	Skin, tongue, adipocyte, macrophage, mammary gland, brain, intestine, kidney, liver, lung, skeletal muscle, testis, retina, lens, spleen, prostate
FABP6	Ileal FABP	Il-FABP	Ileum, ovary, adrenal gland, stomach
FABP7	Brain FABP	B-FABP	Brain, glia cell, retina, mammary gland
FABP8	Myelin FABP	M-FABP	Peripheral

			nervous system
FABP9	Testis FABP	T-FABP	Testis, salivary gland, mammary gland
Fabp10	Liver FABP	L-FABP	Liver of teleost fish
Fabp11	–	–	Liver, intestine, muscle, brain, heart, eye, swim bladder, gills, kidney, skin, ovary and testis of teleost fish
FABP12	–	–	Retinoblastoma cell from human. Retina, testicular germ, kidney

1.7.2 General functions of FABPs

FABPs had come up with many features. As a lipid chaperone, FABPs can actively bind and transport lipids to specific locations or organelles of the cells. These locations or organelles include lipid droplets for lipid storage and endoplasmic reticulum for signal transduction, transport and membrane synthesis (118). Fatty acids can be transported to different destinations inside the cells: to the mitochondria or peroxisomal for oxidation; to cytosolic or other enzymes for regulating enzymes' activity; to the nucleus for lipid mediated transcriptional regulation (118). Fatty acids can also be transported to the extracellular signaling through an autocrine or paracrine mechanism (119) (Figure 1.9).

Furthermore, FABP can enter the nucleus and transfer fatty acids to transcriptional regulators, for example, allowing the peroxisome proliferator-activated receptors (PPARs) family to perform its biological functions (120-122). There is evidence that FABPs transfers fatty acids from the cytoplasm to their receptor PPAR in the nucleus (118). In addition, it has been reported that FABP expression in cancer tissues is located in the cytoplasm and nucleus (121, 123). These investigations suggested that FABPs involve in specific signaling pathways in the nucleus to control gene expression. The process of fatty acid-transportation and the their route of metabolism inside the cell are illustrated in Figure 1.9.

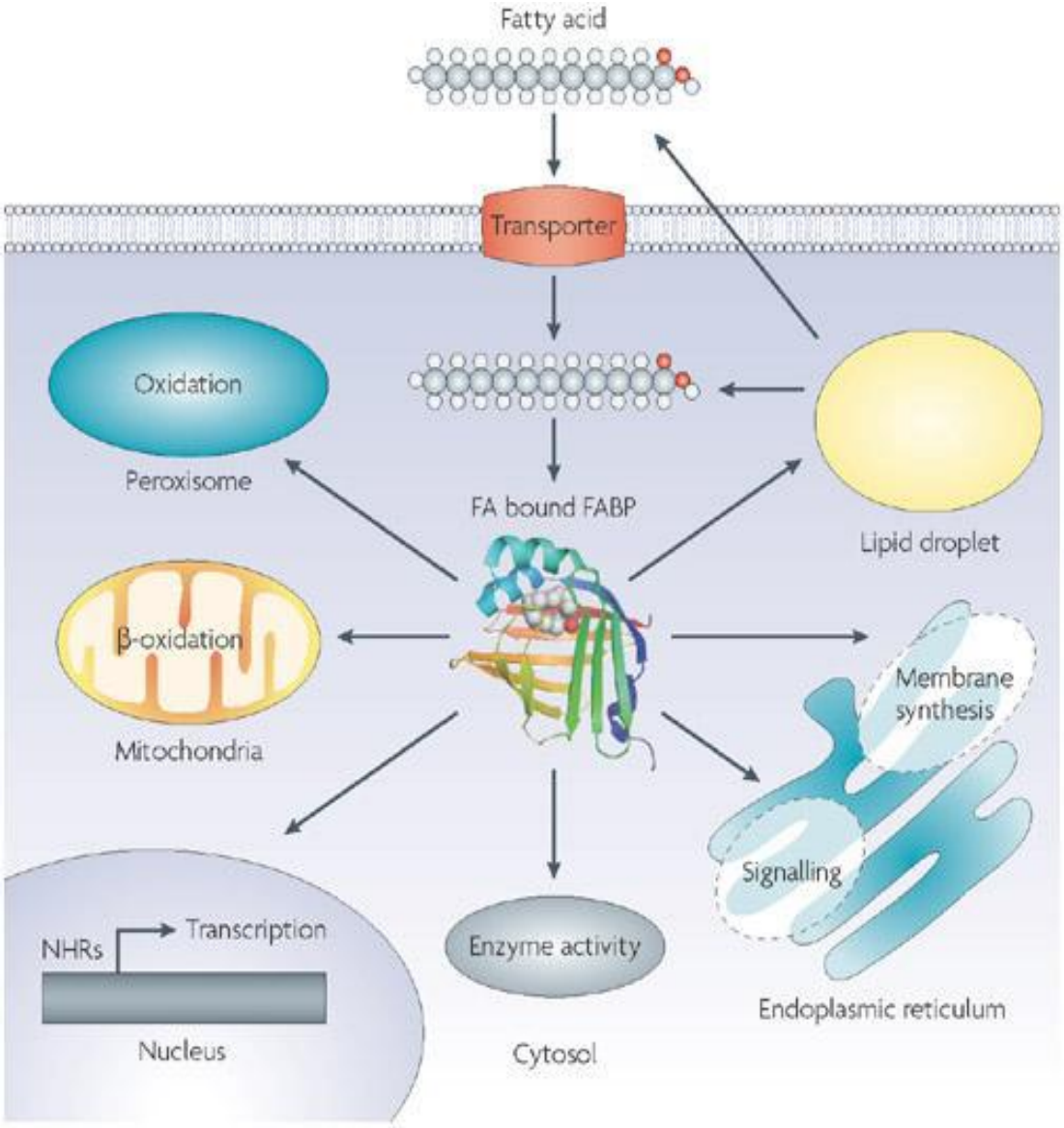

Figure 1.9. Putative functions of FABPs in the cell. FABPs have been put forward to play a role in the transport of lipids tospecific compartments in the cell by passive diffusion or by transporters (e.g. CD36): to lipid droplets for storage; to the endoplasmicreticulum for signalling, trafficking and membrane synthesis; to the mitochondria orperoxisome for oxidation; to cytosolic or other enzymes to regulate their activity; to the nucleus for the control of lipid-mediated transcriptional programs via nuclear hormone receptors (NHRs) (109).

1.7.3 The Structure of FABPs

The FABP structure had been studied by X-ray crystallography, nuclear magnetic resonance and other biochemical methods. FABPs showed a range of 15% to 70% amino acid sequence homology (113). However, highly similar tertiary structures were found amongst FABPs (124). Generally, FABP has a 10-strand antiparallel β-barrel structure. The binding pocket is located in the β-barrel, and one side of binding pocket is consist of an N-terminal helix-loop-helix motif, which is supposed to be the main location to bind to fatty acids (113). It has been shown that all FABPs have a three-element fingerprints (Figure 1.10).

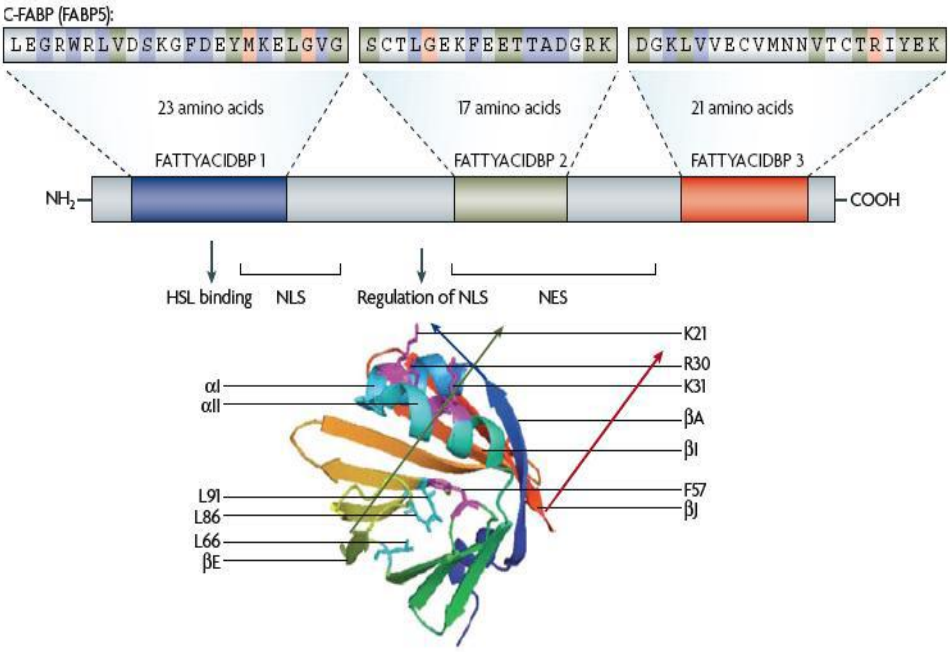

Figure 1.10. Fingerprint for fatty acid binding proteins (109).

All FABPs bind long-chain fatty acids and have ligand selectivity due to small structural differences between isoforms (124). Except for unsaturated fatty acids, the more hydrophobic the ligands are, the higher their binding affinity is (125). The need for target cells may also determine the affinity and selectivity of major isotypes that exist at different sites (113). For example, FABP7 is highly selective for very long-chain fatty acids such as docosahexaenoic acid (125). On the other hand, FABP1 have the binding capacity of a wide range of ligands from lysophospholipids to haem (126).

1.8 FABP5 (or cutanious fatty acid binding protein) in prostate cancer

FABP5 is a member of FABP family and a 15kDa cytosolic protein that binds with high affinity to long and middle chain fatty acids (127). It has been identified that FABP5 widely expresses in the endothelial cells of the placenta, heart, skeletal muscle, small intestine, renal medulla and in the goblet cells of the lung (128). Previous studies indicated that FABP5 level was extremely high in prostate cancer cells (129, 130). Moreover, FABP5, when highly expressed, can induce *in vivo* metastasis by promoting the expression of vascular endothelial growth factor (VEGF) (131-133). FABP5 has been proved to be a potential prognostic marker to predict the prognosis of patients and the target of therapeutic intervention (129, 134). FABP5 inhibition by siRNA can effectively inhibit prostate cancer in nude mice (131). It has been demonstrated that FABP5's tumour-promoting activity on prostate cancer cells depends on its binding and transporting capability with fatty acids, those fatty acids act as signaling molecules to activate its nuclear receptor PPARγ in CRPC cells (107). In addition, it was confirmed that the high expression of cytoplasmic FABP5 was significantly correlated with increasing nuclear PPARγ, and the increased levels of these two proteins were correlated with a lower survival rate of patients (123). Previously, it was demonstrated that fatty acids can activate PPARγ to trigger FABP5-PPARγ-VEGF signaling pathway, which is novel target for therapeutic intervention or angiogenesis inhibition (135) (Figure 1.10). The FABP5-PPARγ-VEGF- signaling transduction axis and how it works inside prostate cancer cells are shown in Figure 1.11.

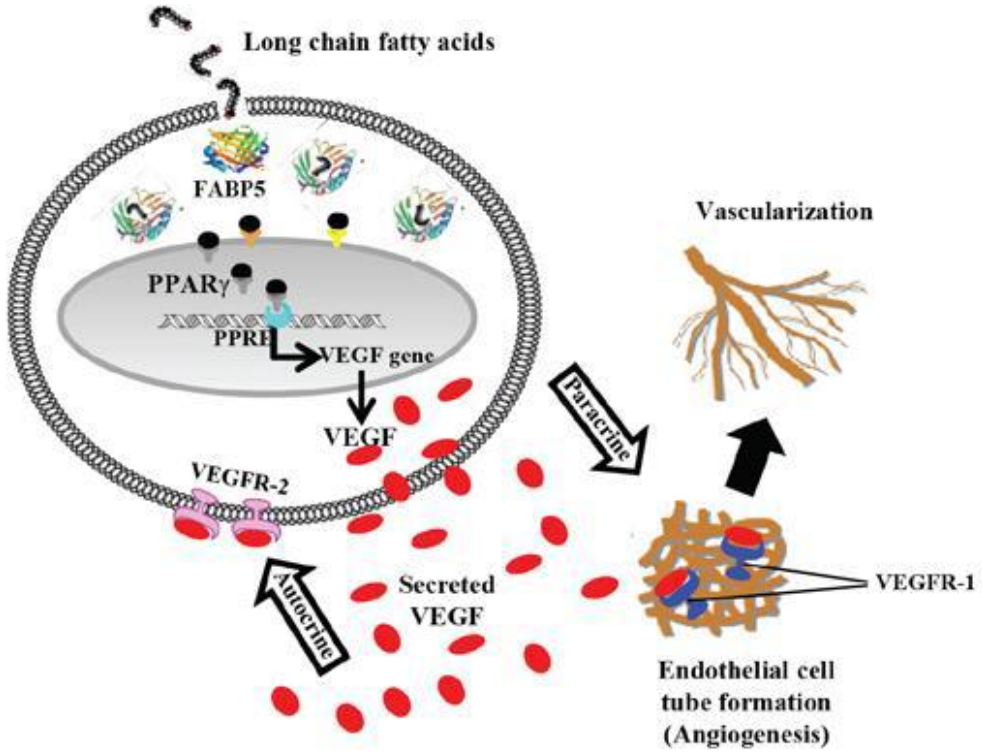

Figure 1.11. Schematic illustrations of FABP5-PPARγ-VEGF pathway (135).

1.9 FABP5 and apoptosis in prostate cancer

The effect of FABP5 on apoptosis of prostate cancer cells has been detected in prostate cancer cells. Previous research showed that the increased level of FABP5 promoted tumorigenicity and metastasis of the prostate cancer cells and it may do so partially by reducing the apoptotic cell number or reducing the response-sensitivity to apoptotic induction signals in prostate cancer cells (107). Some studies also showed that FABP5 had a high influence in suppressing apoptosis in highly malignant DU145 and PC3-M cells; probably by up-regulating some pro-apoptotic factors (136, 137). Furthermore, strong evidence showed that activation of PPARγ pathway inhibited cellular apoptosis in several types of cancers including prostate cancer (138-144). Despite all these previous studies, the true molecular mechanism involved in how FABP5 suppresses apoptosis of the cancer cells and how the FABP5-PPARγ pathway is related to apoptosis in prostate cancer are not known.

1.10 Targeting FABP5 in prostate cancer

To investigate the possibility of targeting FABP5 as a therapeutic strategy for prostate cancer treatment, the gene coding for FABP5 was knocked down by RNA interference in the highly malignant PC3-M cells to generate a subline (Si-clone-2) expressing significantly-reduced level of FABP5 (129). When othotopically implanted into mouse prostate gland and compared with the control, Si-clone-2 produced 63- fold reduction in average tumour size; 7- fold reduction in tumour incidence and 100% reduction in metastasis (129). This result showed that the short FABP5 siRNA generated from inside the cancer cells is very effective on suppressing the malignant progression of the cancer developed in mouse. However, due to the instability and the short life in body temperature, siRNA molecules will be degraded quickly soon after administrated as externally reagents. Thus, siRNA is not a proper treatment drugs for prostate cancer. Even when the siRNA against FABP5 was dissolved in a stabilizing agent (named Atolecollagen, made from cow skin extracts) and was applied directly into the established prostate cancer tumour in nude mouse, these siRNA molecules could only slow and stabilize the tumour growth, but could not reverse the malignant progression or reduce tumour sizes (134). Thus, in order to develop an ideal prostate cancer therapy by suppressing the biological activity of FABP5, discovery of highly effective, specific, and relatively stable novel FABP5 inhibitors is the key issue.

We have recent found an effective FABP5 inhibitor, named SB-FI-26, which was an active component of a Chinese herbal medicine (Incarvillea sinensis) used to reduce pain and to treat rheumatism (145, 146). Our study showed that SB-FI-26 significantly suppressed the proliferation, migration, invasiveness and colony formation of PC3-M cells *in vitro*. This inhibitor also suppressed both the metastases

and the primary tumours developed from cancer cells implanted orthotopically into the prostate glands of nude mice (147).

The normal biological function of FABP5 is to bind to and to transport fatty acids into cells from different extracellular and intracellular sources (148). FABP5 binds to fatty acids with its carboxylate group through a fatty acid-binding motif that consists of 3 key amino acids (Arg^{109}, Arg^{129}, and Tyr^{131}) (148). Previous study revealed that tumor promotion effect of FABP5 in prostate cancer cells depended completely on the structural integrity of fatty acid binding motifs. We tested the possibility of getting an inhibitor of the wild type FABP5 by mutating the fatty acid-binding motif structure. Site-directed mutagenesis was introduced to change 2 of the 3 amino acids (from $Arginine^{109}$ to $Alanine^{109}$ and Arg^{129} to $Alanine^{129}$) of the fatty acid-binding motif (107, 149) to obtain a cDNA coding for a doubly-mutated FABP5; its recombinant product was named dmrFABP5. While wild-type recombinant FABP5 (wtrFABP5) has full ability of binding to fatty acids and significantly promote tumorigenicity of prostate cancer cells by 13 times, dmrFABP5 cannot bind to fatty acids and cannot promote tumorigenicity (107). Our previous results showed that changing 2 of the 3 key amino acids in the fatty acid-binding motif in FABP5 has almost completely deprived of its fatty acid-binding ability (107). DmrFABP5, almost incapable of binding to fatty acids has not only lost its tumour-promoting activity, but also has gained an ability to suppress the biological activity of wtrFABP5, and thus is a novel FABP5 inhibitor. Surprisingly, when used as an therapeutic agent to treat prostate cancer developed in nude mouse, dmrFABP5 produced more than 14-fold reduction in primary tumour mass and 100% inhibition in metastasis (150). The effect achieved by dmrFABP5 the therapeutic test in nude mouse model is much better than that obtained with SB-FI-26.

Thus dmrFABP5 is an excellent potential candidate compound for prostate cancer treatment.

1.11 Apoptosis related pathways

Apoptosis, or programmed cell death, is a fundamental mechanism with a key role throughout development. Apoptosis works through two main, alternative pathways: death receptor-mediated (or extrinsic) pathway and mitochondria-dependent (or intrinsic) pathway (151). The former pathway is initiated by ligation of specific death receptors by their ligands. The latter pathway, which was mainly studied in this work, triggered by mitochondrial outer membranepermeabilization (MOMP), which is partly influenced by BCL-2 family members bound to the mitochondrial membrane, including BAX and BCL-2, which are, respectively, pro- or anti-apoptotic regulatory proteins (151). The anti-apoptotic proteins BCL-2 inhibit the release of cytochrome C, whereas pro-apoptotic proteins (BAX, BAK, and BID) promote its release from mitochondria (152). Cytochrome C, along with Apaf-1 and dATP, form the "apoptosome" – a multiprotein complex that activates caspase-9 to initiate the caspase-3-dependent proteolytic cascade, which is considered a key executioner pathway of apoptotic cell death (153).

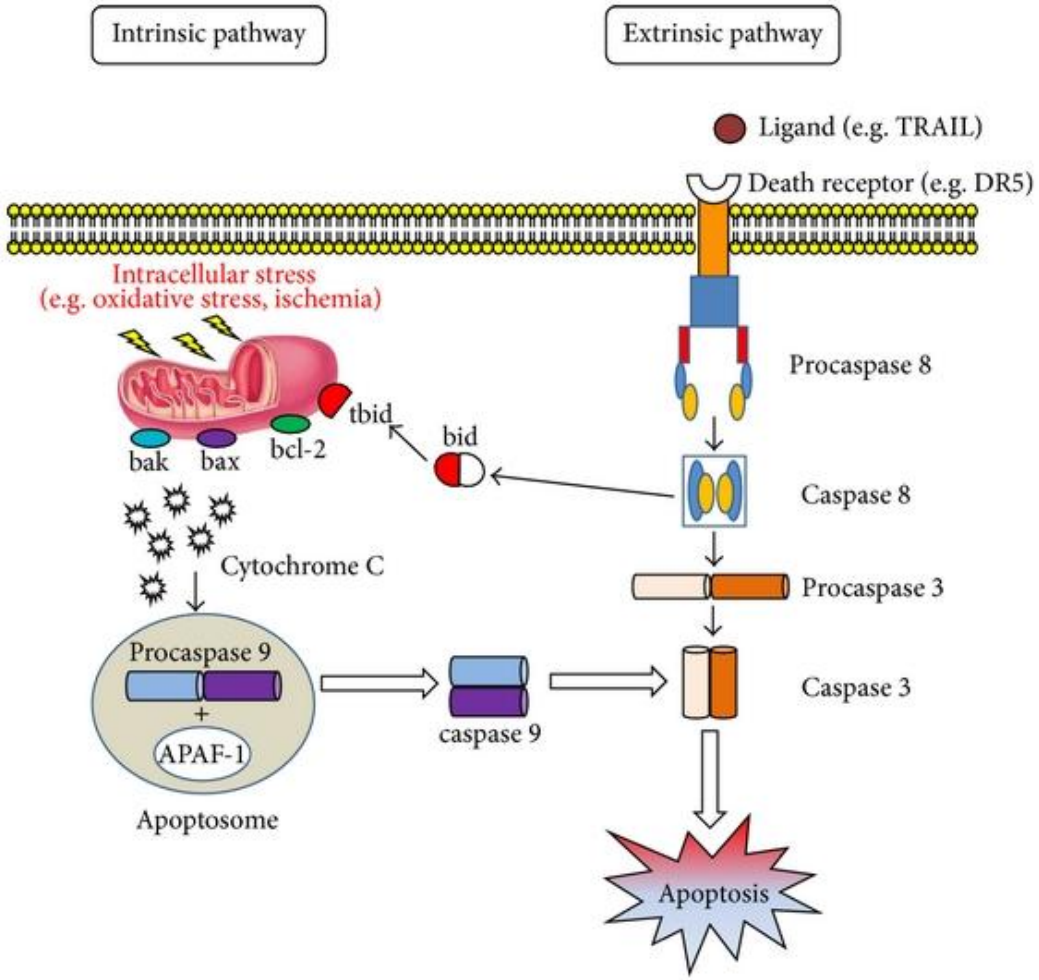

Figure 1.12. Two main pathways related to cell apoptosis: death receptor-mediated (or extrinsic) and mitochondria-dependent (or intrinsic). Extrinsic pathway is initiated by ligation of specific death receptors by their ligands. The main death receptors—Fas and tumour necrosis factor- (TNF-) related apoptosis inducing ligand (TRAIL) receptors DR4 and DR5—induce cell death following ligation with Fas ligand (FasL) or TRAIL, respectively, followed by recruitment of procaspase 8. The intrinsic pathway induces apoptosis by directly activating caspase 3 or by cleaving BID, resulting in mitochondrial dysfunction and subsequent release of cytochrome C and activation of caspases 9 and 3. Caspase 3 promotes the typical apoptosis features,

including DNA fragmentation and cell death. The intrinsic pathway is partly influenced by BCL family members bound to the mitochondrial membrane, including BAX (pro-apoptotic regulatory protein) and BCL-2 (anti-apoptotic regulatory protein) These proteins have opposite effect in affecting cytochrome C release from mitochondria. Cytochrome C and deoxyadenosine triphosphate (dATP) bind to apoptotic protease activating factor (APAF-1) to form a multimeric complex that recruits and activates procaspase 9, an apoptosis-mediating executioner protease that in turn activates caspase 3, resulting in cell apoptosis (154).

1.12 Research Scope

Based on previous investigations, it is reasonable to hypothesize that FABP5 and the fatty acids transported by FABP5 are important pharmacological target. Modulating FABP5 biological activity may provide changes on apoptosis in prostate cancer cells through PPARγ, AKT, NFκB and intrinsic apoptosis pathways.

1.13 Research plan

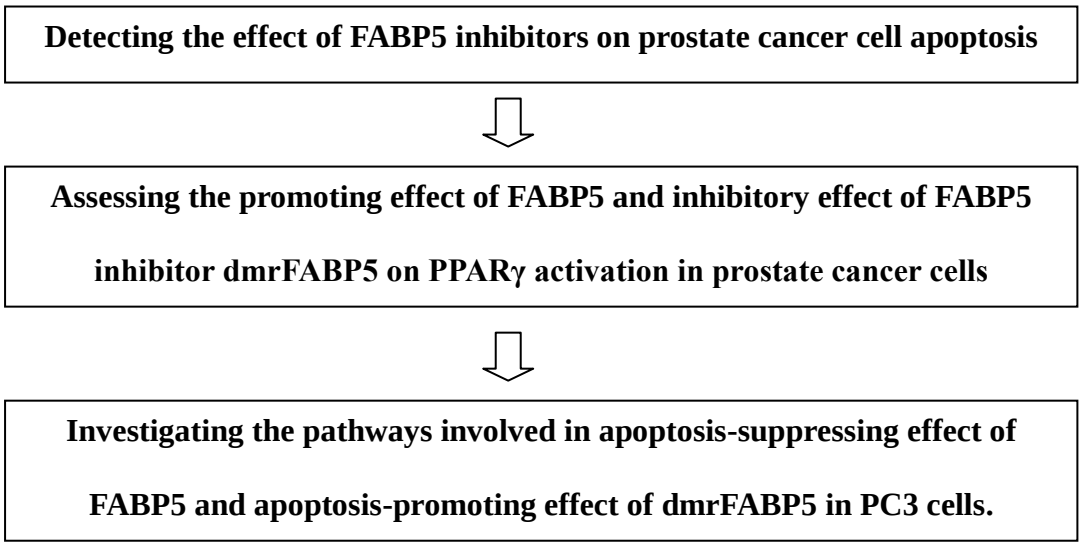

Chapter 2

Materials and Methods

2. Materials and Methods

2.1 Preparation of competent bacterial cells

The *E. coli* (DH5α) glycerol was selected and seeded onto an LB-agar plate and the plate was incubated at 37^{o}C overnight. On the following day, a single colony was inoculated into a conical flask containing 10mls LB broth at 37^{o}C overnight with shaking at 225×g in a shaking incubator. Then, 1ml of overnight culture was transferred into a 250ml flask containing100ml of SOB medium and incubated at 37^{o}C with shaking at 225×g in a shaking incubator until the OD_{550} reached 0.4. The culture solution was then split into 8 × 12ml aliquots and placed on ice for 10-15 minutes to cool down. DH5α bacteria was isolated by centrifuging at 2500×g for 10 minutes at 4^{o}C. The bacterial cell pellets were re-suspended in 8.25ml of pre-cooled RF1 buffer and incubated on ice for 10-15 minutes. After a further centrifuging at 2500×g for 10 minutes at 4^{o}C, the cell pellet was re-suspended in 2ml of RF2 buffer. The DH5α bacteria solution was dispensed into 1ml aliquots in cryovials, flash-frozen in liquid nitrogen and transferred immediately to -80^{o}C freezer for storage (107).

2.2 Miniprep extraction of plasmid DNA

For double mutant FABP5 DNA, Miniprep QIAgen extraction kit was used to extract plasmid DNA of *pQE-32* expression vector (107). Ten mls of overnight growing bacteria (DH5α *E. coli*) in LB medium containing ampicillin was harvested by centrifuging (6,500 × g, 1min). Discarded the supernatant. Cell pellet was re-suspended in 250µl of cell suspension buffer P1 (50mM TrisHCl pH8.0, 10mM EDTA and 100µg/ml RNaseA) by swinging. Then 250µl of cell lysis buffer P2 (200mM NaOH and 1% w/v SDS) was added to the bacterial suspension. The reagents were slowly mixed up by inversion of the Eppendorf for six times. Then 350µl of neutralization buffer N3 (4.2M Gu-HCl, 0.9M potassium acetate pH4.8) was added and mixed up by gentle reversal in eppendorf for six times. The mixture was centrifuged at 15,000×g for 10 minutes and the supernatant was moved to a Miniprep spin column. The column was centrifuged at 17,000×g for 1minute and the supernatant was removed. The column was then washed by adding 750µl of wash buffer PE (10mM Tris-HCl pH7.5 and 80% ethanol) and centrifuged at 17,000×g for 1 minute. Repeat the centrifugation for 1 minute after discarding the flow through. The column was placed in a clean 1.5ml eppendorf, 40µl of distilled water was added. After the incubation for 1 minute at room temperature, the plasmid DNA was eluted by centrifuging at 17,000×g for 1minute. The DNA concentration was evaluated with a NanoDrop spectrophotometer (Labtech International, Ringmer, UK). The plasmid DNA was stored in -20℃ freezer (155).

2.3 Digestion of plasmid DNA using restriction enzymes

Plasmid DNA of double-mutant FABP5 was digested with two different restriction enzymes (*Kpn*I and *Pst*I) from vector *pQE-32* to confirm the presence of insert or to produce the DNA fragment for further application. Empty plasmid *pQE-32*, the cloning vector *pBluescript II SK* harboring wtrFABP5 DNA and the cloning vector *pBluescript II SK* harboring dmrFABP5 DNA was digested with the same two restriction enzymes, respectively. The restriction digestion mixtures were prepared as shown in the following table (107).

Table 2.1: The restriction enzyme digestion mixture (total volume 25 µl)

Reagent	*pQE-32* (Empty)	*pBluescript II SK* (dmrFABP5)	*pBluescript II SK* (wtrFABP5)
Water	0.5µl	5.5µl	17.5µl
*Pst*I	1µl	1µl	1µl
*Kpn*I	1µl	1µl	1µl
Buffer 1	2.5µl	2.5µl	2.5µl
DNA	20µl (2µg)	15µl (1µg)	3µl (3µg)
Total volume	25µl	25µl	25µl

The above restriction digestion mixtures were incubated at 37℃ for 1.5 hours to produce a complete cleavage of template DNA. The enzyme activity was then inactivated by heating to 65℃ for 10 minutes and the resulting DNA fragments were analyzed by electrophoresis in agarose gels to confirm the successful cleavages.

2.4 Analysis of DNA fragments by electrophoresis in agarose gel

Agarose gel electrophoresis was performed in 1×TBE buffer. The agarose concentration was 0.8% to 2.0% (w/v) in the gel, according to DNA size. The agarose was dissolved in 200ml 1×TBE buffer by boiling in microwave for 2 minutes and cooled down for 20 minutes (40-50℃). Five µl safe view blue dye was then added to the gel for visualization of the DNA bands. The gel mixture was placed to 4℃ for solidification. DNA samples were prepared by adding 6× DNA loading buffer and dH_2O to 20µl. Samples were heated at 65℃ for 5minutes and then loaded into each well of the gel. The sample run for 50 minutes in the gel at 90V electricity to separate the DNA fragments. Different sized DNA fragments separated by electrophoresis in the agarose gel were visualized to distinguish the vector and insert fragments on an UV transilluminator (155).

2.5. Purification of DNA from gels

DNA fragments were purified from agarose gel by using a Wizard® SV Gel and PCR Clean-Up kit (Promega, WI, USA). Target fragments were cut off from the gel using a sterile blade. Each cut gel slice was weighed, then three times (W/V) buffer QG was added. The mixture was dissolved by heating at 50-60℃ in a water bath for 10 minutes with occasional vortex. The melted agarose and DNA solution were applied to a QIA quick spin column (Qiagen, UK) and centrifuged for 1 minute at 16,000×g. The column was then washed by 750µl of PE buffer and centrifuged for another 1 minute. The DNA fragments were collected by eluting from the column with 30µl of dH_2O and the concentration of the DAN fragments was evaluated with Nano-Drop and DNA prepared from bacterial cells was kept at -20℃ (155).

2.6 DNA ligation

The wild-type FABP5 cDNA fragment prepared in the way described in section **2.3**. was inserted into the expression vector *pQE-32* by T4 DNA ligase. The components of the ligation reaction mixtures were listed in the following table:

Table 2.2: The ligation reaction mixture (155).

Insert DNA (139ng/µl)	14µl
Vector DNA *pQE-32* (100ng/µl)	1.5µl
Quick Ligation buffer	2µl
T4 DNA Ligase	1µl
Distilled water	1.5µl
Total volume	20µl

2.7 Transformation of competent bacteria with vector DNA

E. coli (DH5α) cells were taken out from -80℃ storage and unfrozen on ice. Ten µl ligation mixtures containing wtrFABP5- and dmrFABP5- expression constructs (contains about 50ng construct DNA) were added to 200ml LB broth with competent *E. coli* (DH5α) cells, respectively. The DNA constructs and *E. coli* cells were first mixed by gentle vortex, incubated on ice for half an hour, briefly heated at a 42℃ water bath for 1.5 minutes, and then immediately put on ice for 2 minutes. To each transformation vial, 800µl SOC reagent was added, and the mixture was then incubated at 37℃ in an orbit-shaking incubator for 1 hour at a shaking speed of 150×g. Then, 200µl of transformed cells was removed and spread on the top of the ampicillin LB agar in a plate and incubated at 37℃ overnight (107).

On the following day, several clones were picked up from each plate and the plasmid DNA was selected from the culture of each colony. The restriction enzymes *Kpn*I and *Pst*I were used again to digest the expression construct and the digestion mixture was applied to electrophoresis in agarose gel. The resulting DNA fragments were visualized on an UV transilluminator. The success of cDNA insertion in the ligation reaction (the FABP5 cDNA was inserted into the pQE-32 vector) was confirmed by the appearance of a short FABP cDNA fragment. The method used for construction of expression vectors was the same as that described previously (107).

2.8 Expression and purification of wtrFABP5 and dmrFABP5

The protocol of expression and purification of recombinant protein was carried out as explained in the QIAexpress Ni-NTA Fast Start Handbook. The protein blotting protocol was carried out as explained in the Bio-Rad Protein Blotting Guide.

2.8.1 Growing *E. coli* cells and inducing protein expression

Single colony harboring construct either pQE-32-wtrFABP5 or construct pQE-32-dmrFABP5 was picked up from the selective antibiotic LB agar plate, and incubated in a 50ml flask containing 10ml LB medium with 100μg/ml ampicillin at 37℃ overnight. The overnight bacterial culture (10ml) was then transferred into a 1-litre flask containing 250ml of pre-warmed LB broth with 100μg/ml ampicillin and inoculated with shaking at 37℃ until OD_{600} reached 0.6 (usually 60-90 minutes). Isopropylthiogalactoside (IPTG, Sigma, USA) was added to induce further protein expression at the concentration of 1mM for 4.5 hours. Cells were collected by centrifugation at 5000×g for 20 minutes and pellet was stored in -20℃.

2.8.2 Protein purification

The recombinant FABP5s produced in *E. coli* cells were purified with a Qiagen Ni-NTA Fast Start Kit. Both wtrFABP5 and dmrFABP5 (fused with a 6×His-tag) were separated from bacterial proteins by affinity chromatography with a 6×His-tag antibody conjugated to Ni-NTA agarose in a column. Cell pellet was lysed by 10ml native lysis buffer for about 1 hour and the clean cell lysate supernatant was collected after centrifugation at 14,000 ×g for 30 minutes at 4℃. Five μl of supernatant was

taken for SDS-PAGE analysis to confirm the presence of relevant His-tag (conjugated with recombinant FABP5) bands. Then the supernatant was applied to a Ni-NTA column and 5µl flow-through fraction was collected for further SDS-PAGE analysis. The column was then washed for 3 times by 4ml native wash buffer. For each fraction, 5µl was collected for SDS-PAGE analysis. The FABP5 proteins (either wtr- or dmr-FABP5) conjugated to 6×His-tagged antibody in the column was eluted by 1ml native elution buffer twice. The recombinant protein (wtrFABP5 or dmrFABP5) was confirmed finally by the presence of the band detected with antiFABP5 antibody on the blot (155).

2.8.3 Cleaning the recombinant protein by dialysis

The D-Tube dialyzer (Novagen) was used to remove the buffer from purified recombinant protein. The D-Tube was treated with deionized water for 5minutes. The water was then removed and protein in the elusion buffer was added to the tube. Tube was placed into PBS in a beaker on a floating rack. The dialysis was conducted with gentle stirring in 4℃ for 3 hours and the protein was then stored in -80℃ after flash freezing in liquid nitrogen (155).

2.8.4 Bradford assay

Bradford assay was used to measure the concentrations of proteins. A standard curve was established by a serial concentrations of BSA (from 50-500µg/µl) in 50µl PBS. Five micro liter of protein samples were diluted with 50µl PBS. Controls and samples were incubated with 1ml of diluted (1/5) dye reagent (Bio-Rad GmbH, Munchen,

Germany), for 15 minutes before measuring the absorbance at 595nm using the MultiSkan plate reader (BioTek Instruments, USA). Standard curve (Figure 2.1) was used to calculate the concentration of proteins (156). Since the linear ranges of target proteins detected in Western blotting could not be tested in this assay, the quantitative analysis was not absolutely accurate. But the results of western blot showed the trend of changes of proteins under different treatments.

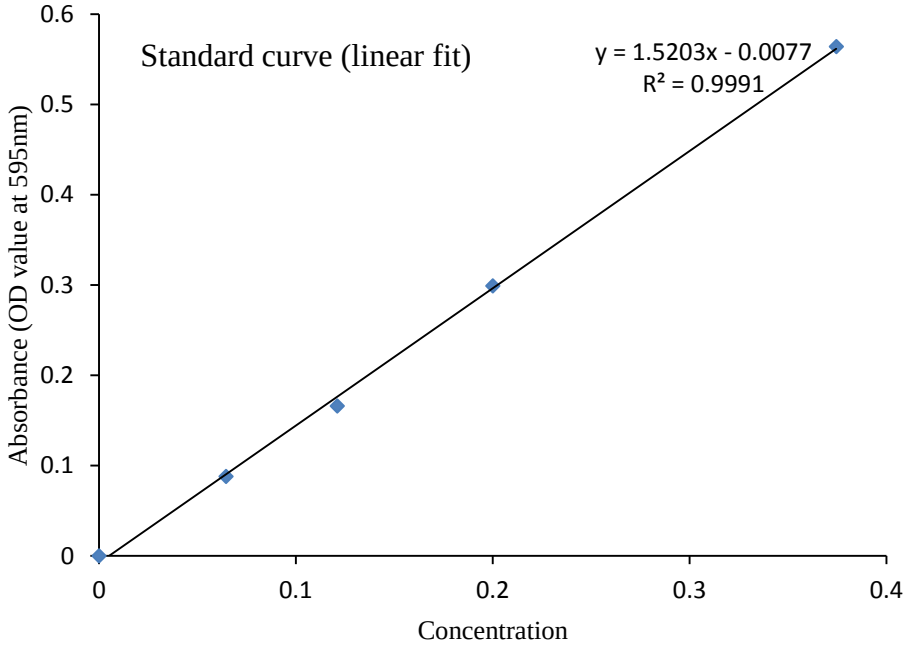

Figure 2.1. Standard curve of Bradford assay. The standard curve showed the variation in the response of proteins in the Bradford assay. The R^2=0.9991 which indicated the curve is linearized. The data allow comparisons to be made between estimates of protein content obtained with these protein standards (156).

2.8.5 Sodium dodecyl sulphate-polyacrylamide protein gel electrophoresis (SDS-PAGE)

Sodium dodecyl sulphate-polyacrylamide protein gel electrophoresis is a very common method for separating proteins according to their molecular weight. This technique is based on the differential rates of migration of protein through a gel under the effect of an applied electrical field. A polyacrylamide gel is applied as a medium and sodium dodecyl sulfate (SDS) to denature the proteins. A plate sandwich of ready gel from Bio-Rad was performed and protein samples were added to 2×SDS-PAGE sample loading buffer, boiled at 95℃ for 10 minutes and treated on ice for 2 minutes, then the samples were loaded. The gel with samples was run for 40-60 minutes at 150V (155).

2.8.6 Transfer of proteins from SDS gel to nitrocellulose membrane

Proteins were Separated based on different molecular weight after SDS-PAGE. The proteins were transferred from SDS gel to a nitrocellulose membrane using the Bio-Rad mini trans-blot system. Two sheets of Bio-Rad thick filter papers and the nitrocellulose membrane were treated in cold in1× transfer buffer for 5 minutes. The cassette, with black side down, was placed on a dish with transfer buffer and the cassette was assembled in following order (from black side on the bottom): a pre-wet fiber pad, 1 sheet of thick filter paper, equilibrated SDS gel, nitrocellulose membrane, 1 sheet of thick filter paper and another pre-wet fiber pad. Air bubbles must be removed. The transfer was performed at 100V, 4℃ for 1 hour in cold in 1x transfer buffer (155).

2.8.7 Immunoblotting for target protein detection

The nitrocellulose membrane with transferred proteins was soaked in 20ml of 5% blocking solution (5g skimmed-milk in 100ml TBST) for an hour at room temperature

with gentle shaking. The membrane was then incubated with antibody in milk-TBS-T mixture in an appropriate concentration (Table 2.1) with gentle shaking at 4℃ overnight, respectively. Washing the membrane with 1× T-TBS for 10 minutes and repeated for 3 times to remove unbound primary antibody. The washed membrane was incubated with a secondary antibody in an appropriate concentration (Table 2.1) for an hour at room temperature, respectively. Washing the membrane again by using 1× T-TBS 10 minutes and repeated for 3 times. The bound antibodies on the membrane were visualized with an ECL reagents kit (mixed with 1ml of Reagent A and of 1ml solution B) for 5 minutes at room temperature. The intensities of visualized protein bands were measured with an imaging analysis machine (ChemiDoc MP Imaging System, Bio-Rad, UK) (155).

2.8.8 Correction of possible loading discrepancies

An anti-β-actin antibody was used to hybridize each blot to normalize the possible loading variations: After the intensities of bands on the blot were measured by imaging analysis, the membrane was washed in 1× T-TBS with gentle shaking overnight. Then the membrane was incubated in 20ml of 5% blocking solution for 30 minutes. Incubated membrane with anti-β-actin antibody at a 1:20,000 dilution for 30 minutes at room temperature. Washing membrane with 1× T-TBS for 5 minutes for 3 times. Secondary antibody was added after washing. The secondary antibody in 1:20,000 dilution was added and incubated with the membrane for 30 minutes with gentle shaking at room temperature. Blots were washed respectively for three times with 1×T-TBS for 5 minutes again and bound β-actin bands were visualized with the

ECL detection and imaging analysis system. The process of recombinant protein production and purification is shown in the following figure:

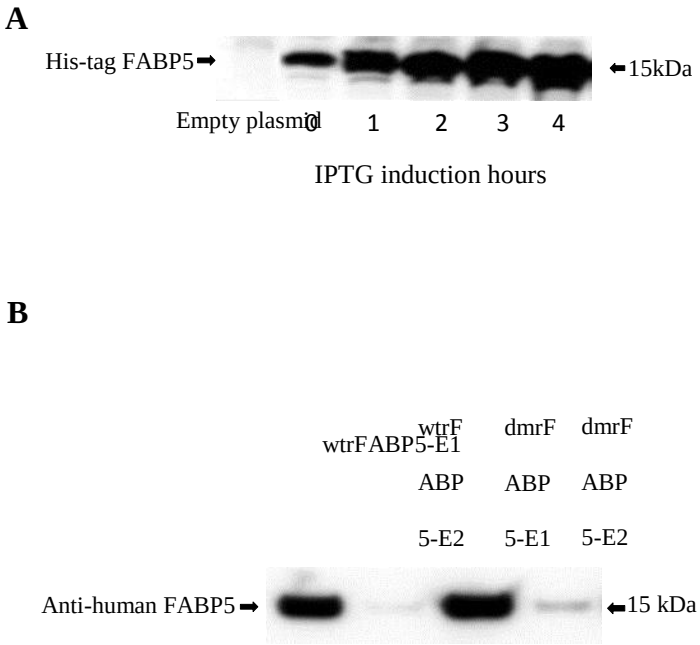

Figure 2.2. Recombinant protein production and purification. A) Western blot confirmation of the optimal experimental time points at which the maximum amount of recombinant protein was synthesized in bacterial cells. After the wild-type and the double-mutated *FABP5* cDNAs were cloned into *pQE32* expression vectors, 2 recombinant FABP5s were produced in the BL21 strain of *E. coli* cells. Bacterial samples were removed once per hour from culture, totally for 5 hours after IPTG was added. Before loading, the total proteins from each lysed bacterial sample was quantified using a Bradford Assay kit (Bio-Rad, Hertfordshire, UK). DH_2O was added to samples to ensure equal amount of protein were loaded. 6×His-tag bound protein

bands were tested by the Penta-His antibody. The wtrFABP5 protein synthesized in bacterial cells at different time points is shown in 7 separate lanes. **B)** Western blot analysis of different recombinant FABP5s purified by affinity chromatography on a Ni-NTA column. FABP5 protein was tested by monoclonal anti-human FABP5 antibody (HycultR Biotech, UK). At the final stage of the purification, 2 eluates were collected, Elution 1 and Elution 2 are the first and the second eluates, respectively. Immunodetection of the first and second elution of the purified recombinant FABP5s showed that the majority of protein is in Elution1.

Table 2.3. Antibodies used in Western blot analysis.

Target Protein	Primary Antibody	Secondary Antibody
FABP5	Monoclonal Rabbit Anti-human FABP5 (1:500) (HycultR Biotech)	Polyclonal Swine Anti-rabbit Immunoglobulins-HRP (1:10,000) (Abcam)
6 ×His-tagged protein	Penta-his antibody Binding (1:1000) (Qiagen)	Polyclonal Swine Anti-rabbit Immunoglobulins-HRP (1:10,000) (Abcam)
β-Actin	Monoclonal Mouse Anti-β-Actin (1:20,000) (Abcam)	Polyclonal Rabbit Anti-mouse Immunoglobulins-HRP (1:20,000) (Abcam)

2.9 Cell culture

2.9.1 Routine cell culture

Cell lines were cultured in flasks and incubated at 37℃ in a humidified incubator with 5% (v/v) CO_2. Three cell lines PNT2, 22Rv1 and PC3 were cultured in RPMI-1640 medium supplemented with 10% (v/v) foetal calf serum (FCS), 2mM L-glutamine, 100IU penicillin- 50μg/ml streptomycin (PEN-STREP). All routine culture media were replaced every other day. Authenticity of each cell line was confirmed by DNA fingerprinting or STR analysis (shown in Appendix) and cell culture was routinely examined for mycoplasma contamination every 3 weeks. The cell authenticity was performed by the department STR Test Centre and the certificates for each cell line was included I the appendix. The mycoplasma contamination test was conducted by a designated department technician (155).

2.9.2 Cells thawing

Vials of cells were taken out from a liquid nitrogen storage tank and defrosted in a 37℃ water bath. Cells were moved to a universal tube containing 10ml complete medium and separated by centrifugation at 800 g for 3 minutes. The supernatant was discarded and the cell pellet was re-suspended in complete medium. Cells were placed in cell culture flask and incubated in an incubator at 37℃ with 5% (v/v) CO_2 (155).

2.9.3 Cells sub-culture

When cells grew to approximately 60-80% confluence, sub-culture was performed to split the culture into more flasks so that the cells can continue to grow. To start the sub-culture of the cells, the old medium was aspirated from the flask and flask was rinsed by PBS for 2 times. Adequate amount of 2.5% (v/v) trypsin/versene mixed solution was added into flask and incubated in an incubator for 3-5 minutes. Complete medium containing double amount of FSC was added to inactivate the effect of trypsin/versene mixture. Centrifugation at 800 g was applied for 3 minutes, re-suspended cell pellet in complete medium in a new flask and incubated in an incubator at 37℃ with 5% (v/v) CO_2 (155).

2.9.4 Cell counting

The number of cells was counted with an improved Neuberger double counting chamber haemocytometer. Cells were detached from the culture flask with the method as previously described. After thoroughly mixed, 10μl of cell suspension was loaded to a counting chamber of haemocytometer with 9 (3×3) squares. Then, cells were counted in four corner squares under the microscope. The total number of cells is calculated using the following equation:

Total number of cells = Average cell count per square $\times$ Dilution $\times 10^4 \times$ Total volume (ml).

2.9.5 Freezing cells

Cells were frozen down when they reached approximately 65-85% confluence. Cells were detached and washed as described in section 2.9.3. Cell pellets were re-suspended with freezing medium (complete medium with 0.75% (v/v) DMSO). For each cryogenic vial, 1ml cell suspension was added and placed into a Nalgene cryo-preserver box containing 250ml isopropyl alcohol. The box was then stored in a -80℃ freezer overnight before moving to a liquid nitrogen tank for long-term storage (155).

2.10. Detection of cellular apoptosis by Annexin V-FITC staining

This staining was with Annexin V-FITC apoptosis detection kit following the protocol (Abcam, UK). Cell apoptosis was induced with 5 μM camptothecin. The cells were first treated by either wtrFABP5, dmrFABP5, SB-FI-26 or PBS for 48 hours, respectively. A number of 3×10^5 cells were collected from each group and re-suspended in 500 μl binding buffer. Five μl of Annexin V-FITC and 5μl of propidium iodide (PI) were added into the buffer and incubated in dark place at room temperature for 5 minutes.

Samples were analyzed by flow cytometry with FACSCanto II Flow Cytometer (BD) using FITC signal detector (FL1) and phycoerythrin emission signal detector (FL2).

2.11. The assay of NFκB transcription factor activity test

The DNA binding activity of NFκB in cell nucleus was detected with an NFκB transcription factor (p65) assay kit following the protocol of the manufacturer (Abcam, UK). Nuclear extracts of control cells (treated with PBS) and cells treated with wtrFABP5 or dmrFABP5 were collected with a nuclear extraction kit (Abcam, UK).

2.11.1 Nuclear extraction

Control cells (treated with PBS) and cells treated with wtrFABP5 or dmrFABP5 were grown to 70-80% confluence in flasks and 5×10^6 cells were sub-cultured by trypsin/versene solution and collected from each group. Cell pellet was collected and re-suspended in 500µl 1×Pre-extraction buffer, then flat on ice for 10 minutes. Samples were mixed and centrifuged at 10,000 g for 1 minute, then carefully removed the cytoplasmic extract from the nuclear pellet.

A volume of 50µl of Extraction buffer with DTT and PIC mixture (1000:1) was added to each nuclear pellet. The extracts were flat on ice for 15 minutes with 5-10 seconds vortex every 3 minutes.

Each suspension was centrifuged for 10 minutes at 12,000 g at 4℃ and supernatant was collected and transferred to another microcentrifuge tube.

The concentration of nuclear extracts were measured with Bradford assay described in section 2.8.4.

2.11.2 NFκB transcription factor assay with ELISA method

The transcription factor antibody binding buffer (10×) was diluted 1:10 by adding UltraPure water. The wash buffer (400×) was diluted 1:400, 5 ml of 400×wash buffer was diluted by adding 2 L UltraPure water and 1 ml of Polysorbate 20. Complete transcription factor binding assay buffer (CTFB) was prepared prior to use in 1.5 ml centrifuge tubes as shown in following table.

Table 2.4. Preparation of Complete Transcription Factor Binding Assay Buffer.

Reagents	Volume/ well
UltraPure water	73 µl
Transcription factor binding assay buffer (4×)	25 µl
Reagent A	1 µl
300mM DTT	1µl
Total volume	100µl

Move the 96-well plate and buffers to room temperature for warming. Unseal the plate and chose number of wells needed.

Non-specific binding wells, positive control wells, specific competitor double-stranded DNA (dsDNA) wells and test wells were set up in duplicates in different wells of a transcription factor NFκB 96-well strip plate as shown in figure 2.2. The

appropriate amout of reagents liste below to the designated wells as follows:

Non-specific binding wells: 100µl CTFB

Specific competitor dsDNA wells: 80µl of CTFB on the bottom and 10µl of Transcription Factor NFκB competitor dsDNA to designated wells. Then add 10µl of control cell lysate.

Sample wells: add 90 µl of CTFB and then add 10 µl (5µg) of sample Nuclear Extract

Positive control wells: add 90 µl of CTFB and then add 10 µl of positive control

The plate was then sealed with cover and incubated at room temperature for 1 hour without agitation. The reagents in the wells were then removed and washed 5 times with 200 µl of 1× wash buffer. Remove any residual wash buffer after 5 times washing.

The plate was incubated with NFκB primary antibody (1: 100) for 1 hour and washed 5 times with 200µl of 1× wash buffer. Remove any residual wash buffer after 5 times washing.

Then conjugated to goat anti-rabbit HRP antibody (1:100) was applied to each well for 1 hour and washed 5 times with 200µl of 1× wash buffer. Remove any residual wash buffer after 5 times washing.

A volume of 100µl transcription factor-developing solution was added to each well for 30 min in the dark at room temperature. Before adding Transcription Factor Stop Solution, monitor the wells to turn medium to dark blue. The stop solution was added and absorbance at 450nm was measured within five minutes.

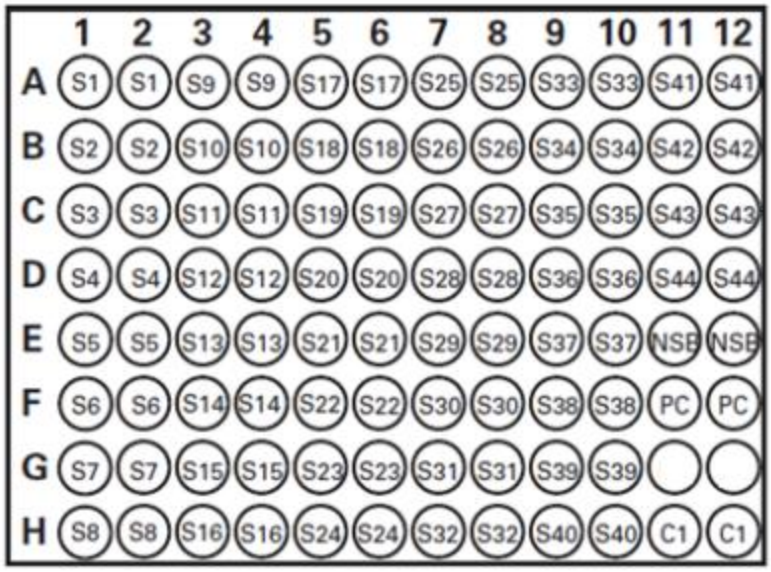

Figure 2.2. 96-well strip plate format

2.12. Western blot analysis for apoptosis-related factors.

Expression of proteins in control cells and cells treated with wtrFABP5 or dmrFABP5 were detected by Western blot technique and ECL detection system (Millipore, UK).

Proteins were loaded and run with SDS-PAGE in a 12.5% (w/v) acrylamide gel, and transferred onto a nitrocellulose membrane (Hybond ECL, Amersham Pharmacia, Amersham, UK). Primary antibody against p-PPARγ (Ser 112) (Thermo Fisher, UK) was diluted at 1:200 and incubated with the blot overnight. After incubating with horseradish peroxidase-conjugated anti-rabbit IgG (Santa-cruz, USA) diluted at 1: 10,000 protein bands were detected and measured by exposing the membrane in a imaging analysis machine (ChemiDoc MP Imaging System, Bio-Rad, UK). The primary antibodies against PPARγ, AKT, p-AKT (Ser 473), BAX, BCL-2, the cleaved-Capase-9 (Santa-Cruz, USA) and the cleaved-Caspase-3 (Cell Signaling, UK) were diluted at 1:200-500 and incubated with the blots for 1 hour. After incubating with horseradish peroxidase-conjugated anti-rabbit (AKT, p-AKT and cleaved-Caspase-3) - or anti-mouse (PPARγ, BAX, BCL-2, cleaved-Caspase-9) - IgG (Santa-Cruz, USA) diluted at 1:10,000, respectively, protein bands were detected and measured in the same way as p-PPARγ. The antibody against β-actin was used to quantify the actin bands on each blot to correct for possible loading discrepancies.

Table 2.5. Antibodies used in Western blot analysis.

Target Protein	Primary Antibody	Secondary Antibody
PPARγ	Monoclonal Mouse anti-PPARγ Antibody (1:500) (Santa cruz)	Polyclonal Rabbit Anti-mouse Immunoglobulins-HRP (1:20,000) (Abcam)
p-PPARγ	Phospho-PPARγ (Ser112) Polyclonal Rabbit antibody (1:250) (Thermo Fisher)	Polyclonal Swine Anti-rabbit Immunoglobulins-HRP (1:10,000) (Abcam)
AKT	Monoclonal Mouse anti-AKT Antibody (1:500) (Santa cruz)	Polyclonal Rabbit Anti-mouse Immunoglobulins-HRP (1:20,000) (Abcam)
p-AKT	Monoclonal Mouse anti-p-AKT (Ser 473) Antibody (1:500) (Santa cruz)	Polyclonal Rabbit Anti-mouse Immunoglobulins-HRP (1:20,000) (Abcam)
BAX	Monoclonal Mouse anti-BAX Antibody (1:500) (Santa cruz)	Polyclonal Rabbit Anti-mouse Immunoglobulins-HRP (1:20,000) (Abcam)
BCL-2	Monoclonal Mouse anti-BCL-2 Antibody (1:500) (Santa cruz)	Polyclonal Rabbit Anti-mouse Immunoglobulins-HRP (1:20,000) (Abcam)
Cleaved Caspase-9	Monoclonal Mouse anti-Caspase-9 Antibody (1:500) (Santa cruz)	Polyclonal Rabbit Anti-mouse Immunoglobulins-HRP (1:20,000) (Abcam)
Cleaved Caspase-3	Monoclonal Rabbit anti-Cleaved Caspase-3 Antibody (1:200) (Cell signaling)	Polyclonal Swine Anti-rabbit Immunoglobulins-HRP (1:10,000) (Abcam)
β-Actin	Monoclonal Mouse Anti-β-Actin (1:20,000) (Abcam)	Polyclonal Rabbit Anti-mouse Immunoglobulins-HRP (1:20,000) (Abcam)

2.13. Statistical analysis

Student's *t*-test was carried out using GraphPad Prism software to compare the differences of the means between control and experimental groups and the data is presented as mean ± SE. the *P*-value less than 0.05 was regarded as statistical significance.

Chapter 3

Result 1

The effect of FABP5 inhibitors on prostate cancer cell apoptosis

3. Result 1: The effect of FABP5 inhibitors on prostate cancer cell apoptosis

3.1 Introduction

Previous work in our research group confirmed that FABP5 had a tumour-promoting effect on prostate cancer cells and this effect depended on its ability to bind to and to transport fatty acids from intracellular and extracellular sources into cells to activate their nuclear receptor PPARγ (107, 129). FABP5 binds to medium- and long- chain fatty acids with a high affinity (128) through a binding motif that consists of 3 key amino acids (Arg^{109}, Arg^{129}, and Tyr^{131}) (107, 149). In previous studies, we altered 2 of 3 key amino acids (from Arg^{109} to Ala^{109} and Arg^{129} to Ala^{129}) and produced the mutant dmrFABP5 (107), which is almost incapable of binding to fatty acids, and which can suppress the biological activity of wtrFABP5 (150).

Although both FABP5 inhibitors SB-FI-26 and dmrFABP5 can suppress the tumourigenicity of prostate cancer cells (147), the molecular mechanisms involved in their tumour-suppressing activities are not known and whether these inhibitors can affect the apoptosis of the prostate cancer cells is not fully investigated.

The target of this chapter is to detect the effect of FABP5 and FABP5 inhibitors on apoptosis in prostate cancer cells. To investigate the possible relationship between FABP5 inhibitors and apoptosis in prostate cancer cells, sufficient quantities of wtrFABP5 and dmrFABP5 had been produced and purified using the experimental

procedures described in chapter 2. The chemically synthesized FABP5 inhibitor SB-FI-26 was purchased from commercial source (Cayman Chemical Company, USA). Using these experimental materials, we first investigated whether FABP5 inhibitors were involved in promoting apoptosis in both the androgen-responsive 22Rv1 cells and the AR-negative PC3 cells; then assessed whether FABP5 inhibitors suppressed tumourigenicity of the cancer cells by promoting apoptosis.

3.2 WtrFABP5 suppressed apoptosis of the prostate cancer cells

WtrFABP5 was used to treat 22Rv1 and PC3 cells to test the change on apoptosis. The androgen-responsive prostate cancer cell line 22RV1 and the androgen-independent cell line PC3 were cultured to 90% confluence and harvested; equal number (1×10^5) of cells were then sub-cultured in triplicates. Each different dose (From 0.1 μM to 1 μM) of wtrFABP5 was added to each of the triplicate cultures and the cells were allowed to grow for a further 48h. Cells were harvested by centrifuge and Annexin V-FITC staining and flow cytometry were then performed to each group. The dot graph and histogram graph records were collected from flow cytometry and the records of control groups and optimal dose of wtrFABP5 (0.5 μM) groups were shown in Figure 3.1.

For each dot graph, dots in the first quadrant (up right) represent the late stage apoptotic cells. Dots in the second quadrant (up-left) represent dead cells and cell debris. Dots in the third quadrant (low-left) represent normal living cells, which do not undergo apoptosis. Dots in the fourth quadrant (low right) represent cells undergoing apoptosis. For the histograms, the peak on the left represents living cells

without undergoing apoptosis, the right peak represents apoptotic cells.

The results of flow cytometry quantitative analysis shown in Figure 3.1 and Figure 3.2 revealed that the apoptosis rate of 22Rv1 cells was significantly higher than that of PC3 cells by 6.48% ($p<0.01$, Student's t-test) with the treatment of PBS (Figure 3.2). For the groups treated with wtrFABP5, all doses used produced reductions in apoptosis and the highest reduction was achieved in both cell lines with 0.5 μM wtrFABP5. Higher doses produced no more reductions in apoptosis. In 22Rv1 cells, when treated with this optimal dosage of wrtFABP5, 10.30% of cells underwent apoptosis. It is a significant reduction (17.18%) compared with that of control group ($p<0.05$, Student's t-test). Thus, wtrFABP5 treatment reduced apoptotic fraction of the cells by 40.08% in 22Rv1 culture. In PC3 cells, the optimal dose of wtrFABP5 reduced the fraction of cells undergoing apoptosis by 3.03% ($p<0.05$, Student's t-test) when compared with that of control (10.70%). Therefore, in wtrFABP5-treated PC3, the apoptotic cells were reduced by 28.3%, compared to that in the control PC3 cells.

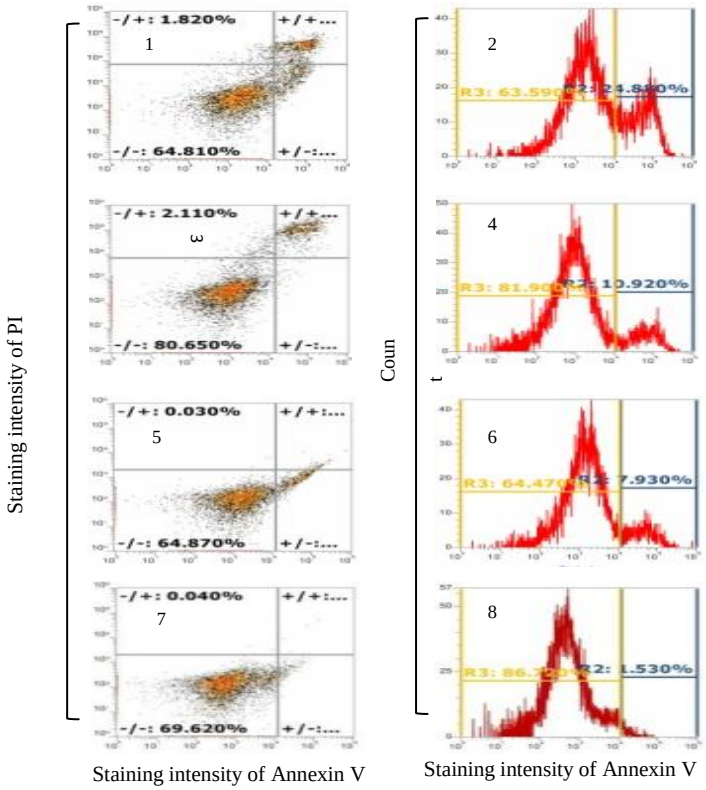

Figure 3.1. Records of dot graph and histogram graph of wtrFABP5 treated 22Rv1 and PC3 cells. 1, dot graph record of control 22RV1 cells (treated with PBS). 2, histogram record of control 22RV1 cells. 3, dot graph record of control PC3 cells (treated with PBS). 4, histogram record of control PC3 cells. 5, dot graph record of 22RV1 cells treated with 0.5 μM wtrFABP5. 6, histogram record of 22RV1 cells treated with 0.5 μM wtrFABP5. 7, dot graph record of control PC3 cells treated with 0.5 μM wtrFABP5. 8, histogram record of PC3 cells treated with 0.5 μM wtrFABP5.

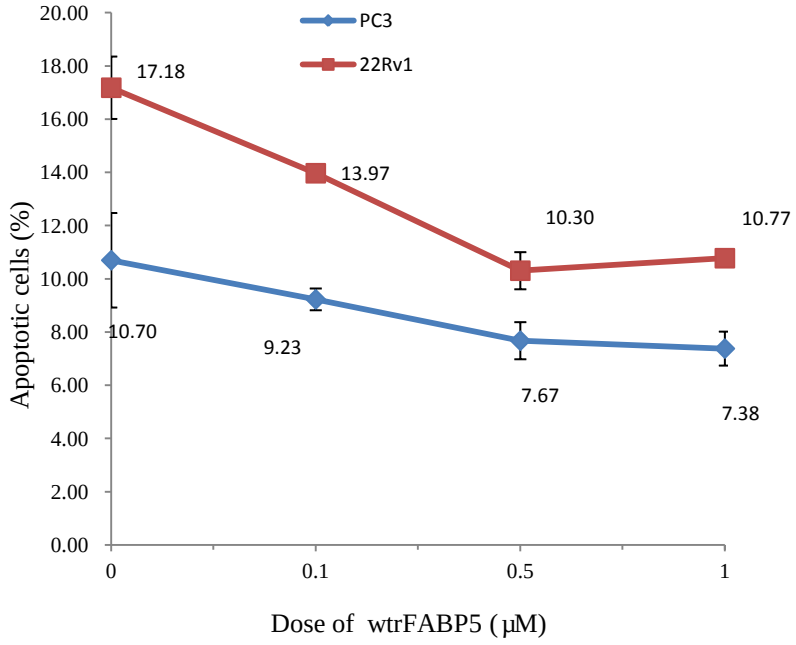

Figure 3.2. Line chart of percentages of the apoptotic cells in 22RV1 and PC3 cell lines treated with 4 different doses of wtrFABP5, respectively. Results were obtained from three separate measurements (mean ± SE) and the differences between the control and treatment were assessed by 2-tailed unpaired Student's t test.

3.3 Chemical inhibitor SB-FI-26 promote apoptosis of the prostate cancer cells

Chemical inhibitor of FABP5, SB-FI-26, was used to treat 22Rv1 and PC3 cell lines and the effect on apoptosis was tested. 22RV1 and PC3 cell lines were cultured to 90% confluent and harvested; equal number (1×10^5) of cells were then sub-cultured in triplicates. Each different dose (From 50μM to 150μM) of SB-FI-26 was added to each triplicate culture and the cells were continued to grow for 48h. Cells were harvested by centrifuge and Annexin V-FITC staining and flow cytometry were then performed to each group. The dot graph and histogram graph records were collected from flow cytometry and the records of control groups and highest dose of SB-FI-26 (150μM) groups were shown in Figure 3.3.

Quantitative analysis of flow cytometry showed that all used doses of SB-FI-26 promoted apoptosis and the increase was positively correlated to the increase in dose. With the treatment of 150μM of SB-FI-26, 46.6% of 22Rv1 cells underwent apoptosis, a significant increase of 29.40% over that (17.2%) in the control ($p<0.001$, Student's t-test). Thus, SB-FI-26 produced 1.71 fold more apoptotic cells in 22Rv1 cultures (Figure 3.4). In PC3 cells, 150μM of SB-FI-26 significantly increased by 7.78% of the proportion of cells undergoing apoptosis ($p<0.05$, Student's t-test) when compared with that of the control (10.70%). Thus, there was 0.72 fold more cells undergoing apoptosis in SB-FI-26-treated PC3 cells in comparison with the control (Figure 3.4).

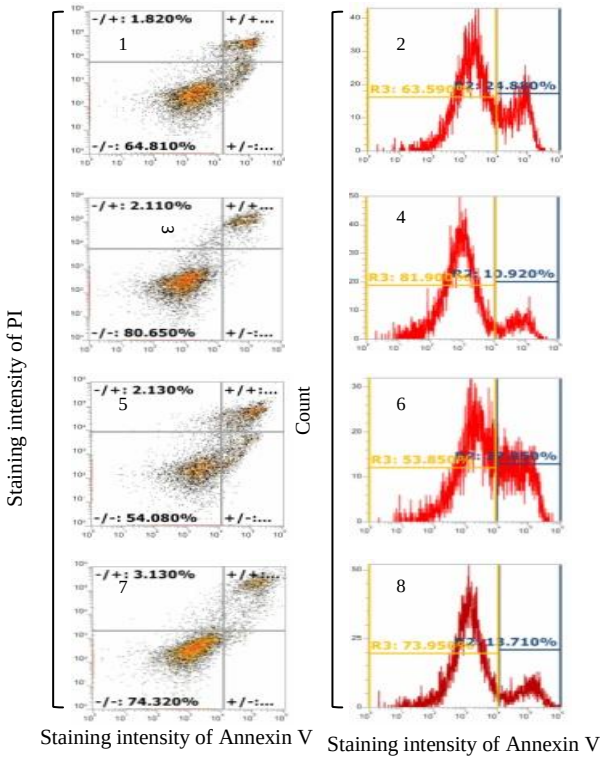

Figure 3.3. Records of dot graph and histogram graph of SB-FI-26 treated 22Rv1 and PC3 cells. 1, dot graph record of control 22RV1 cells (treated with PBS). 2, histogram record of control 22RV1 cells. 3, dot graph record of control PC3 cells (treated with PBS). 4, histogram record of control PC3 cells. 5, dot graph record of 22RV1 cells treated with 150 μM SB-FI-26. 6, histogram record of 22RV1 cells treated with 150 μM SB-FI-26. 7, dot graph record of control PC3 cells treated with 150 μM SB-FI-26. 8, histogram record of PC3 cells treated with 150 μM SB-FI-26.

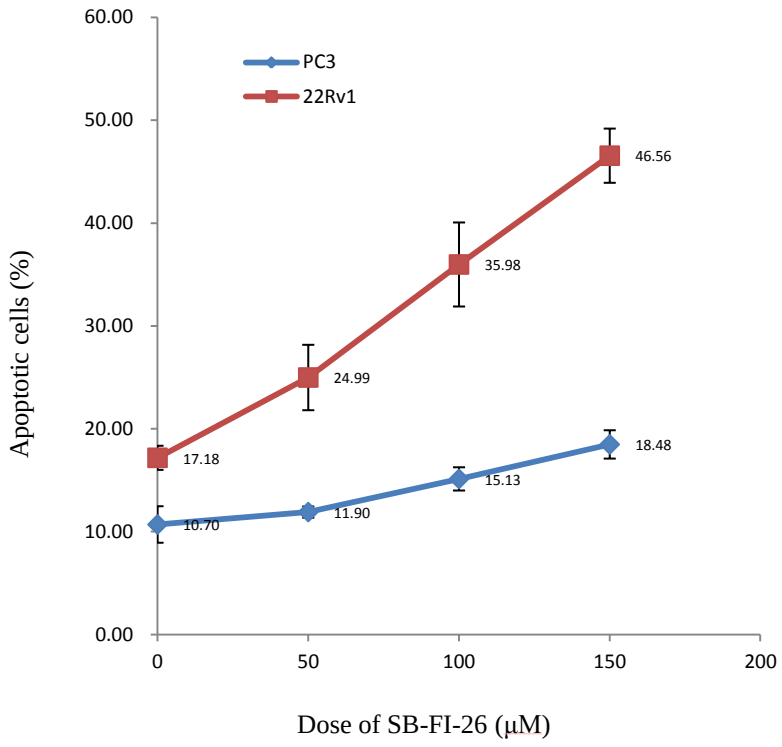

Figure 3.4. Line chart of percentages of the apoptotic cells in 22RV1 and PC3 cell lines treated with 4 different doses of SB-FI-26, respectively. Results were obtained from three separate measurements (mean ± SE) and the differences between the control and treatment were assessed by 2-tailed unpaired Student's t test.

3.4 DmrFABP5 promote apoptosis of the prostate cancer cells

The effect of the dmrFABP5 on apoptosis of 22Rv1 and PC3 cells was studied and the results were shown below. 22RV1 and PC3 cell lines were cultured to 90% confluent and harvested; equal number (1×10^5) of cells were then sub-cultured in triplicates. Each different dose (From 0.1 μM to 1 μM) of dmrFABP5 was added to each triplicate culture and the cells were continued to grow for 48h. Cells were harvested, Annexin V-FITC staining and flow cytometry were then performed to each group. As shown by Figure 3.5 and Figure 3.6, dmrFABP5 promoted apoptosis in both cell lines. The dot graph and histogram graph records were collected from flow cytometry and the records of control groups and optimal dose of dmrFABP5 (0.5 μM) groups were shown in Figure 3.5.

With the treatment of dmrFABP5, quantitative analysis of flow cytometry showed that all groups had increased apoptosis rates and the highest increase was achieved in both cell lines when 0.5 μM dmrFABP5 was used (Figure 3.6). Higher dose in dmrFABP5 did not produced more significant increases in apoptosis. In 22Rv1 cells, with the treatment of optimal dosage of dmrFABP5, 40.31% of cells underwent apoptosis, a significant increase by 23.12% from that (17.18%) in the control ($p<0.001$, Student's t-test). Thus, dmrFABP5 treatment produced 134.60% more apoptotic cells in 22Rv1 cells. In PC3 cells, the optimal dose of dmrFABP5 produced 26.46% of cells undergoing apoptosis; or an increase in the proportion of cells undergoing apoptosis by 15.76% ($p<0.001$, Student's t-test) when compared with that of the control (10.70%) (Figure 3.6). Therefore, dmrFABP5 produced 1.47 fold more cells undergoing apoptosis in PC3 cells.

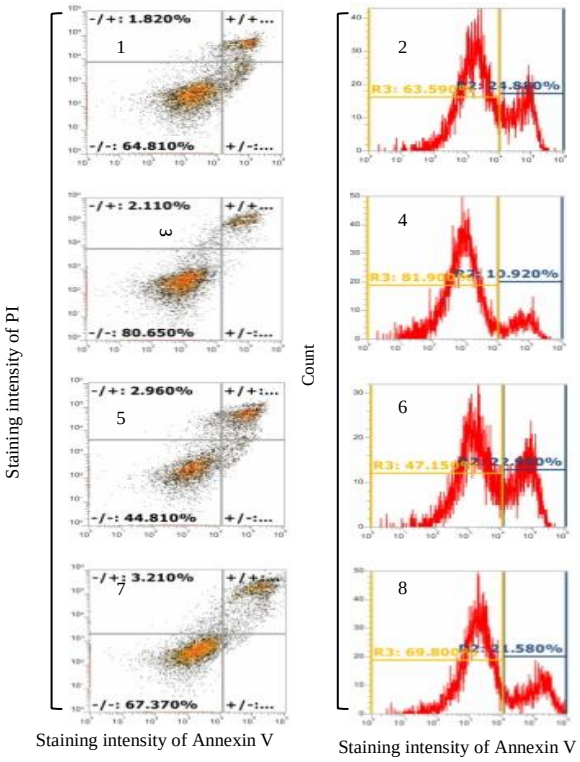

Figure 3.5. Records of dot graph and histogram graph of dmrFABP5 treated 22Rv1 and PC3 cells. 1, dot graph record of control 22RV1 cells (treated with PBS). 2, histogram record of control 22RV1 cells. 3, dot graph record of control PC3 cells (treated with PBS). 4, histogram record of control PC3 cells. 5, dot graph record of 22RV1 cells treated with 0.5 μM dmrFABP5. 6, histogram record of 22RV1 cells treated with 0.5 μM dmrFABP5. 7, dot graph record of control PC3 cells treated with 0.5 μM dmrFABP5. 8, histogram record of PC3 cells treated with 0.5 μM dmrFABP5.

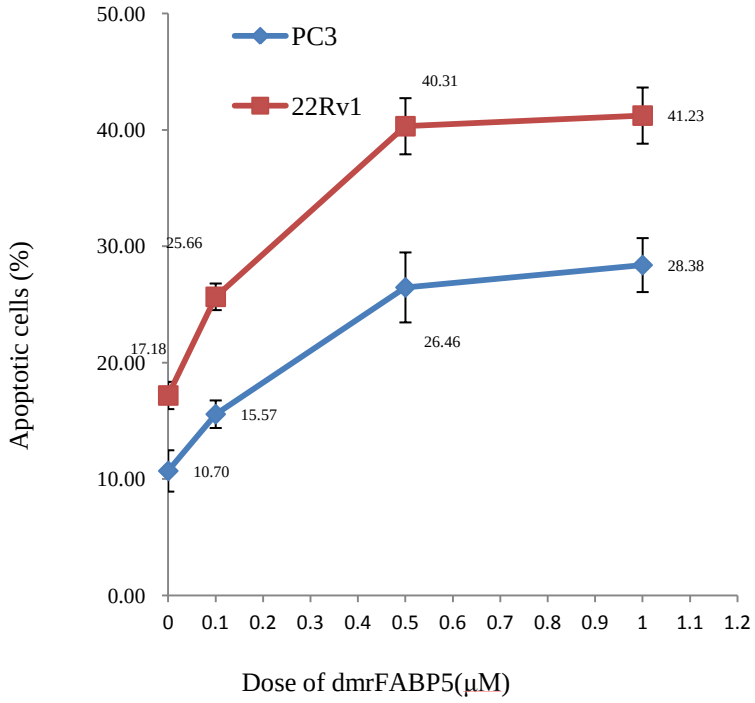

Figure 3.6. Line chart of percentages of the apoptotic cells in 22RV1 and PC3 cell lines treated with 4 different doses of SB-FI-26, respectively. Results were obtained from three separate measurements (mean ± SE) and the differences between the control and treatment were assessed by 2-tailed unpaired Student's t test.

3.5 Discussion

FABP5-related signal transduction pathway plays an important role in promoting malignant progression of CRPC cells and suppression of FABP5 to inhibit the tumorigenicity and metastasis of the prostate cancer cells (107, 123, 135, 147). Previously, studies of FABP5 were mainly focused on its tumorigenicity and metastasis promoting effect (107, 129, 132). It is also suggested that fatty acids carried by FABP5 can activate PPARγ to trigger FABP5-PPARγ-VEGF signaling pathway, which is novel target for therapeutic intervention or angiogenesis inhibition (135). Furthermore, one of the molecular mechanisms for the FABP5 inhibitors could be related to cellular apoptosis (107). Here in order to study the possible relationship between the suppressive effect of FABP5 inhibitors on cell apoptosis, the moderately malignant androgen sensitive 22Rv1 cells and the highly malignant androgen independent PC3 cells were treated with wtrFABP5 first and then treated with two FABP5 inhibitors: the chemical inhibitor SB-FI-26 and the bio-inhibitor dmrFABP5. SB-FI-26, a chemically synthesized inhibitor of FABP5, exhibited an ability to suppress both tumorigenicity and metastasis of prostate cancer (147). It can competitively bind to FABP5 to prevent intracellular and extracellular fatty acids from being transported into the cytoplasm and hence to reduce the cellular fatty acid uptake (147). The reduced fatty acid uptake can lead to a reduction or cessation of the fatty acid activation to their nuclear receptor PPARγ, and thus inhibited the biological activity of PPARγ. DmrFABP5 has a very similar structure to that of wtrFABP5, but is almost unable to bind to fatty acids (107), and does not affect the cellular fatty acid-uptake. Although the mechanism involved is not clear currently, dmrFABP5 can also reduce the biological activity of PPARγ, as that caused by SB-FI-26. Thus it was

suggested that both SB-FI-26 and dmrFABP5 significantly suppressed the tumorigenicity and metastasis of prostate cancer (147, 150) via suppressing the biological activation of the nuclear fatty acid-receptor PPARγ.

In this chapter, treatment with wtrFABP5 significantly suppressed apoptosis in both 22Rv1 (40%) and PC3 (28.3%) cells (Fig 3.2), indicating that FABP5 possibly promote the malignant progression of the CRPC cells by suppressing apoptosis, or at least, suppressing apoptosis is a part of the mechanisms involved in the cancer-promoting effect of FABP5. As shown in figure 3.4, treatment with 150μM SB-FI-26 caused 1.71 and 0.72 fold more cells to undergo apoptosis in 22Rv1 and PC3, respectively. Treatments with 0.5μM dmrFABP5 triggered 1.34 fold and 1.47 fold more cells to undergo apoptosis in 22Rv1 and PC3 cells, respectively (Fig 3.6). These results suggested that, while the increased level of FABP5 may significantly suppress apoptosis in prostate cancer cells, the opposite effect was achieved when cells were treated with inhibitors SB-FI-26 or dmrFABP5, which demonstrated that both FABP5 inhibitors suppressed prostate cancer by promoting the cancer cells to undergo apoptosis. These results provided a theoretical basis for possible therapeutic strategies for CRPC by inducing apoptosis obtained by FABP5 inhibitors. Although these results are very encouraging, further investigations are needed on the molecular mechanisms of how FABP5 affects cellular apoptosis and how the highly suppressed apoptosis by FABP5 can be increased by the FABP5 inhibitors.

Chapter 4

Result 2

FABP5 inhibitors suppress PPARγ activation in prostate cancer cells

4. Result 2: FABP5 inhibitors suppress PPARγ activation in prostate cancer cells

4.1. Introduction

Previously, it was found that FABP5 expression was highly increased in prostate cancer cells and the increased FABP5 level is significantly correlated with the increasing malignancy of the cancer cells (107, 129). Since in the physiological state, the biological function of FABP5 is to transporting fatty acids into cells, the increased FABP5 in prostate cancer cells can transport a large amount of fatty acids into the cancer cells (107). While most of these fatty acids are used as alternative energy sources, the excessive amount of fatty acids were transported into nucleus (157). FABP5 performed as signaling molecules to activate its nuclear receptor PPARγ (135). When PPARγ is activated by fatty acids and is phosphorylated, it can suppress the nuclear membrane and promoted the downstream cancer-related genes through DNA response element (PPRE) which may lead to enhanced tumourigenicity and metastasis with promoting angiogenesis and suppressing apoptosis (107, 158).

Further studies revealed that FABP5- PPARγ- VEGF may gradually replace the AR-related signal pathway in the CRPC cells to play a predominant role in promoting malignant progression in CRPC cells (123, 135, 137). While wtrFABP5 promoted malignant progression through affect PPARγ, the inhibitors of FABP5 (SB-FI-26 and dmrFABP5) have an exactly the opposite effect on PPARγ, and they inhibited the malignant progression of the cancer cells through reversing the biological function of

the wtrFABP5 (147, 150). Although both wtrFABP5 and its two inhibitors affect the malignant progression of the prostate cancer cells through interfering the biological activity of PPARγ, it is not clear whether their influence on apoptosis of the cancer cells is via PPARγ.

The target of this chapter is to identify the effect of wtrFABP5 and dmrFABP5 on PPARγ activation during the process of influencing apoptosis in prostate cancer cells. In order to investigate the molecular mechanisms involved in how FABP5 and its two inhibitor exhibited any effect on the biological activity of PPARγ during the processes of influencing apoptosis, we first treated prostate cancer cells with wtrFABP5 to investigate whether the biological activity of PPARγ was increased. Then we treated the cancer cells with two FABP5 inhibitors to investigate whether the inhibitors can influence the biological activity of PPARγ. Since the effect of SB-FI-26 on PPARγ has already investigated in our previous work (147), the here we focused on the conformation of wtrFABP5 and dmrFABP5 .

4.2. Levels of FABP5, PPARγ and p-PPARγ in benign and malignant prostate epithelial cells

Levels of of the FABP5 were detected by Western blot and the results were shown in Figure 4.1 (A, B). The benign PNT2 cells, the androgen-sensitive 22RV1 cells and the androgen-independent PC3 cells were cultured to 80% confluence, harvested and disrupted with a cell lyse buffer. Cell extracts were first subjected to SDS-PAGE and then Western blot analysis. An antibody against non-muscle β-actin was applied with each blot to correct possible loading discrepancies. Based on the bands in Figure 4.1A, level of FABP5 in the benign PNT2 cells were much lower than those in the medium malignant 22Rv1 and in the highly malignant PC3 cells. When the level of FABP5was set at 1 in PNT2 cells, its relative levels were greatly increased to 4.90±0.37 and 42.47±1.53 in 22Rv1 and PC3 cells, respectively (Figure 4.1B).

Level of of the PPARγ was measured by Western blot and the results were shown in Figure 4.2 (A, B). Based on the bands in Figure 4.2A, level of PPARγ in the benign PNT2 cells were much higher than those in the medium malignant 22Rv1 and in the highly malignant PC3 cells. Level of the phosphorylated form PPARγ (biologically activated form p-PPARγ) was measured by Western blot and the result was shown in Figure 4.2 (C, D). Based on the bands in Figure 4.2C, the expression of p-PPARγ was greatly increased in the malignant cells comparing with those in PNT2 cells. While the level of p-PPARγ was set at 1 in PNT2 cells, its relative levels were greatly increased to 18.74±2.46 and 16.47±1.45 in 22Rv1 and PC3 cells, respectively (p<0.01, Student t-test) (Figure 4.2D).

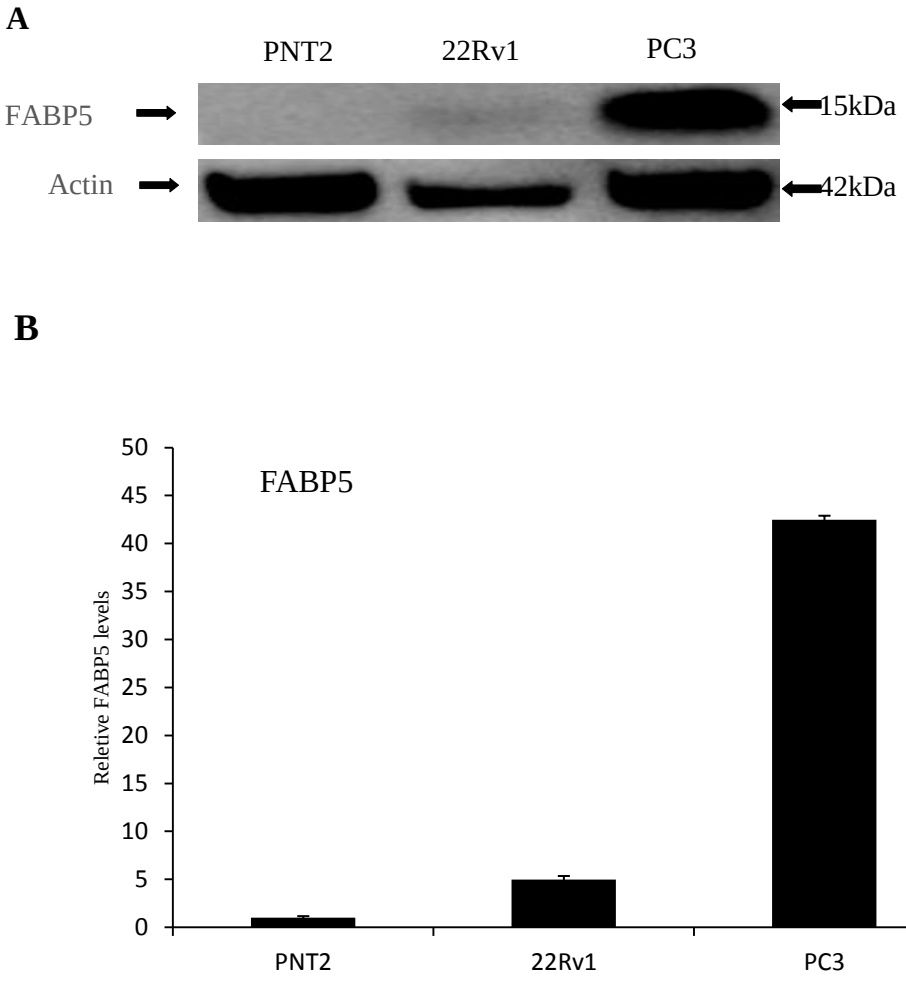

Figure 4.1. Levels of FABP5 in benign and malignant prostate cells by Western blot. **A)** Western blot analyses of FABP5 expression in the benign PNT2 cells, moderately malignant 22RV1 and highly malignant PC3 cells. **B)** Quantitative assessment of the relative levels of FABP5 by densitometry scanning of the intensities of the bands on each blot. The level of FABP5 in the benign PNT2 cells was set at 1; the levels of other cell lines on the same blot were calculated by relating to that of PNT2. Results were obtained from three separate measurements (mean ± SE, n=3), the differences between the control PNT2 and 22Rv1, PC3 cells were assessed by 2-tailed unpaired Student's t test.

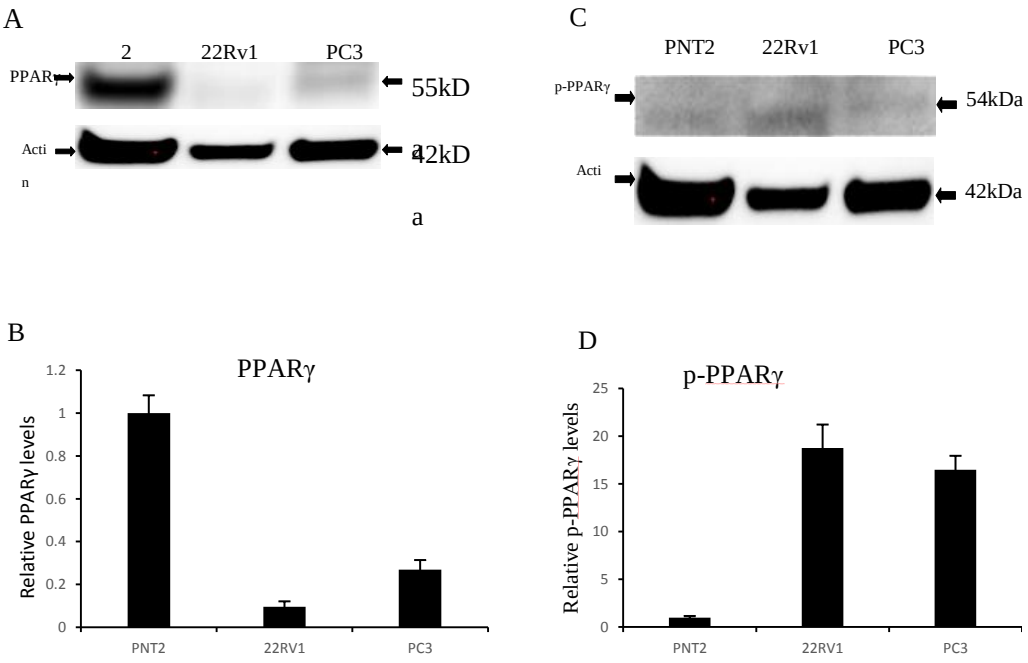

Figure 4.2. Levels of PPARγ and p-PPARγ in benign and malignant prostate cells. **A)** Western blot analyses of FABP5 expression in the benign PNT2 cells, moderately malignant 22RV1 and highly malignant PC3 cells. **B)** Quantitative assessment of the relative levels of FABP5 by densitometry scanning of the intensities of the bands on each blot. The level of PPARγ in the benign PNT2 cells was set at 1; the levels of other cell lines on the same blot were calculated by relating to that of PNT2. **C)** Western blot analyses of FABP5 expression in the benign PNT2 cells, moderately malignant 22RV1 and highly malignant PC3 cells. **D)** Quantitative assessment of the relative levels of FABP5 by densitometry scanning of the intensities of the bands on each blot. The level of p-PPARγ in the benign PNT2 cells was set at 1; the levels of other cell lines on the same blot were calculated by relating to that of PNT2. Results were obtained from three separate measurements (mean ± SE, n=3), the differences

between the control PNT2 and 22Rv1, PC3 cells were assessed by 2-tailed unpaired Student's t test.

4.3. The effect of wtrFABP5 and dmrFABP5 on levels of PPARγ and p-PPARγ expression in PC3 cells

The effect of wtrFABP5 and dmrFABP5 on level of PPARγ expression in PC3 cells was measured by Western blot (Fig 4.3A,B). PC3 cells were cultured to 80% and counted, equal number (1×10^5) of cells were then sub-cultured in triplicates: the control group was treated with PBS, the other 2 groups were treated with either 0.5μM wtrFABP5 or 0.5μM dmrFABP5 for 48 hours, respectively. All the cells were harvested and disrupted with a cell lyse buffer. Cell extracts were first subjected to SDS-PAGE and then Western blot analysis. An antibody against non-muscle β-actin was incubated with each blot to correct possible loading discrepancies. As shown in Figure 4.3, wtrFABP5 and dmrFABP5 produced no obvious changes in the sizes of the bands (A) and the quantitative assessments showed that neither wtrFABP5 nor dmrFABP5 treatment produced significant changes to the levels of both PPARγ ($p>0.05$, Student T-test) (B).

The effect of wtrFABP5 and dmrFABP5 on level of p-PPARγ expression and in PC3 cells was measured by Western blot (Fig 4.3C,D). As shown in Figure 4.3, treatment with wtrFABP5 promoted the expression of p-PPARγ (C). Quantitative analysis showed that wtrFABP5 produced a significant increase ($p<0.001$, Student T-test) in p-PPARγ level by about 39% (D). Treatment with dmrFABP5 suppressed the expression of p-PPARγ (C). Quantitative analysis showed that significant reduction ($p<0.001$, Student T-test) was produced in level of p-PPARγ by about 48% (D).

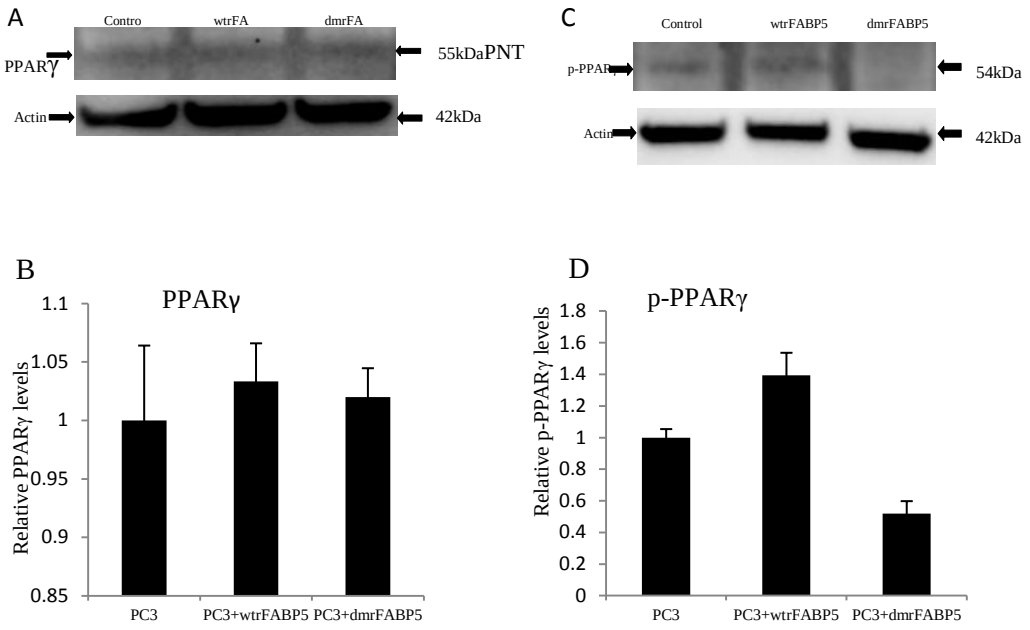

Figure 4.3. The effect of wtrFABP5 and dmrFABP5 on levels of PPARγ and p-PPARγ in PC3 cells. **A)** Western blot analyze of the effects of the treatments with PBS (Control), 0.5 µM wtrFABP5 and 0.5 µM dmrFABP5, respectively, on levels of PPARγ expression. **B)** Quantitative assessments by densitometry scanning of the intensities of the blot bands representing relative levels of PPARγ. The level of the control band (treated with PBS) in each panel was set at 1. The levels in cells treated with 0.5 µM wtrFABP5 and dmrFABP5 were calculated, respectively, by relating to that in control. **C)** Western blot analyze of the effects of the treatments with PBS (Control), 0.5 µM wtrFABP5 and 0.5 µM dmrFABP5, respectively, on levels of p-PPARγ expression. **D)** Quantitative assessments by densitometry scanning of the intensities of the blot bands representing relative levels of p-PPARγ. The level of the control band (treated with PBS) in each panel was set at 1. The levels in cells treated with 0.5 µM wtrFABP5 and

dmrFABP5 were calculated, respectively, by relating to that in control. Results were obtained from three separate measurements (mean ± SE, n=3), the differences between the control and treatments were assessed by 2-tailed unpaired Student's t test.

4.4. Discussion

PPARγ is located on nuclear membrane, it is highly expressed in adipose tissue and plays an important role to regulate adiposity and insulin sensitivity (159). Recent studies confirmed that PPARγ had key influence in promoting malignant progression of prostate cancer (160, 161). Our previous study suggested that the FABP5-PPARγ-VEGF was a key signaling pathway in CRPC malignant signals transduction (135). While wtrFABP5 increased the level of p-PPARγ and dmrFABP5 has an opposite effect, the promoting effect of wtrFABP5 on p-PPARγ in prostate cancer cells could be completely reversed by dmrFABP5 when both were used together. Thus it was concluded that dmrFABP5 suppressed the tumorigenicity and metastasis by reversing the promoting effect of wtrFABP5 on p-PPARγ (150). Some studies also indicated that PPARγ could affect cell growth and apoptosis by targeting AKT pathway in human cells, and changes of expression levels of PPARγ were found when human cancer cells underwent apoptosis (165, 166). Recently, patients with CRPC are not curable and no effective therapy has been developed. Therefore, targeting CRPC is an imperative clinical requirement. In this work, we focused on PC3 cell line which was an androgen-independent CRPC cells.

In this study, results showed that the total PPARγ levels in 22Rv1 and PC3 cells were much lower than that in the benign PNT2 cells, but the p-PPARγ levels in 22Rv1 and

PC3 cells were significantly higher (18.74 ± 2.46 fold and 16.47 ± 1.45 fold, respectively) than that in PNT2 (Fig 4.2). Results also showed that expressions of PPARγ were not significantly different in PC3 cells when treated with wtrFABP5 or dmrFABP5. However, the level of p-PPARγ was significantly increased in highly malignant PC3 cells by about 39% when treated with wtrFABP5(Fig 4.3A,B), whereas treatment with dmrFABP5 significantly reduced the level of p-PPARγ by about 48% in PC3 cells. This result suggested dmrFABP5 played a completely opposite role to wtrFABP5 and suppressed the activation of PPARγ (Fig 4.3C,D). Therefore, it is possible that the increased apoptosis shown in previous chapter is caused by the reduction of the p-PPARγ level.

To further study how p-PPARγ could affect apoptosis, levels of some factors related to cell surviving pathways were measured when cells were treated with wtrFABP5 or dmrFABP5.

Chapter 5

Result 3

DmrFABP5 suppresses AKT and NFκB signaling pathway activities in prostate cancer cells

5. Result 3: DmrFABP5 suppresses AKT and NFκB signaling pathway activities in prostate cancer cells

5.1. Introduction

Now that we have demonstrated that wtrFABP5, its inhibitors SB-FI-26 and dmrFABP5 can modulate PPARγ (162, 163). Therefore, it is very likely that the effect on apoptosis produced by these molecules are through PPARγ. However, whether and how PPARγ is exactly connected to apoptosis of the prostate cells is not known. Some recent studies reported that AKT had a key influence on regulating apoptosis in different types of cancers, including prostate cancer (164-166). Previous investigations in other cell systems suggested that activated AKT pathway is often associated with the biologically active PPARγ (167-169). Despite of these previous observations in other cells systems, it is not clear whether PPARγ may regulate AKT pathway to influence apoptosis in prostate cancer cells.

AKT pathway, also named as PI3K-AKT- signal pathway, was identified to be an important pathway, which controls cell survival and apoptosis. This pathway can be activated through the stimulation of PI3K (170-172), which promotes the phosphorylation of AKT at Thr-308 or Ser-473 (173). Biologically activated AKT (p-AKT) can regulate individual members of the downstream BCL-2 family factors to disrupt their balance. This may lead to a reduced level of Caspase-9 and hence suppression of apoptosis (174-176).

Nuclear factor (NF)- κB (NFκB) is a protein that controls DNA transcription, cytokine production, cell survival and apoptosis in human cells (177-179). Some kinases,

including AKT, can influence the upstream factors of the NFκB pathway. For example, phosphorylated AKT at Thr 308 or Ser 473 can up-regulate the p65 subunit of NFκB (180, 181). Some stimulations could cause the phosphorylation, ubiquitination and subsequent degradation of IκB proteins, thereby enabling translocation of NFκB into the nucleus (182). NFκB transcription factors bind to DNA sequences as dimers to regulate the downstream genes expression involved in cell growth and apoptosis (183-185). Although NFκB pathway plays an important role in malignant progression, it is not known whether it is related to PPARγ in prostate cancer cells.

The target of this chapter is to access the possible effect of wtrFABP5 and dmrFABP5 on survival pathways AKT and NFκB during the process of influencing apoptosis in prostate cancer cells. To investigate the possible relationship of PPARγ and AKT pathway or NFκB pathway, we first tested levels of AKT and p-AKT expression in prostate cancer cells in this set of experimental work. Then we investigated the changes in levels of AKT, p-AKT after the treatment of either wtrFABP5 or dmrFABP5. We also investigated the changes in the activity of NFκB factors produced by the treatment of either wtrFABP5 or dmrFABP5 in prostate cancer cells.

5.2. Levels of AKT and p-AKT in benign and malignant prostate epithelial cells

Levels of of AKT were measured by Western blot and the results were shown in Figure 5.1 (A, B). The benign PNT2 cells, the androgen-sensitive 22RV1 cells and the androgen-independent PC3 cells were cultured to 80% confluence, harvested and disrupted with a cell lyse buffer. The cell extracts were first subjected to SDS-PAGE and then Western blot analysis. An antibody against non-muscle β-actin was incubated with each blot to correct possible loading discrepancies. Based on the bands in Figure 5.1A, level of total AKT in the benign PNT2 cells were much higher than those in the medium malignant 22Rv1 and in the highly malignant PC3 cells.

Levels of p-AKT were measured by Western blot and the results were shown in Figure 5.1 (C, D). Based on the bands in Figure 5.1C, the expression of p-AKT was greatly increased in the malignant cells comparing with those in PNT2 cells. When the level of p-AKT was set at 1 in PNT2 cells, its relative levels were greatly increased to 1.27 ± 0.09 and 2.57 ± 0.3 in 22Rv1 and PC3 cells, respectively ($p<0.01$, Student T-test) (Figure 5.1D).

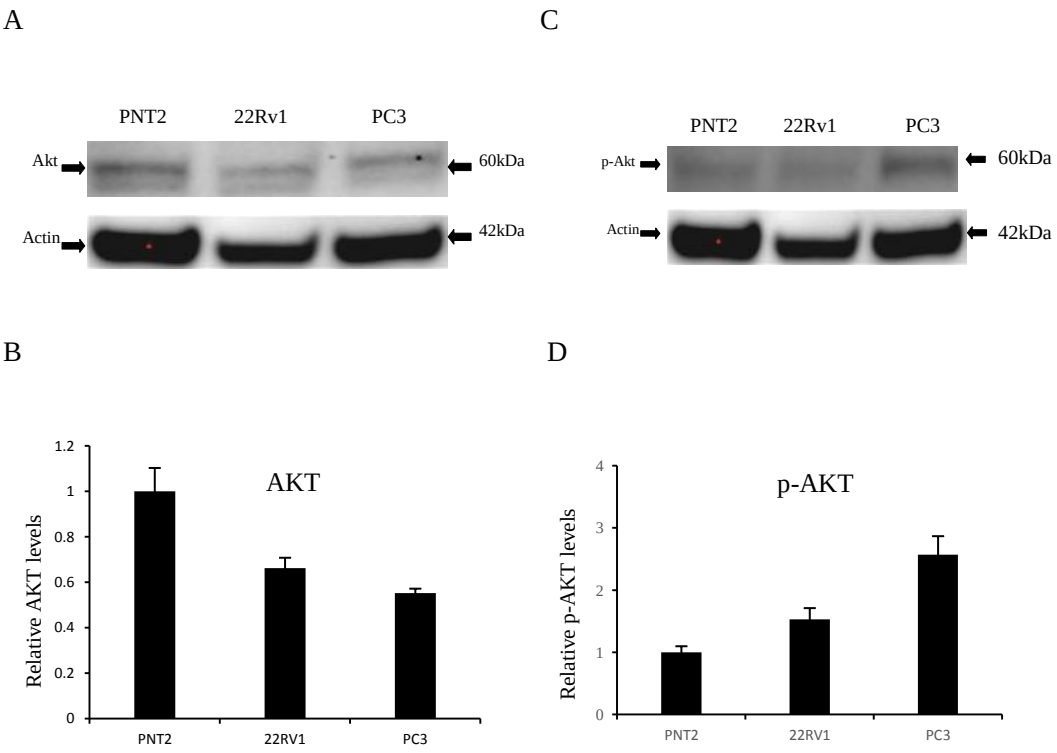

Figure 5.1. Levels of AKT and p-AKT in benign and malignant prostate cells by Western blot. **A)** Western blot analyses of AKT expression in the benign PNT2 cells and in the malignant 22RV1 and PC3 cells. **B)** Quantitative assessment of the relative levels of AKT by densitometry scanning of the intensities of the bands on each blot. The level of each of AKT in the benign PNT2 cells was set at 1; levels of other cell lines on the same blot were calculated by relating to that of PNT2. **C)** Western blot analyses of p-AKT expression in the benign PNT2 cells and in the malignant 22RV1 and PC3 cells. **D)** Quantitative assessment of the relative levels of p-AKT by densitometry scanning of the intensities of the bands on each blot. The level of each of p-AKT in the benign PNT2 cells was set at 1; the levels of other cell lines on the same blot were calculated by relating to that of PNT2. Results were obtained from three separate measurements (mean ± SE, n=3), the differences between the control PNT2 and 22Rv1, PC3 cells were assessed by 2-tailed unpaired Student's t test.

5.3. The effect of wtrFABP5 and dmrFABP5 on levels of AKT and p-AKT expression in PC3 cells

The effect of wtrFABP5 and dmrFABP5 on levels of AKT expression and in PC3 cells were measured by Western blot (Fig 5.2). The androgen-independent cancer cell line PC3 were cultured to 80% and counted, equal number (1×10^5) of cells were then sub-cultured in triplicates: the control group was treated with PBS, the other 2 groups were treated with either 0.5μM wtrFABP5 or 0.5μM dmrFABP5 for 48 hours, respectively. All the cells were harvested and disrupted with a cell lyse buffer. The cell extracts were first subjected to SDS-PAGE and then Western blot analysis. An antibody against non-muscle β-actin was incubated with each blot to correct possible loading discrepancies. As shown in Figure 5.2, wtrFABP5 and dmrFABP5 produced no obvious changes in the sizes of the bands (A) and the quantitative assessments showed that neither wtrFABP5 nor dmrFABP5 treatment produced significant changes to the levels of both AKT (p>0.05, Student T-test) (B).

The effect of wtrFABP5 and dmrFABP5 on levels of p-AKT expression and in PC3 cells were measured by Western blot (Fig 5.2). The androgen-independent cancer cell line PC3 were cultured to 80% and counted, equal number (1×10^5) of cells were then sub-cultured in triplicates: the control group was treated with PBS, the other 2 groups were treated with either 0.5μM wtrFABP5 or 0.5μM dmrFABP5 for 48 hours, respectively. All the cells were harvested and disrupted with a cell lyse buffer. The cell extracts were first subjected to SDS-PAGE and then Western blot analysis. An antibody against non-muscle β-actin was incubated with each blot to correct possible loading discrepancies. As shown in Figure 5.2, treatment with wtrFABP5 promoted

the expression of p-AKT (C). Quantitative analysis showed that wtrFABP5 produced a significant increase (p<0.001, Student T-test) in p-AKT level by about 69% (D). Treatment with dmrFABP5 suppressed the expression of p-AKT (C). Quantitative analysis showed that significant reduction (p<0.001, Student T-test) was produced in level of p-AKT by about 21% (D).

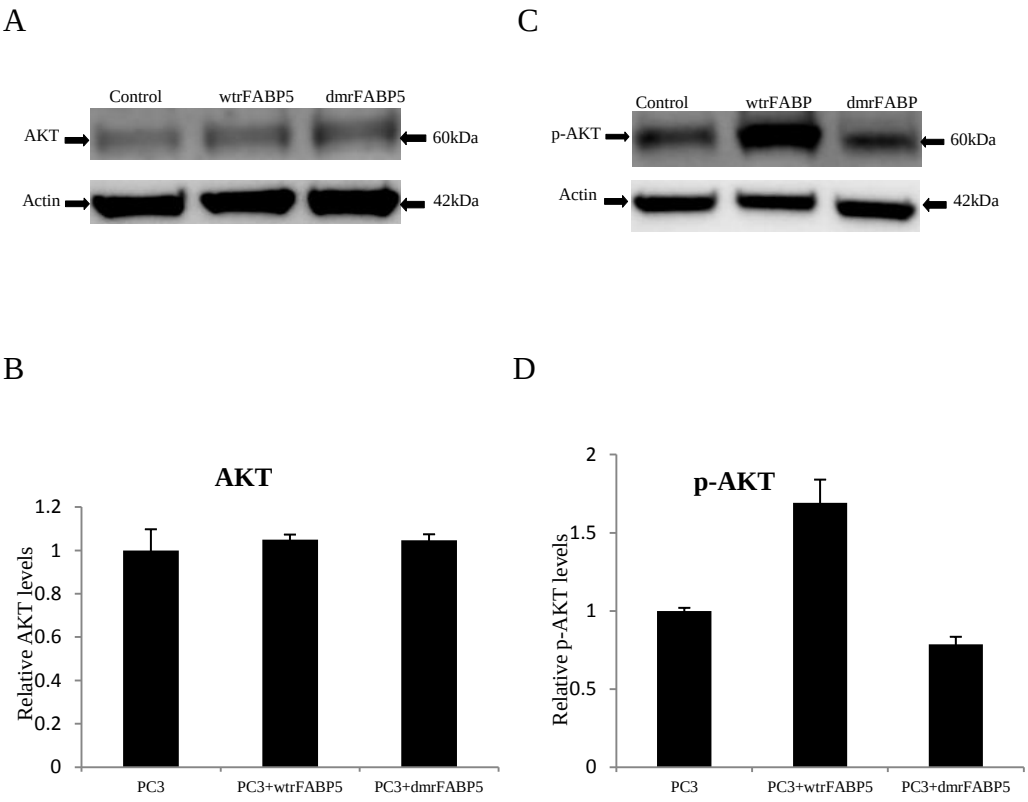

Figure 5.2. The effect of wtrFABP5 and dmrFABP5 on levels of AKT in PC3 cells. **A)** Western blot analyze of the effects of the treatments with PBS (Control), 0.5μM wtrFABP5 and 0.5μM dmrFABP5, respectively, on levels of AKT expression. **B)** Quantitative assessments by densitometry scanning of the intensities of the blot bands representing relative levels of AKT. The level of the control band (treated with PBS) in each panel was set at 1. The levels in cells treated with 0.5μM wtrFABP5 and

dmrFABP5 were calculated, respectively, by relating to that in control. **C)** Western blot analyze of the effects of the treatments with PBS (Control), 0.5 μM wtrFABP5 and 0.5 μM dmrFABP5, respectively, on levels of p-AKT expression. **D)** Quantitative assessments by densitometry scanning of the intensities of the blot bands representing relative levels of p-AKT. The level of the control band (treated with PBS) in each panel was set at 1. The levels in cells treated with 0.5 μM wtrFABP5 and dmrFABP5 were calculated, respectively, by relating to that in control. Results were obtained from three separate measurements (mean ± SE, n=3), the differences between the control and treatments were assessed by 2-tailed unpaired Student's t test.

5.4. The effect of dmrFABP5 on NF-κB activity in PC3 cells

The effect of wtrFABP5 and dmrFABP5 on NF-κB transcription factor activity in PC3 cells was measured with a transcription factor-binding assay. As shown in Fig 5.3, when the level of NF-κB transcription factor activity in the benign PNT2 cells was set at 1; the level in the PC3 cells was significantly ($p<0.05$, Student's t-test) increased to 1.09 ± 0.02. The treatment of the PC3 cells with wtrFABP5 significantly (Student's t-test, $p<0.0001$) increased the NF-κB transcription factor activity by 24.77% to 1.36 ± 0.01. The treatment with dmrFABP5 significantly ($p<0.0005$, Student's t-test) reduced NF-κB transcription factor activity in PC3 cells by 27.61% to 0.80 ± 0.05.

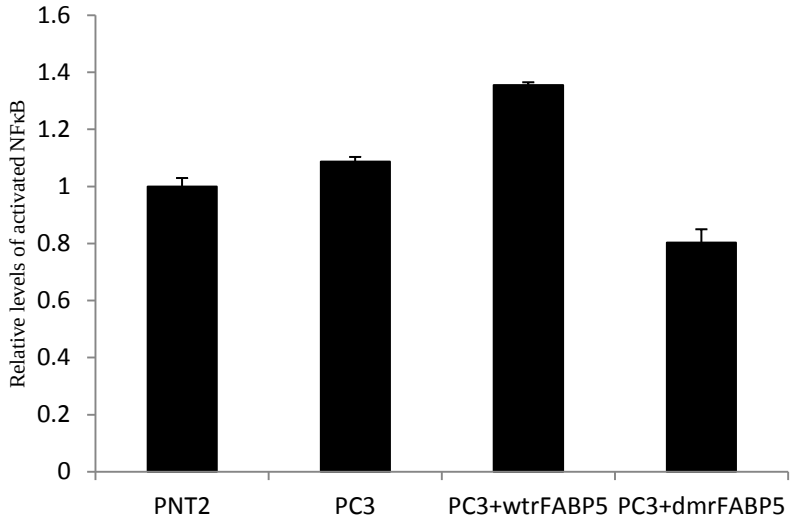

Figure 5.3. The effect of dmrFABP5 on NF-κB activity in PC3 cells. Quantitative analysis of relative OD level of each group was made and the OD level of PNT2 group was set at 1; the levels in wtrFABP5-treated and dmrFABP5-treated PC3 cells were calculated by relating to that in control PC3 cells. Results were obtained from three separate measurements (mean ± SE, n=3), the differences between the control and treatments were assessed by 2-tailed unpaired Student's t test.

5.5. Discussion

Previous results demonstrated that FABP5 affected cell apoptosis by regulating the activation of PPARγ and the inhibitor of FABP5 played opposite roles to FABP5 to influencing the biological activity. To study the molecular mechanism of how p-PPARγ could affect apoptosis, we investigated its effect on the PI3K-AKT- signal pathway, which controls cell survival and apoptosis. Other studies demonstrated that the activation of AKT promotes cell survival and reduces apoptosis in different types of cancer cells including prostate cancer (164-166, 186-188). Some studies reported that AKT can affect apoptosis by regulating the proteins in BCL-2 family and hence

lead to a reduction of the cleavage of Caspase-9 (174-176). AKT can also influence the upstream factor p65 subunit of the NFκB pathway (180, 181), which triggers the activation of NFκB and then regulate the expression of downstream genes involved in cell growth and apoptosis (183-185).

In this work, when PC3 cells were treated with wtrFABP5, the level of p-AKT was significantly increased by about 69%, whereas the level of p-AKT was significantly reduced by about 21% (Fig 5.2) when treated with dmrFABP5. Results also showed that the wtrFABP5 treatment in PC3 cells increased NFκB activity by about 25%, but dmrFABP5 reduced the NFκB activity by about 27%. These results suggested that the reduction in the level of p-PPARγ produced by dmrFABP5 lead to a significant suppression of p-AKT and hence suppressed the activity of NFκB. These suppressions inevitably caused an increased apoptosis of CRPC cells. Although the changes in levels of activated AKT and NFκB were observed together with the change in level of p-PPARγ when PC3 cells were treated with wtrFABP5 or dmrFABP5, the molecular mechanisms involved in how FABP5 and FABP5 inhibitors affected the activities of AKT and NFκB by regulating activated PPARγ was not known.

Chapter 6

Result 4

DmrFABP5 affects expression levels of apoptosis-related factors- BAX, BCL-2, Caspase-9 and Caspase-3 in prostate cancer cells

6. Result 4: DmrFABP5 affects expression levels of apoptosis-related factors- BAX, BCL-2, Caspase-9 and Caspase-3 in prostate cancer cells

6.1. Introduction

Caspases are a family of protease enzymes which have key influences in protein-degradation in cells, thus they are essential molecules in the progress of apoptosis, pyroptosis and necroptosis (189, 190). BCL-2 is a cytoplasmic protein and an important member of apoptosis- regulating factor family (191) and is a crucial suppressor of apoptosis (192, 193). BCL-2 and BAX form a heterodimer, which inhibits the promoting function of BAX in apoptosis. Biologically activated AKT can act with the down-stream individual members of BCL family of proteins to disrupt BCL-2/BAX balance (194, 195). This may lead to a reduced level of Caspase-9 and hence suppression of apoptosis (174, 175, 196). Previous studies showed that the effect of NFκB activity on apoptosis was achieved through influencing the balance of BAX/BCL-2 and its subsequent effect on the levels of Caspase family members, particular Caspase-3 (197, 198). Cytochrome C, along with APAF-1 and dATP, then bind to procaspase-9 form the "apoptosome", which is a multi-protein complex. The apoptosome hydrolyzes adenosine triphosphate to cleave and activate caspase 9. The initiator Caspase-9 then cleaves and activates the executioner Caspases 3, 6, and 7, resulting in cell apoptosis (153).

The target of this chapter is to investigate the changes in intrinsic pathway involved in apoptosis-suppressing prosess of FABP5 and apoptosis-promoting process of dmrFABP5 in PC3 cells. In order to find out whether and how FABP5 affect apoptosis through possible PPARγ-downstream pathways, we stimulated the cancer cells with both wtrFABP5 and dmrFABP5, and measured the level or the biological activity of AKT or NFκB. We found that both AKT and NFκB responded to treatments of both wtrFABP5 and dmrFABP5.

6.2. Levels of BAX in benign and malignant prostate epithelial cells

Levels of of BAX expressed in different prostatic epithelial cell lines were measured by Western blot and the results were shown in Figure 6.1 (A, B). The level of BAX in the benign PNT2 cells was much higher than that in the moderately malignant 22Rv1 cells, which is higher than that in the highly malignant PC3 cells. When the level in the benign PNT2 cells was set at 1, its relative levels in the moderately malignant 22Rv1 and the highly malignant PC3 cells were 0.49 ± 0.08 and 0.31 ± 0.02, respectively (Figure 6.1B); significant reductions by about 51% and 61%, respectively ($p<0.005$, Student's t-test).

A

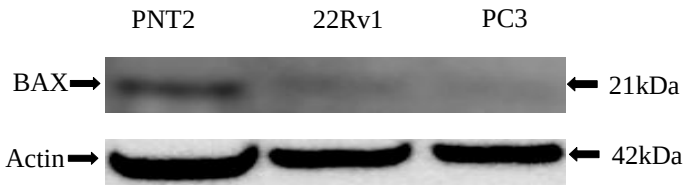

B

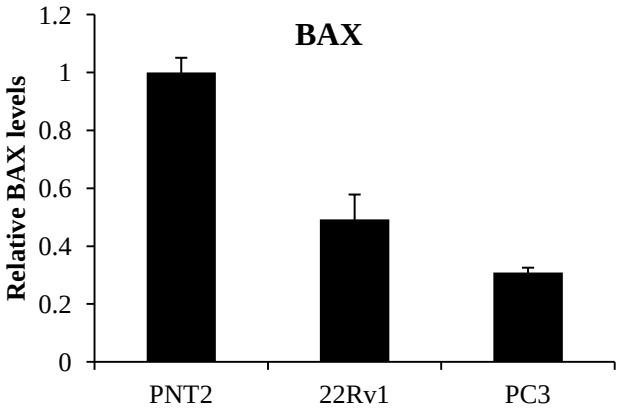

Figure 6.1. Levels of BAX in benign and malignant prostate epithelial cells by Western blot. **A)** Western blot analyses of BAX expression in the benign PNT2 cells, the malignant 22RV1 and the highly malignant PC3 cells. **B)** Quantitative assessment of the relative levels of BAX by densitometry scanning of the intensities of the bands on the blot. The level of BAX in the benign PNT2 cells was set at 1; the levels in other cell lines on the same blot were calculated by relating to that of PNT2. Results were obtained from three separate measurements (mean ± SE, n=3), the differences between the control PNT2 and 22Rv1, PC3 cells were assessed by 2-tailed unpaired Student's t test.

6.3. Levels of BCL-2 in benign and malignant prostate epithelial cells

Levels of BCL-2 was measured by Western blot and the results were shown in Figure 6.2 (A, B). Based on the intensities of the bands in Figure 6.2A, the level of BCL-2 in the benign PNT2 cells was similar (no significant difference) to those in 22Rv1 and PC3 cells.

A

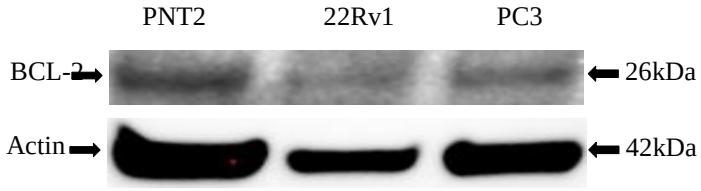

B

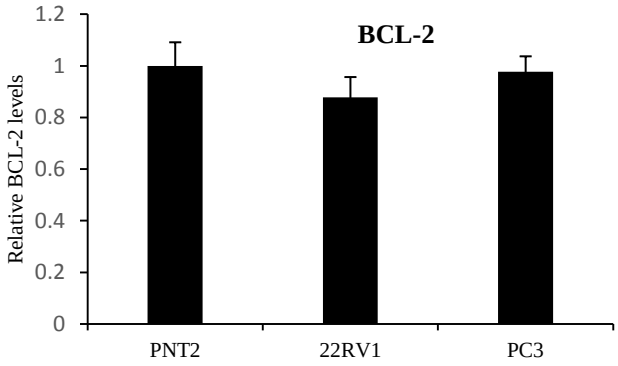

Figure 6.2. The levels of BCL-2 in benign and malignant prostate epithelial cells by Western blot. **A)** Western blot analyses of BCL-2 expression in the benign PNT2 cells and in the malignant 22RV1 and PC3 cells. **B)** Quantitative assessment of the relative

levels of BCL-2 by densitometry scanning of the intensities of the bands on each blot. The level of each of BCL-2 in the benign PNT2 cells was set at 1; the levels of other cell lines on the same blot were calculated by relating to that of PNT2. Results were obtained from three separate measurements (mean ± SE, n=3), the differences between the control PNT2 and 22Rv1, PC3 cells were assessed by 2-tailed unpaired Student's t test.

6.4. Levels of cleaved-Caspase-9 in benign and malignant prostate epithelial cells

Levels of cleaved-Caspase-9 were measured by Western blot and the results were shown in Figure 6.3 (A, B). Based on the intensities of bands in Figure 6.3A, level of cleaved-Caspase-9 in the benign PNT2 cells was similar to that in the 22Rv1 cells but was significantly higher than that in the highly malignant PC3 cells. When the level of cleaved-Caspase-9 in PNT2 was set at 1, its relative levels in 22Rv1 and PC3 were 0.97 ± 0.06 and 0.69 ± 0.03, respectively (Figure 6.3B). While the levels between PNT2 and 22Rv1 cells were very similar, the cleaved-Caspase-9 level in the highly malignant PC3 cells was significantly ($p<0.01$, Student's t-test) reduced by 31% when compared with that in the benign PNT2 cells.

A

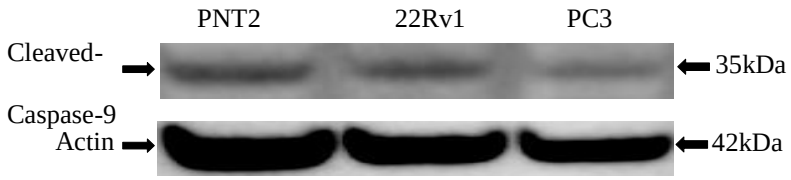

B

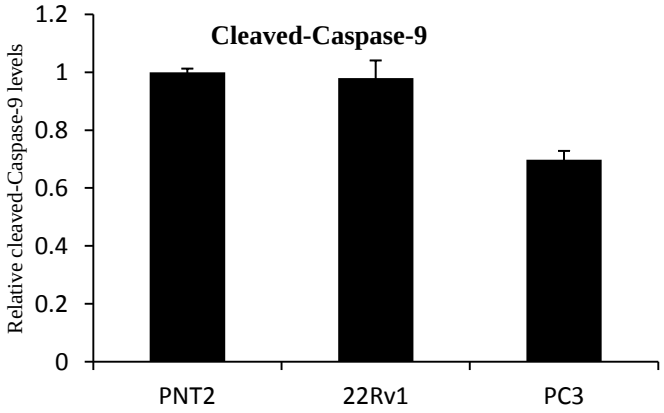

Figure 6.3. The levels of Cleaved-Caspase-9 in benign and malignant prostate cells by Western blot. **A)** Western blot analyses of Cleaved-Caspase-9 expression in the benign PNT2 cells and in the malignant 22RV1 and PC3 cells. **B)** Quantitative assessment of the relative levels of cleaved-Caspase-9 by densitometry scanning of the intensities of the bands on each blot. The level of each of cleaved-Caspase-9 in the benign PNT2 cells was set at 1; the levels of other cell lines on the same blot were calculated by relating to that of PNT2. Results were obtained from three separate measurements (mean ± SE, n=3), the differences between the control PNT2 and 22Rv1, PC3 cells were assessed by 2-tailed unpaired Student's t test.

6.5. Levels of cleaved-Caspase-3 in benign and malignant prostate epithelial cells

Levels of cleaved-Caspase-3 were measured by Western blot and the results were shown in Figure 6.4 (A, B). Based on the intensities of the bands in Figure 6.4A, the level of the cleaved-Caspase-3 in the benign PNT2 cells was much higher than those in 22Rv1 and in PC3 cells. When the level in PNT2 was set at 1, its relative levels in 22Rv1 and PC3 were 0.54 ± 0.09 and 0.42 ± 0.03, respectively (Figure 6.4B), significant reductions by about 46% and 58%, respectively ($p<0.01$; $p<0.05$, Student's t-test).

A

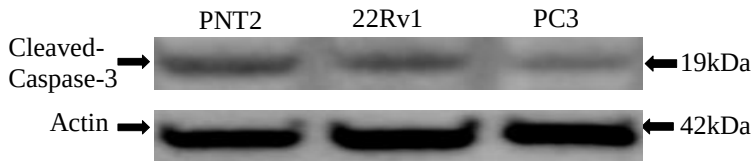

B

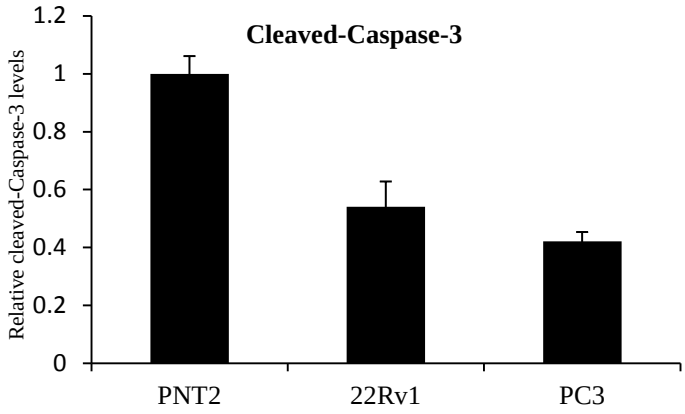

Figure 6.4. The levels of cleaved-Caspase-3 in benign and malignant prostate cells by Western blot. **A)** Western blot analyses of cleaved-Caspase-3 expression in the benign PNT2 cells and in the malignant 22RV1 and PC3 cells. **B)** Quantitative assessment of the relative levels of cleaved-Caspase-3 by densitometry scanning of the intensities of the bands on each blot. The level of each of cleaved-Caspase-3 in the benign PNT2 cells was set at 1; the levels of other cell lines on the same blot were calculated by relating to that of PNT2. Results were obtained from three separate measurements (mean ± SE, n=3), the differences between the control PNT2 and 22Rv1, PC3 cells were assessed by 2-tailed unpaired Student's t test.

6.6. The effect of dmrFABP5 on levels of BAX expression in PC3 cells

The effect of dmrFABP5 on the level of BAX in PC3 cells was measured by Western blot (Fig 6.5). The androgen-independent cancer cell line PC3 was cultured to 80% confluence, the cells were harvested, counted, equal number (1×10^5) of cells were then sub-cultured in triplicates: the control group was treated with PBS, the other 3 groups were treated with 0.5μM wtrFABP5, 0.5μM dmrFABP5 or combination of 0.5μM wtrFABP5 and 0.5μM dmrFABP5 for 48 hours, respectively. All the cells were harvested and disrupted with a cell lyse buffer. The cell extracts were first subjected to SDS-PAGE and then Western blot analysis. An antibody against non-muscle β-actin was incubated with each blot to correct possible loading discrepancies. As shown in Figure 6.5, treatment with wtrFABP5 reduced the expression of BAX (A). Quantitative analysis showed that wtrFABP5 produced a significant decrease ($p<0.001$, Student t-test) in BAX level by about 34% (B). Treatment with dmrFABP5 promoted the expression of BAX (A). Quantitative analysis showed that significant increase ($p<0.001$, Student t-test) was produced in level of BAX by about 45% (B). Treatment with both wtrFABP5 and dmrFABP5 produced no significant difference compared with benign group.

A

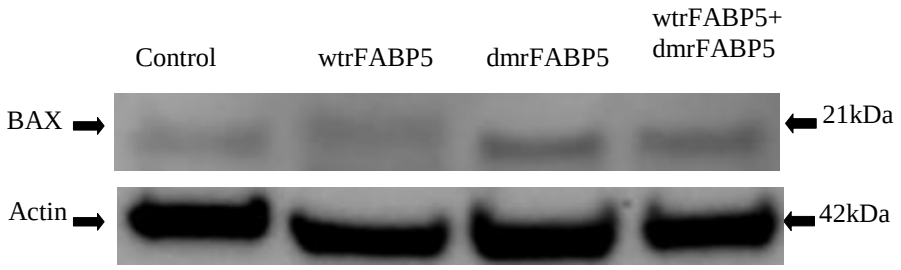

B

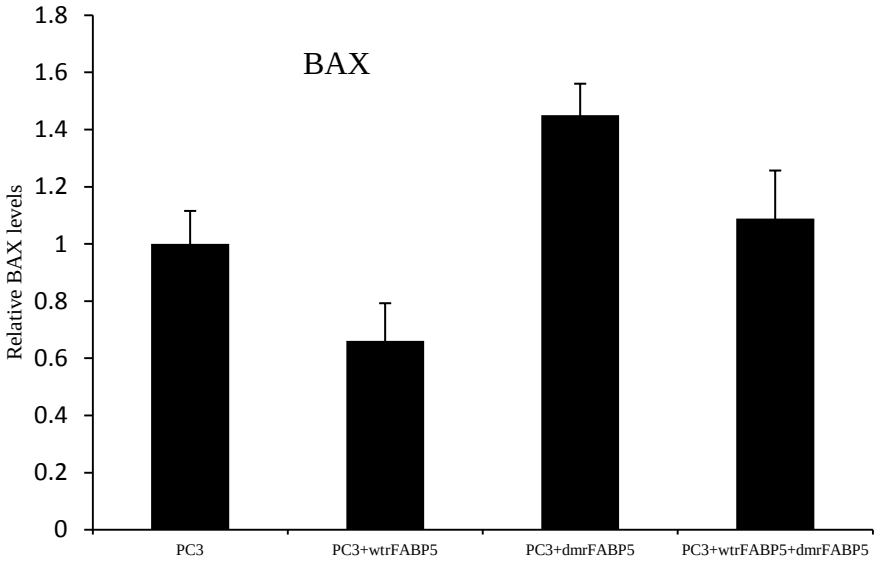

Figure 6.5. The effect of wtrFABP5 and dmrFABP5 on levels of BAX in PC3 cells. **A)** Western blot analyze of the effects of the treatments with PBS (Control), 0.5µM wtrFABP5, 0.5µM dmrFABP5 and combination of 0.5µM wtrFABP5 and 0.5µM dmrFABP5 , respectively, on levels of BAX expression. **B)** Quantitative assessments by densitometry scanning of the intensities of the blot bands representing relative levels of BAX. The level of the control band (treated with PBS) in each panel was set

at 1. The levels in cells treated with 0.5 μM wtrFABP5, dmrFABP5 and combination of 0.5 μM wtrFABP5 and 0.5 μM dmrFABP5 were calculated, respectively, by relating to that in control. Results were obtained from three separate measurements (mean ± SE, n=3), the differences between the control and treatments were assessed by 2-tailed unpaired Student's t test.

6.7. The effect of dmrFABP5 on levels of BCL-2 expression in PC3 cells

The effect of dmrFABP5 on level of BCL-2 expression and in PC3 cells was measured by Western blot (Fig 6.6). The androgen-independent cancer cell line PC3 were cultured to 80% and counted, equal number (1×10^5) of cells were then sub-cultured in triplicates: the control group was treated with PBS, the other 3 groups were treated with 0.5μM wtrFABP5, 0.5μM dmrFABP5 or combination of 0.5μM wtrFABP5 and 0.5μM dmrFABP5 for 48 hours, respectively. All the cells were harvested and disrupted with a cell lyse buffer. The cell extracts were first subjected to SDS-PAGE and then Western blot analysis. An antibody against non-muscle β-actin was incubated with each blot to correct possible loading discrepancies. As shown in Figure 6.6, treatment with wtrFABP5 reduced the expression of BCL-2 (A). Quantitative analysis showed that wtrFABP5 produced a significant increase ($p<0.001$, Student t-test) in BCL-2 level by about 316% (B). Treatment with dmrFABP5 promoted the expression of BCL-2 (A). Quantitative analysis showed that significant reduction ($p<0.05$, Student t-test) was produced in level of BCL-2 by about 44% (B). Treatment with both wtrFABP5 and dmrFABP5 produced no significant difference compared with benign group.

A

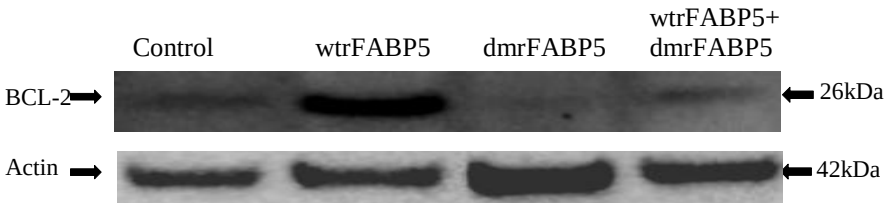

B

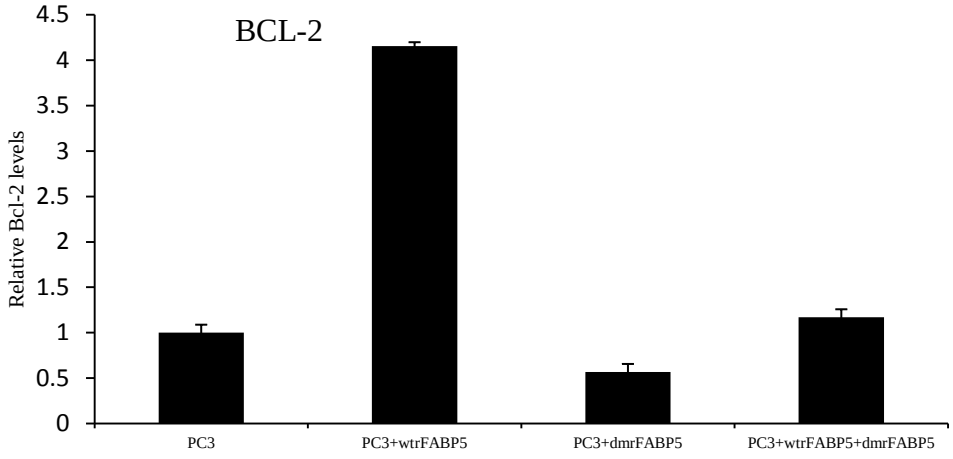

Figure 6.6. The effect of wtrFABP5 and dmrFABP5 on levels of BCL-2 in PC3 cells. **A)** Western blot analyze of the effects of the treatments with PBS (Control), 0.5μM wtrFABP5, 0.5μM dmrFABP5 and combination of 0.5μM wtrFABP5 and 0.5μM dmrFABP5 , respectively, on levels of BCL-2 expression. **B)** Quantitative assessments by densitometry scanning of the intensities of the blot bands representing relative levels of BCL-2. The level of the control band (treated with PBS) in each panel was

set at 1. The levels in cells treated with 0.5 μM wtrFABP5, dmrFABP5 and combination of 0.5 μM wtrFABP5 and 0.5 μM dmrFABP5 were calculated, respectively, by relating to that in control. Results were obtained from three separate measurements (mean ± SE, n=3), the differences between the control and treatments were assessed by 2-tailed unpaired Student's t test.

6.8. The effect of dmrFABP5 on levels of cleaved-Caspase-9 expression in PC3 cells

The effect of dmrFABP5 on the level of cleaved-Caspase-9 expression and in PC3 cells was measured by Western blot (Fig 6.7). The androgen-independent cancer cell line PC3 was cultured to 80% confluent and counted, equal number (1×10^5) of cells were then sub-cultured in triplicates: the control group was treated with PBS, the other 3 groups were treated with 0.5μM wtrFABP5, 0.5μM dmrFABP5 or combination of 0.5μM wtrFABP5 and 0.5μM dmrFABP5 for 48 hours, respectively. All the cells were harvested and disrupted with a cell lyse buffer. The cell extracts were first subjected to SDS-PAGE and then Western blot analysis. An antibody against non-muscle β-actin was incubated with each blot to correct possible loading discrepancies. As shown in Figure 6.7, treatment with wtrFABP5 reduced the expression of cleaved-Caspase-9 (A). Quantitative analysis showed that wtrFABP5 produced a significant reduction ($p<0.001$, Student t-test) in cleaved-Caspase-9 level by about 61% (B). Treatment with dmrFABP5 promoted the expression of cleaved-Caspase-9 (A). Quantitative analysis showed that significant increase ($p<0.001$, Student t-test) was produced in level of cleaved-Caspase-9 by about 31% (B).

Treatment with both wtrFABP5 and dmrFABP5 produced a reduction in levels of cleaved-Caspase-9 by about 31%, which was significantly reversed from the effect of wtrFABP5 and dmrFABP5.

A

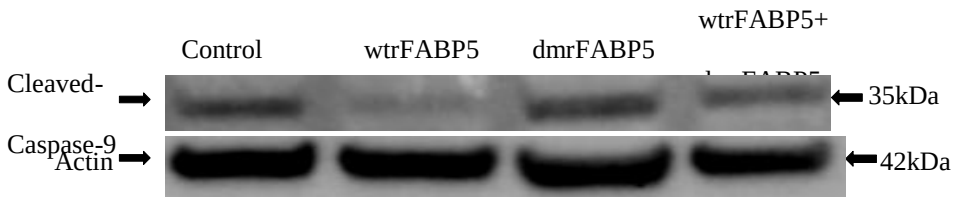

B

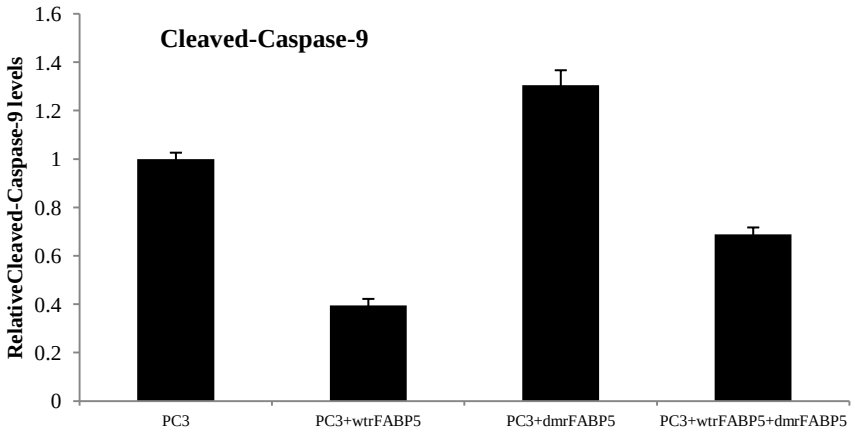

Figure 6.7. The effect of wtrFABP5 and dmrFABP5 on levels of cleaved-Caspase-9 in PC3 cells. **A)** Western blot analyze of the effects of the treatments with PBS (Control), 0.5μM wtrFABP5, 0.5μM dmrFABP5 and combination of 0.5μM wtrFABP5 and 0.5μM dmrFABP5 , respectively, on levels of cleaved-Caspase-9 expression. **B)**

Quantitative assessments by densitometry scanning of the intensities of the blot bands representing relative levels of cleaved-Caspase-9. The level of the control band (treated with PBS) in each panel was set at 1. The levels in cells treated with 0.5μM wtrFABP5, 0.5μM dmrFABP5 and combination of 0.5μM wtrFABP5 and 0.5μM dmrFABP5 were calculated, respectively, by relating to that in control. Results were obtained from three separate measurements (mean ± SE, n=3), the differences between the control and treatments were assessed by 2-tailed unpaired Student's t test.

6.9. The effect of dmrFABP5 on levels of cleaved-Caspase-3 expression in PC3 cells

The effect of dmrFABP5 on level of cleaved-Capase-3 expression and in PC3 cells was measured by Western blot (Fig 6.8). The androgen-independent cancer cell line PC3 were cultured to 80% and counted, equal number (1×10^5) of cells were then sub-cultured in triplicates: the control group was treated with PBS, the other 3 groups were treated with 0.5μM wtrFABP5, 0.5μM dmrFABP5 or combination of 0.5μM wtrFABP5 and 0.5μM dmrFABP5 for 48 hours, respectively. All the cells were harvested and disrupted with a cell lyse buffer. The cell extracts were first subjected to SDS-PAGE and then Western blot analysis. An antibody against non-muscle β-actin was incubated with each blot to correct possible loading discrepancies. As shown in Figure 6.8, treatment with wtrFABP5 reduced the expression of cleaved-Capase-3 (A). Quantitative analysis showed that wtrFABP5 produced a significant decrease (p<0.001, Student t-test) in cleaved-Capase-3 level by about 64% (B). Treatment with dmrFABP5 promoted the expression of cleaved-Capase-3 (A). Quantitative analysis

showed that significant promotion (p<0.05, Student t-test) was produced in level of cleaved-Capase-3 by about 23% (B). Treatment with both wtrFABP5 and dmrFABP5 produced no significant difference compared with benign group.

A

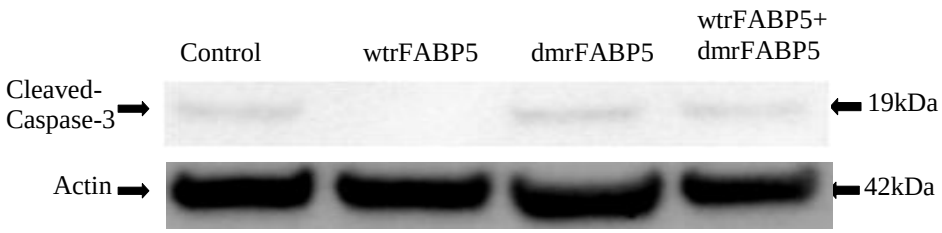

B

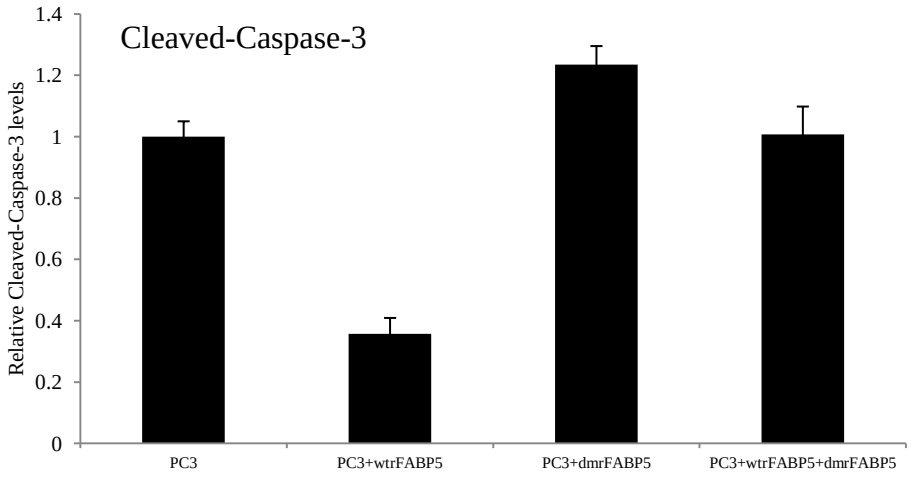

Figure 6.8. The effect of wtrFABP5 and dmrFABP5 on levels of cleaved-Caspase-3 in PC3 cells. **A)** Western blot analyze of the effects of the treatments with PBS (Control), 0.5μM wtrFABP5, 0.5μM dmrFABP5 and combination of 0.5μM wtrFABP5 and 0.5μM dmrFABP5 , respectively, on levels of cleaved-Caspase-3 expression. **B)** Quantitative assessments by densitometry scanning of the intensities of

the blot bands representing relative levels of cleaved-Caspase-3. The level of the control band (treated with PBS) in each panel was set at 1. The levels in cells treated with 0.5μM wtrFABP5, dmrFABP5 and combination of 0.5μM wtrFABP5 and 0.5μM dmrFABP5 were calculated, respectively, by relating to that in control. Results were obtained from three separate measurements (mean ± SE, n=3), the differences between the control and treatments were assessed by 2-tailed unpaired Student's t test.

6.10. Discussion

Previous studies suggested that the effect of biological activities of both AKT and NFκB on apoptosis were achieved through influencing levels of different BCL-2 family members and hence the balance of the apoptosis-promoting and -suppressing elements. Tipping this balance may result in an activated or an inhibited biological activity of the Caspase family, particularly Caspase-9 and Caspase-3 (186, 199-202). The heterodimer formed by BCL-2 and BAX can suppress the biological activity of BAX (203, 204), thus, the reduction of BAX/BCL-2 ratio to disrupt this balance suppressed the cleavages of Caspase-9 and Caspase-3 and resulted in an inhibited apoptosis and an enhanced malignant progression (205-207).

In this study, we first detected the levels of BAX, BCL-2, cleaved-Caspase-9 and cleaved-Caspase-3 in benign PNT2 cells and in the malignant 22Rv1 and PC3 cells. As showed in the results, the level of BAX (Fig 6.1) and cleaved-Caspase-3 (Fig 6.4) in the benign PNT2 cells was much higher than that in the moderately malignant 22Rv1 cells, which is higher than that in the highly malignant PC3 cells. Whereas the level of cleaved-Caspase-9 in the benign PNT2 cells was similar to that in the 22Rv1 cells but was significantly higher than that in the highly malignant PC3 cells (Fig 6.3). The levels of BCL-2 were similar amongst these cell lines (Fig 6.2). These results suggested that in the malignant prostate cancer cells, the cleaved caspases is less active than that in the benign cells indicating a suppressed apoptosis is related to the increased level of FABP5 expression.

It was shown that PC3 cells treated with wtrFABP5 greatly reduced the level of BAX by about 34% (Fig 6.5), and greatly increased the level of BCL-2 by about 316% (Fig

6.6). In contrast, the treatment with dmrFABP5 significantly increased the level of BAX by about 45% (Fig 6.5) but reduced the level of BCL-2 by about 44% (Fig 6.6). Whereas the treatment with both wtrFABP5 and dmrFABP5 showed no significant difference on levels of BAX and BCL-2 in PC3 cells. This result showed that changes in both BAX and BCL-2 levels obtained by wtrFABP5 were completely reversed (not significantly different from control) with the treatment with dmrFABP5 in PC3 cells. Similarly, Changes in both BAX and BCL-2 levels obtained by dmrFABP5 were completely reversed with the treatment with wtrFABP5. Further investigation showed that wtrFABP5 produced significant reduction in levels of cleaved-Caspase-9 by about 61%, whereas dmrFABP5 promoted the levels of cleaved-Caspase-9 by about 31%. Treatment with both wtrFABP5 and dmrFABP5 have neutralised about 51% of the effect produced by wtrFABP5, but this level was still significantly lower than that in the control by about 31%. Thus, the promoting effect of dmrFABP5 in level of cleaved-Caspase-9 was not strong enough to completely reverse that suppressive effect of wtrFABP5 (Fig 6.7), indicating that a more complicated mechanism maybe involved in the cleavage of Caspase-9, apart from the effect of FABP5. Thus, further investigation is needed to find out what other factors are involved in suppressing the biological activity of Caspase-9. The results in this work also showed that wtrFABP5 produced significant reduction in levels of cleaved-Caspase-3 by about 64%, whereas dmrFABP5 promoted the levels of cleaved-Caspase-3 by about 23% (Fig 6.8). Changes in cleaved-Caspase-3 level obtained by wtrFABP5 was completely reversed with the treatment with dmrFABP5 in PC3 cells. Similarly, changes in cleaved-Caspase-3 level obtained by dmrFABP5 was completely reversed with the treatment with wtrFABP5.

Chapter 7

General Discussion and future work

7. General Discussion, conclusion and future work

Prostate cancer is the most commonly diagnosed male cancer and the second leading cancer-related death in male in the rich western countries (4). Since Higgins and associates discovered that the growth and expansion of prostate cancer cells are dependent on the stimulations of male hormone supplied through peripheral blood circulation (208), androgen deprivation by physical or pharmaceutical castration or suppressing the biological activity of AR has been the primary treatment for patients with prostate cancer over the past 50 years (209). Despite the initial effectiveness, prostate cancer usually come back in about two years with a more aggressive hormone-independent phenotype, called CRPC. CRPC does not effectively sensitive to ADT anymore because the growth and progression of CRPC cells are no longer dependent on circulating hormones (210). The conversion of androgen-dependent cancer cells to androgen-independent CRPC cells is a fundamental change, and the molecular mechanism involved in this change is not fully understood (211). To develop new therapeutic strategies, it is necessary to conduct further investigations on molecular mechanisms involved in the malignant progression of prostate cancer. Our previous studies suggest that AR may be unrelated to the malignant progression of CRPC. Instead of AR-mediated signaling pathway, FABP5-PPARγ-VEGF axis possibly play a more effective role in CRPC (123, 135). Fatty acids were demonstrated to function in cellular building and initiation of signaling pathway in cancer cells and have important influences in tumourigenisity and metastasis of cancer cells (212, 213). High level of FABP5 in prostate cancer has been suspected as

a promoter for cell growth and metastasis (214). It has been proved that FABP5 delivers fatty acids from intracellular and extracellular sources into cells and enhance the activity of their nuclear receptor PPARγ in prostate cancer cells (123, 135). The siRNA knockdown of FABP5 shown an effective inhibition of growth in highly malignant prostate cancer cells *in vivo* (134), however, the siRNA was unstable and loss their function in a short time. Thus, targeting FABP5 biological function could be considered a new way for CRPC treatment. Our previous studies demonstrated that with the treatment of both chemically-synthesized inhibitor (SB-FI-26) and a bio-inhibitor (dmrFABP5) for FABP5, its biological activity was suppressed and hence the tumour growth and metastasis were significantly reduced (147). Our previous studies also demonstrated that FABP5-related signal transduction pathway plays an crucial role in promoting malignant progression of prostate cancer cells and it is possible for FABP5 to promote tumorigenicity and metastasis through the inhibition of cellular apoptosis (107, 129, 131). To study the possible molecular mechanisms underlying the tumour-suppressing effect of the FABP5 inhibitors, here for the first time, we conducted a systematic assessment on whether promoting cellar apoptosis is part of the mechanisms for these inhibitors to suppress the malignant progression of the CRPC cells. The results in this study can be summarized as following:

1- FABP5 inhibitors promoted the apoptosis in both moderately malignant androgen sensitive 22Rv1 cells and the highly malignant androgen independent PC3 cells.

2- The increased apoptosis caused by dmrFABP5 is possibly caused by the reduction of p-PPARγ level.

3- The increased level of p-PPARγ produced by wtrFABP5 treatment lead to a significant promotion of p-AKT and hence promote the activity of NFκB, whereas the reduced level of p-PPARγ produced by dmrFABP5 lead to a significant suppression of p-AKT and hence suppressed the activity of NFκB.

4- Pro-apoptotic BAX and cleaved-Caspases in malignant prostate cancer cells were much less active than those in benign PNT2 cells but the anti-apoptotic BCL-2 remained a similar levels amongst the benign and the malignant cells.

5- WtrFABP5 suppressed pro-apoptotic BAX level and increased the anti-apoptotic BCL-2 level, which led to a significant reduction in BAX/BCL-2 ratio in PC3 cells. Wheras dmrFABP5 promoted pro-apoptotic BAX level and suppressed the anti-apoptotic BCL-2 level, which led to a significant increasing in BAX/BCL-2 ratio in PC3 cells.

6- WtrFABP5 produced significant reduction in the level of cleaved-Caspase-9 and cleaved-Caspase-3, whereas dmrFABP5 promoted the level of cleaved-Caspase-9 and cleaved-Caspase-3 in PC3 cells.

7.1 FABP5 and FABP5 inhibitors implicated apoptosis in prostate cancer cells.

In order to investigate the possible effect of FABP5 on cell apoptosis, the moderately malignant androgen sensitive 22Rv1 cells and the highly malignant androgen independent PC3 cells were treated with wtrFABP5 first and then treated with two FABP5 inhibitors: the chemical inhibitor SB-FI-26 and the bio-inhibitor dmrFABP5. Before treatment, we found that the percentage of apoptotic cells in 22Rv1 was significantly higher than that in PC3 (Fig. 3.2). Considering that fact that the level of FABP5 in 22Rv1 is lower and the malignancy in 22Rv1 is lower than those in PC3,

the result in this work suggested that the increased level of FABP5 is closely associated with the reduced level of the percentage of cells undergoing apoptosis. When treated with wtrFABP5, significant suppression of apoptosis were found in both 22Rv1 and PC3 cells (Fig 3.2). This result plus our previous work suggested that the increased level of FABP5 may play a suppressive role in apoptosis and this role may contribute, at least partially, to the caner-promoting activity of FABP5 in prostate cancer. As showed in figure 3.4, when treated with 150μM SB-FI-26, more 22Rv1 and PC3 cells underwent apoptosis. Whereas when treated with 0.5μM dmrFABP5, more 22Rv1 and PC3 cells underwent apoptosis (Fig 3.6). These results showed that completely opposite to wtrFABP5, the role of the inhibitors SB-FI-26 or dmrFABP5 are promoting apoptosis. DmrFABP5 had a better promotion effect (about 1.5 fold promotion) in apoptosis of the highly malignant PC3 cells compared with SB-FI-26 (about 0.7 fold promotion). Thus, it is possible that the FABP5 inhibitors suppressed the malignant progression of prostate cancer cells, at least partly, by promoting the apoptosis of cancer cells. These results provided a theoretical basis for possible therapeutic strategies for prostate cancer, especially CRPC, by inducing apoptosis obtained by FABP5 inhibitors.

7.2 PPARγ was correlated with modulating changes in apoptosis caused by wtrFABP5 and dmrFABP5 in prostate cancer cells.

FABP5 can transport a large amount of fatty acids into prostate cancer cells (215). While most of these fatty acids are used as alternative energy sources, the excessive amount of fatty acids were transported into nucleus, as signaling molecules, to stimulate the nuclear receptor PPARγ (216). PPARγ is located in nuclear membrane, it is highly expressed in adipose tissue and plays an important role to regulate

adiposity and insulin sensitivity (159). Our Previous studies demonstrated that the FABP5-PPARγ-VEGF influenced malignant progression and cellular apoptosis of CRPC (107, 123, 135). In this work, we detected the change in levels of PPARγ and p-PPARγ in untreated prostate cancer cells and in highly malignant PC3 cells when treated with wtrFABP5 or dmrFABP5. Results showed that the total PPARγ levels in PC3 cells were higher than that in 22Rv1 cells and lower than that in the benign PNT2 cells, (Fig 4.1); and the levels of PPARγ were not significantly different in PC3 cells when treated with wtrFABP5 or dmrFABP5 (Fig 4.2). However, the p-PPARγ levels in 22Rv1 and PC3 cells were significantly higher than that in PNT2 (Fig 4.1); the level of p-PPARγ was significantly increased in highly malignant PC3 cells by 39% when treated with wtrFABP5, whereas treatment with dmrFABP5 significantly reduced the level of p-PPARγ in PC3 cells (Fig 4.3). These results showed that the total level of PPARγ did not respond to the treatments with either wtrFABP5 or dmrFABP5, but the level of p-PPARγ or the biologically active PPARγ was significantly increased when treated with wtrFABP5. Whereas when treated with dmrFAB5, the level of p-PPARγ was significantly reduced, which suggested that dmrFABP5 played a completely opposite role to wtrFABP5 and suppressed the activation of PPARγ. Thus, the increased apoptosis caused by dmrFABP5 shown in previous results is possibly caused by the reduction of p-PPARγ level; PPARγ may play a central role in modulating changes related to apoptosis.

7.3 AKT and NFκB pathways were correlated with modulating changes in apoptosis caused by wtrFABP5 and dmrFABP5 in prostate cancer cells.

To study the molecular mechanism of how p-PPARγ affected apoptosis, we first investigated the change in prostate cancer cells on the PI3K-AKT- signal pathway,

which controls cell survival and apoptosis, and which is influenced by the changes of the p-PPARγ level. The activation of AKT pathway promotes cell survival and reduces cellular apoptosis in different types of cancer cells including prostate cancer (164-166). It was reported that the way that AKT affected apoptosis was through regulating the individual protein members of the BCL-2 family and changing the balance of cancer- promotive- or suppressive- forces, hence triggering the change of caspase-9 (174-176). As AKT also affects the activation of NFκB by influencing the upstream factor p65 subunit of the NFκB pathway (180, 181), and the activation of NFκB can regulate the expression of downstream genes involved in cell growth and apoptosis (183-185), we then detected the level of activation of NFκB in prostate cancer cells. Result showed that the level of total AKT in the benign PNT2 cells were much higher than that in the moderately malignant 22Rv1 and in the highly malignant PC3 cells (Figure 5.1). Whereas compared with the level of the expression of p-AKT in PNT-2 cells, the level was greatly increased in 22Rv1 cells and PC3 cells (Fig. 5.1). These results suggested that the levels of activated AKT were increased in the moderately malignant 22Rv1 cells and further greatly increased in the highly malignant PC3 cells. Another result showed that when PC3 cells were treated with wtrFABP5, the level of p-AKT was significantly increased, the level of p-AKT was significantly reduced (Fig. 5.2) when treated with dmrFABP5. Results also showed that the wtrFABP5 treatment in PC3 cells increased NFκB activity, but dmrFABP5 reduced the NFκB activity when compared with the PC3 control (Fig. 5.3). These results proved that the increase in level of p-PPARγ produced by wtrFABP5 lead to a significant promotion of p-AKT and hence promote the activity of NFκB and cell survival. Whereas the reduction in level of p-PPARγ produced by dmrFABP5 lead to a

significant suppression of p-AKT and hence suppressed the activity of NFκB. These suppressions maybe inevitably caused an increased apoptosis of CRPC cells.

7.4 Highly malignant prostate cancer cells expressed lower level of BAX compared with benign cells.

Previous studies proved that the effect of biological activities of both AKT and NFκB on apoptosis were achieved through influencing levels of different BCL-2 family members and hence disrupting the balance of the apoptosis-promoting and -suppressing elements (217-219). Tipping this balance may result in an activated or an inhibited biological activities of the Caspase family, particularly Caspase-9 and Caspase-3 (186, 199-201). Since AKT and NFκB activities were suppressed through p-PPARγ with the treatment of dmrFABP5, detailed investigation on levels of the related apoptosis-inducer and apoptosis-suppressor may help to understand the mechanisms involved in how p-PPARγ influencing cellular apoptosis. Results showed that the level of pro-apoptotic BAX (Fig 6.1) in the benign PNT2 cells was much higher than that in the moderately malignant 22Rv1 cells, which is higher than that in the highly malignant PC3 cells. The levels of cleaved-Caspase-3 (Fig 6.4) in the benign PNT2 cells was much higher than that in 22Rv1 cells, which is higher than that in PC3 cells. Whereas the level of cleaved-Caspase-9 in the benign PNT2 cells was similar to that in the 22Rv1 cells but was significantly higher than that in the highly malignant PC3 cells (Fig 6.3). The levels of anti-apoptotic BCL-2 were similar amongst these cell lines (Fig 6.2). These results suggested that in the malignant prostate cancer cells, pro-apoptotic BAX and cleaved-Caspases were much less active than those in benign PNT2 cells but the anti-apoptotic BCL-2 remained a similar levels amongst the benign and the malignant cells, which indicated that apoptosis was

suppressed in the cancer cells but it is very active in the benign cells. In another word, in the benign PNT2 cells which express low or undetected level of FABP5, apoptosis mechanism is active and the programmed cell death occurred normally. However, in the CRPC cells 22Rv1 and PC3 which express an increased level of FABP5, the opposite to the PNT2 cells was observed and the apoptotic mechanism is highly suppressed and much less cells undergoing apoptosis, and thus as a result of the reduced apoptosis, the malignant progression is obtained and enhanced.

7.5 WtrFABP5 and dmrFABP5 affected the levels of BAX, BCL-2, cleaved-Caspase-9 and cleaved-Caspase-3 in prostate cancer cells.

When PC3 cells were treated with wtrFABP5, the level of BAX was reduced (Fig 6.5), but the level of BCL-2 was greatly increased (Fig 6.6). On the contrary, when PC3 cells were treated with dmrFABP5, the level of BAX was significantly increased (Fig 6.5) but the level of BCL-2 was greatly reduced by (Fig 6.6). Whereas the treatment with both wtrFABP5 and dmrFABP5 showed no significant difference on levels of BAX and BCL-2 in PC3 cells (Fig 6.5, 6.6). These results provided a direct evidence that wtrFABP5 suppressed pro-apoptotic BAX and increased the anti-apoptotic BCL-2, which led to a significant reduction in BAX/BCL-2 ratio. These results also showed that the apoptosis-suppressive effect exerted by wtrFABP5 was reversed completely by the treatment of dmrFABP5. Similarly, the effect in both pro-apoptotic BAX and anti-apoptotic BCL-2 levels produced by dmrFABP5 were completely reversed with the treatment with wtrFABP5. Further studies also showed that wtrFABP5 produced significant reduction in the level of cleaved-Caspase-9, whereas dmrFABP5 promoted the level of cleaved-Caspase-9 in PC3 cells. Treatment with both wtrFABP5 and dmrFABP5 have neutralised effect produced by wtrFABP5, but this level was still

significantly lower than that in the control by about 30%. Therefore, the promoting effect of dmrFABP5 on level of cleaved-Caspase-9 was not strong enough to completely reverse that suppressive effect of wtrFABP5 (Fig 6.7), indicating that a more complicated mechanisms or other unknown factors maybe involved in the cleavage of Caspase-9, apart from the effect of FABP5. Further studies is needed to investigate all pathways and factors that are involved in suppressing the biological activity of Caspase-9 when the cellular apoptosis is influenced by FABP5 inhibitor. Further investigation in this work showed that wtrFABP5 produced significant reduction in levels of cleaved-Caspase-3, whereas dmrFABP5 promoted the levels of cleaved-Caspase-3 (Fig 6.8). These changes in level of cleaved-Caspase-3 obtained by wtrFABP5 was completely reversed with the treatment with dmrFABP5 in PC3 cells. Similarly, Changes in cleaved-Caspase-3 level obtained by dmrFABP5 was completely reversed with the treatment with wtrFABP5. Thus, wtrFABP5 and dmrFABP5 played opposite roles inside cancer cells, and affected the malignant progression through exerting opposite influences on apoptosis.

7.6 Possible *in vivo* detection on apoptosis and potential clinical implementation of FABP5 inhibitors in prostate cancer cells

Previously, it is reported that suppression of the biological function of FABP5 by inhibitors inhibited the migration and invasion of prostate cancer cells *in vitro* and *in vivo*. These results suggest that both FABP5 inhibitors are potent inhibitors on malignant progression of CRPC cells *in vitro* and *in vivo* and the suppression effect of the bio-inhibitor dmrFABP5 is much stronger than that of the chemically synthesised SB-FI-26 (155). In this work, the *in vitro* results showed the suppression of the FABP5 by inhibitors promoted the apoptosis of prostate cancer cells. Further

detection of the effect of FABP5 inhibitors on apoptosis in prostate cancer should be done in the future.

Currently, ADT is a main therapy against prostate cancer. Since the growth of prostate cancer is dependent on androgen at early stages of treatment, blockage of androgen is an effective therapy against prostate cancer. However, ADT can not fully cure prostate cancer and prolonged therapy usually make conversion to CRPC. Therefore, Previous pathological studies have shown that FABP5 overexpression is strongly associated with prostate cancer progression and metastasis (155). Some studies indicated that inhibition of the biological functions of FABP5 could be an effective treatment to suppress multiple steps that are important in tumour progression and metastasis in nude mice (155). The results on prostate cancer proliferation, metastasis and apoptosis obtained from targeting FABP5 biological function provided clues for a new way to treat patients with CRPC, and they also provided a theoretical basis for resolving possible problems raised from the treatment by targeting PPARγ or VEGF (123).

7.7 Conclusion

In conclusion, as shown by the schematic illustration in Figure 7.1, by transporting excessive amount of fatty acids to stimulate PPARγ, the increased level of FABP5 up-regulated the level of p-PPARγ, which directly or indirectly promoted both level of p-AKT and the activity of NFκB in prostate cancer cells. The up-regulation of p-AKT and activated NFκB led to the reduction of BAX and the subsequent change of the BAX/BCL-2 ratio, suppressed the cleavages of Caspase-9 and Caspase-3 and thus inhibited cellular apoptosis and promoted malignant progression. In contrast, the FABP5 inhibitors SB-FI-26 (147) and dmrFABP5 inhibited the level of p-PPARγ by

cessation of fatty acid stimulation through competitively binding to fatty acids (SB-FI-26) or a possible obstruction of fatty acid delivery (dmrFABP5). Then the reduced level of p-PPARγ triggered the suppression in p-AKT and activity of NFκB and an increase of the ratio of BAX/BCL-2, which increased the levels of cleaved-Caspase-9 and cleaved-Caspase-3 and hence promoted apoptosis and inhibited the malignant progression of the cancer cells.

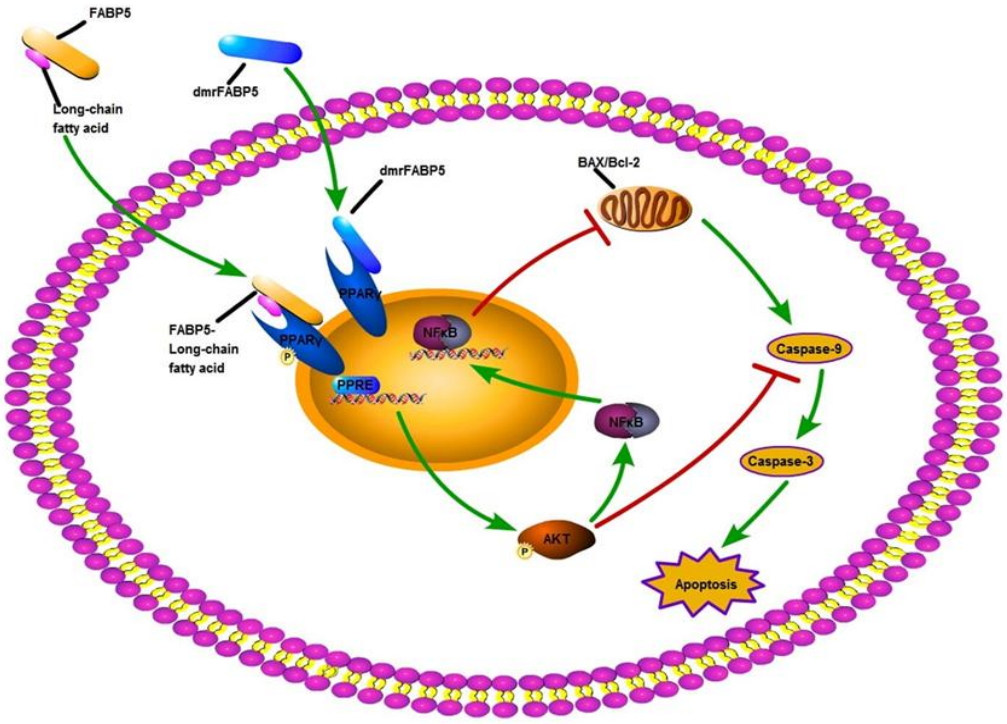

Figure 7.1 Schematic illustration of the possible FABP5-related signaling pathway leading to apoptosis-inhibition and the apoptosis-promoting effect of dmrFABP5 in prostate cancer cells. In untreated prostatic cancer, high level of FABP5 transports a large amount of fatty acids into cells and the excessive amount of fatty acids activate nuclear fatty acid receptor PPARγ by phosphorylation. The p-PPARγ binds to DNA at

peroxisome proliferator response elements (PPREs) and activate the downstream regulatory factors, which may then activate AKT directly or indirectly. The p-AKT can suppress apoptosis by promoting the activity of NF-kB, which can influence the mitochondrial BAX/BCL-2 balance in the way favoring apoptosis-inhibition. The activation of AKT can also lead to a increased cleaved-Caspase-9 level. DmrFABP5 is incapable of binding to fatty acids, but it has a very similar structure to wtrFABP5. DmrFABP5 may bind to PPARγ in the same way as wtrFABP5 to competitively occupy the space without carrying fatty acid, thus dmrFABP5 prevent wtrFABP5 from contacting PPARγ to deliver the fatty acids. This disruption of the fatty acid transportation and stimulation of PPARγ may lead to a cessation of PPARγ activation. The reduced level of p-PPARγ can lead to an increased apoptosis of the cancer cells either by the reduction of the level of p-AKT, which causes the cleavage of Caspase-3 or by the suppression of the NF-kB activity, which can influence the BAX/BCL2 balance and the cleavage of Caspase-3 in the direction favoring apoptosis-promotion.

7.8 Future work

In this work, we detected the changes in apoptosis under the treatments of FABP5 inhibitors in prostate cancer cells and studied some possible mechanisms involved in the apoptosis promotion under the suppression of FABP5 biological function in CRPC. The bio-inhibitor dmrFABP5 suppresses the biological function of FABP5 and works by blocking the fatty-acid stimulation of PPARγ to prevent it from activating the down-stream regulatory cancer-promoting and surviving genes. Since the exact pathway of fatty acid delivery to PPARγ is not clear, how dmrFABP5 inhibits PPARγ is not fully understood. Furthermore, the exact mechanisms of how suppressed p-PPARγ affect AKT activation and the following pathways involved in this apoptosis

promoting effect are not fully studied. Further investigation is needed to understand the detailed molecular mechanisms involved in the suppressive effect of dmrFABP5 on PPARγ activation and the clear apoptosis related (intrinsic and extrinsic) pathways involved in FABP5-apoptosis promoting effect. In addition, further preclinical work on toxicity and pharmacokinetics studies are needed before the true clinical application of FABP5 inhibitors.

References

1. Ferlay J, Soerjomataram I, Dikshit R, Eser S, Mathers C, Rebelo M, et al. Cancer incidence and mortality worldwide: sources, methods and major patterns in GLOBOCAN 2012. International journal of cancer. 2015;136:359-386.

2. ONS. Cancer Registration Statistics, England: 2015. 2017; Available from: https://www.ons.gov.uk/peoplepopulationandcommunity/healthandsocialcare/conditionsanddiseases/bulletins/cancerregistrationstatisticsengland/2015

3. Torre LA, Bray F, Siegel RL, Ferlay J, Lortet‐Tieulent J, Jemal A. Global cancer statistics, 2012. CA: a cancer journal for clinicians. 2015;65:87-108.

4. CRUK. Prostate cancer statistics. 2018 [cited 2018 06]; Available from: http://www.cancerresearchuk.org/health-professional/cancer-statistics/statistics-by-cancer-type/prostate-cancer#heading-Zero

5. Hsing AW, Tsao L, Devesa SS. International trends and patterns of prostate cancer incidence and mortality. International journal of cancer. 2000;85:60-7.

6. Ferlay J, Soerjomataram I, Ervik M, Dikshit R, Eser S, Mathers C, et al. GLOBOCAN 2012 v1. 0, cancer incidence and mortality worldwide: IARC CancerBase no. 11. Lyon: International Agency for Research on Cancer; 2013. 2014.

7. Bray F, Lortet-Tieulent J, Ferlay J, Forman D, Auvinen A. Prostate cancer incidence and mortality trends in 37 European countries: an overview. European journal of cancer. 2010;46:3040-52.

8. CRUK. Prostate cancer incidence statistics. 2018. http://www.cancerresearchuk.org/health-professional/cancer

9. CRUK. Prostate cancer mortality statistics. 2018. http://www.cancerresearchuk.org/health-professional/cancer-statistics/statistics-by-

cancer-type/prostate-cancer/mortality#heading-Zero

10. Brenner H, Stegmaier C, Ziegler H. Long-term survival of cancer patients in Germany achieved by the beginning of the third millenium. Annals of oncology. 2005;16:981-6.

11. Lin DW, Porter M, Montgomery B. Treatment and survival outcomes in young men diagnosed with prostate cancer. Cancer. 2009;115:2863-71.

12. Merrill RM, Bird JS. Effect of young age on prostate cancer survival: a population-based assessment (United States). Cancer Causes & Control. 2002;13:435-43.

13. Lunenfeld B. The ageing male: demographics and challenges. World journal of urology. 2002;20:11-6.

14. Krieger N, Quesenberry C, Peng T, Horn-Ross P, Stewart S, Brown S, et al. Social class, race/ethnicity, and incidence of breast, cervix, colon, lung, and prostate cancer among Asian, Black, Hispanic, and White residents of the San Francisco Bay Area, 1988–92 (United States). Cancer Causes & Control. 1999;10:525-37.

15. Woods VD, Montgomery SB, Belliard JC, Ramírez-Johnson J, Wilson CM. Culture, black men, and prostate cancer: What is reality? Cancer Control. 2004;11:388-96.

16. Baade PD, Youlden DR, Cramb SM, Dunn J, Gardiner RA. Epidemiology of prostate cancer in the Asia-Pacific region. Prostate international. 2013;1:47-58.

17. Goldgar DE, Easton DF, Cannon-Albright LA, Skolnick MH. Systematic population-based assessment of cancer risk in first-degree relatives of cancer probands. JNCI: Journal of the National Cancer Institute. 1994;86:1600-8.

18. Bratt O. Hereditary prostate cancer: clinical aspects. The Journal of urology.

2002;168:906-13.

19. Kalish LA, McDougal WS, McKinlay JB. Family history and the risk of prostate cancer. Urology. 2000;56:803-6.

20. Cerhan JR, Parker AS, Putnam SD, Chiu BC, Lynch CF, Cohen MB, et al. Family history and prostate cancer risk in a population-based cohort of Iowa men. Cancer Epidemiology and Prevention Biomarkers. 1999;8:53-60.

21. Powell IJ. The precise role of ethnicity and family history on aggressive prostate cancer: a review analysis. Archivos espanoles de urologia. 2011;64:711-719.

22. Kiciński M, Vangronsveld J, Nawrot TS. An epidemiological reappraisal of the familial aggregation of prostate cancer: a meta-analysis. PloS one. 2011;6:e27130.

23. Beebe‐Dimmer JL, Yee C, Cote ML, Petrucelli N, Palmer N, Bock C, et al. Familial clustering of breast and prostate cancer and risk of postmenopausal breast cancer in the Women's Health Initiative Study. Cancer. 2015;121:1265-72.

24. Wolk A. Diet, lifestyle and risk of prostate cancer. Acta Oncologica. 2005;44:277-81.

25. Norrish AE, Jackson RT, Sharpe SJ, Skeaff CM. Prostate cancer and dietary carotenoids. American Journal of Epidemiology. 2000;151:119-23.

26. Terry P, Lichtenstein P, Feychting M, Ahlbom A, Wolk A. Fatty fish consumption and risk of prostate cancer. The Lancet. 2001;357:1764-6.

27. Baade PD, Youlden DR, Krnjacki LJ. International epidemiology of prostate cancer: geographical distribution and secular trends. Molecular nutrition & food research. 2009;53:171-84.

28. Whittemore AS, Kolonel LN, Wu AH, John EM, Gallagher RP, Howe GR, et al. Prostate cancer in relation to diet, physical activity, and body size in blacks, whites,

and Asians in the United States and Canada. JNCI: Journal of the National Cancer Institute. 1995;87:652-61.

29. Pelser C, Mondul AM, Hollenbeck AR, Park Y. Dietary fat, fatty acids, and risk of prostate cancer in the NIH-AARP diet and health study. Cancer Epidemiology and Prevention Biomarkers. 2013;22:697-707.

30. Rose DP, Connolly JM. Effects of fatty acids and eicosanoid synthesis inhibitors on the growth of two human prostate cancer cell lines. The Prostate. 1991;18:243-54.

31. Hiatt RA, Armstrong MA, Klatsky AL, Sidney S. Alcohol consumption, smoking, and other risk factors and prostate cancer in a large health plan cohort in California (United States). Cancer Causes & Control. 1994;5:66-72.

32. McNeal JE. The zonal anatomy of the prostate. The prostate. 1981;2:35-49.

33. Labelled HA. Photos Of Male Reproductive System 2016; Available from: http://anatomybody101.org/photos-of-male-reproductive-system/photos-of-male-reproductive-system-male-reproductive-health-urology-promedica/

34. Greene DR, Wheeler TM, Egawa S, Dunn JK, Scardino PT. A comparison of the morphological features of cancer arising in the transition zone and in the peripheral zone of the prostate. The Journal of urology. 1991;146:1069-76.

35. Cohen RJ, Shannon BA, Phillips M, Moorin RE, Wheeler TM, Garrett KL. Central zone carcinoma of the prostate gland: a distinct tumor type with poor prognostic features. The Journal of urology. 2008;179:1762-7.

36. Kayhan A, Fan X, Oommen J, Oto A. Multi-parametric MR imaging of transition zone prostate cancer: imaging features, detection and staging. World journal of radiology. 2010;2:180-187.

37. Wadhera P. An introduction to acinar pressures in BPH and prostate cancer. Nature Reviews Urology. 2013;10:358-366.

38. Hayward SW, Cunha GR. The prostate: development and physiology. Radiologic Clinics. 2000;38:1-14.

39. Mawhinney M, Mariotti A. Physiology, pathology and pharmacology of the male reproductive system. Periodontology 2000. 2013;61:232-51.

40. Humphrey PA. Histological variants of prostatic carcinoma and their significance. Histopathology. 2012;60:59-74.

41. Foster C, Bostwick D, Bonkhoff H, Damber J-E, Van der Kwast T, Montironi R, et al. Cellular and molecular pathology of prostate cancer precursors. Scandinavian Journal of Urology and Nephrology. 2000;34:19-43.

42. MORRISSEY C, FITZPATRICK JM, WATSON RWG. Prostate epithelial cell differentiation and its relevance to the understanding of prostate cancer therapies. Clinical science. 2005;108:1-11.

43. Bonkhoff H, Stein U, Remberger K. The proliferative function of basal cells in the normal and hyperplastic human prostate. The Prostate. 1994;24:114-8.

44. Rizzo S, Attard G, Hudson D. Prostate epithelial stem cells. Cell Proliferation. 2005;38:363-74.

45. Ruscica M, Dozio E, Motta M, Magni P. Role of neuropeptide Y and its receptors in the progression of endocrine-related cancer. Peptides. 2007;28:426-34.

46. Ruscica M, Dozio E, Motta M, Magni P. Relevance of the neuropeptide Y system in the biology of cancer progression. Current topics in medicinal chemistry. 2007;7:1682-91.

47. Elterman DS, Barkin J, Kaplan SA. Optimizing the management of benign

prostatic hyperplasia. Therapeutic advances in urology. 2012;4:77-83.

48. Miah S, Catto J. BPH and prostate cancer risk. Indian journal of urology: IJU: journal of the Urological Society of India. 2014;30:214-218.

49. Sausville J, Naslund M. Benign prostatic hyperplasia and prostate cancer: an overview for primary care physicians. International journal of clinical practice. 2010;64:1740-5.

50. McVary KT. BPH: epidemiology and comorbidities. The American journal of managed care. 2006;12:S122-8.

51. Wise GJ, Ostad E. Hormonal treatment of patients with benign prostatic hyperplasia: pros and cons. Current urology reports. 2001;2:285-91.

52. Djavan B. α1-Adenoceptor Antagonists for the Treatment of Lower Urinary Tract Symptoms Suggestive of Benign Prostatic Hyperplasia (LUTS/BPH): State of the Art. European Urology Supplements. 2004;3:23-30.

53. Bostwick DG, Qian J. High-grade prostatic intraepithelial neoplasia. Modern pathology. 2004;17:360-379.

54. Bostwick DG, Brawer MK. Prostatic intra‐epithelial neoplasia and early invasion in prostate cancer. Cancer. 1987;59:788-94.

55. Zlotta A, Schulman C. Clinical evolution of prostatic intraepithelial neoplasia. European urology. 1999;35:498-503.

56. Sakr W, Grignon D, Crissman J, Heilbrun L, Cassin B, Pontes J, et al. High grade prostatic intraepithelial neoplasia (HGPIN) and prostatic adenocarcinoma between the ages of 20-69: an autopsy study of 249 cases. In Vivo (Athens, Greece). 1994;8:439-43.

57. Cheville JC, Reznicek MJ, Bostwick DG. The focus of “atypical glands,

suspicious for malignancy" in prostatic needle biopsy specimens: incidence, histologic features, and clinical follow-up of cases diagnosed in a community practice. American journal of clinical pathology. 1997;108:633-40.

58. Ayala AG, Ro JY. Prostatic intraepithelial neoplasia: recent advances. Archives of pathology & laboratory medicine. 2007;131:1257-66.

59. Molini é V. Le score de Gleason en 2008. Annales de pathologie; 2008: Elsevier. p. 350-3.

60. Roehrborn CG. Clinical management of lower urinary tract symptoms with combined medical therapy. BJU international. 2008;102:13-7.

61. Humphrey PA. Gleason grading and prognostic factors in carcinoma of the prostate. Modern pathology. 2004;17:292-306.

62. Shah RB. Current perspectives on the Gleason grading of prostate cancer. Archives of pathology & laboratory medicine. 2009;133:1810-6.

63. Epstein JI, Zelefsky MJ, Sjoberg DD, Nelson JB, Egevad L, Magi-Galluzzi C, et al. A contemporary prostate cancer grading system: a validated alternative to the Gleason score. European urology. 2016;69:428-35.

64. Mottet N, Bellmunt J, Bolla M, Briers E, Cumberbatch MG, De Santis M, et al. EAU-ESTRO-SIOG guidelines on prostate cancer. Part 1: screening, diagnosis, and local treatment with curative intent. European urology. 2017;71:618-29.

65. Caram M, Skolarus TA, Cooney KA. Limitations of Prostate-specific Antigen Testing After a Prostate Cancer Diagnosis. 2016, 70: 209-210.

66. Freedland SJ, Humphreys EB, Mangold LA, Eisenberger M, Dorey FJ, Walsh PC, et al. Death in patients with recurrent prostate cancer after radical prostatectomy: prostate-specific antigen doubling time subgroups and their associated contributions

to all-cause mortality. Journal of Clinical Oncology. 2007;25:1765-71.

67. Huggins C, Hodges CV. Studies on prostatic cancer. Cancer Res. 1941;1:293-297.

68. Perlmutter MA, Lepor H. Androgen deprivation therapy in the treatment of advanced prostate cancer. Rev Urol. 2007;9 Suppl 1:S3-S8.

69. Crawford ED, Hou AH. The role of LHRH antagonists in the treatment of prostate cancer. Prostate. 2009;23 (7): 626-30.

70. Loblaw DA, Virgo KS, Nam R, Somerfield MR, Ben-Josef E, Mendelson DS, et al. Initial hormonal management of androgen-sensitive metastatic, recurrent, or progressive prostate cancer: 2006 update of an American Society of Clinical Oncology practice guideline. Journal of Clinical Oncology. 2007;25:1596-605.

71. Chen Y, Clegg NJ, Scher HI. Anti-androgens and androgen-depleting therapies in prostate cancer: new agents for an established target. Lancet Oncol. 2009;10:981-91.

72. Ross RW, Xie W, Regan MM, Pomerantz M, Nakabayashi M, Daskivich TJ, et al. Efficacy of androgen deprivation therapy (ADT) in patients with advanced prostate cancer: association between Gleason score, prostate‐specific antigen level, and prior ADT exposure with duration of ADT effect. Cancer: Interdisciplinary International Journal of the American Cancer Society. 2008;112:1247-53.

73. Waltering KK, Urbanucci A, Visakorpi T. Androgen receptor (AR) aberrations in castration-resistant prostate cancer. Molecular and cellular endocrinology. 2012;360:38-43.

74. Cussenot O, Berthon P, Berger R, Mowszowicz I, Faille A, Hojman F, et al. Immortalization of human adult normal prostatic epithelial cells by liposomes

containing large T-SV40 gene. The Journal of urology. 1991;146:881-6.

75. BERTHON P, CUSSENOT O, HOPWOOD L, LEDUC A, MAITLAND NJ. Functional expression of sv40 in normal human prostatic epithelial and fibroblastic cells-differentiation pattern of nontumorigenic cell-lines. International journal of oncology. 1995;6:333-43.

76. Sobel R, Sadar M. Cell lines used in prostate cancer research: a compendium of old and new lines—part 1. The Journal of urology. 2005;173:342-59.

77. Horoszewicz JS, Leong SS, Kawinski E, Karr JP, Rosenthal H, Chu TM, et al. LNCaP model of human prostatic carcinoma. Cancer research. 1983;43:1809-18.

78. Sramkoski RM, Pretlow TG, Giaconia JM, Pretlow TP, Schwartz S, Sy M-S, et al. A new human prostate carcinoma cell line, 22Rv1. In Vitro Cellular & Developmental Biology-Animal. 1999;35:403-9.

79. Hartel A, Didier A, Pfaffl M, Meyer HH. Characterisation of gene expression patterns in 22RV1 cells for determination of environmental androgenic/antiandrogenic compounds. The Journal of steroid biochemistry and molecular biology. 2003;84:231-8.

80. van Bokhoven A, Varella‐Garcia M, Korch C, Johannes WU, Smith EE, Miller HL, et al. Molecular characterization of human prostate carcinoma cell lines. The Prostate. 2003;57:205-25.

81. Stone KR, Mickey DD, Wunderli H, Mickey GH, Paulson DF. Isolation of a human prostate carcinoma cell line (DU 145). International journal of cancer. 1978;21:274-81.

82. Kaighn M, Narayan KS, Ohnuki Y, Lechner J, Jones L. Establishment and characterization of a human prostatic carcinoma cell line (PC-3). Investigative

urology. 1979;17:16-23.

83. Kozlowski JM, Fidler IJ, Campbell D, Xu Z-l, Kaighn ME, Hart IR. Metastatic behavior of human tumor cell lines grown in the nude mouse. Cancer research. 1984;44:3522-9.

84. Stanbrough M, Leav I, Kwan PW, Bubley GJ, Balk SP. Prostatic intraepithelial neoplasia in mice expressing an androgen receptor transgene in prostate epithelium. Proceedings of the National Academy of Sciences. 2001;98:10823-8.

85. Taplin ME, Ho S-M. The endocrinology of prostate cancer. The Journal of Clinical Endocrinology & Metabolism. 2001;86:3467-77.

86. Attar RM, Takimoto CH, Gottardis MM. Castration-resistant prostate cancer: locking up the molecular escape routes. Clinical Cancer Research. 2009;15:3251-5.

87. Heinlein CA, Chang C. Androgen receptor in prostate cancer. Endocrine reviews. 2004;25:276-308.

88. Heinlein CA, Chang C. Androgen receptor (AR) coregulators: an overview. Endocrine reviews. 2002;23:175-200.

89. Buchanan G, Irvine RA, Coetzee GA, Tilley WD. Contribution of the androgen receptor to prostate cancer predisposition and progression. Prostate Cancer: New Horizons in Research and Treatment: Springer; 2002. p. 71-87.

90. Balk SP, Knudsen KE. AR, the cell cycle, and prostate cancer. Nuclear receptor signaling. 2008;6:nrs. 06001.

91. Jenster G. The role of the androgen receptor in the development and progression of prostate cancer. Seminars in oncology; 1999. p. 407-21.

92. Knudsen KE, Penning TM. Partners in crime: deregulation of AR activity and androgen synthesis in prostate cancer. Trends in Endocrinology & Metabolism.

2010;21:315-24.

93. Magnan S, Zarychanski R, Pilote L, Bernier L, Shemilt M, Vigneault E, et al. Intermittent vs continuous androgen deprivation therapy for prostate cancer: a systematic review and meta-analysis. JAMA oncology. 2015;1:1261-9.

94. Miyamoto H, Messing EM, Chang C. Androgen deprivation therapy for prostate cancer: current status and future prospects. The Prostate. 2004;61:332-53.

95. Taplin M-E, Rajeshkumar B, Halabi S, Werner CP, Woda BA, Picus J, et al. Androgen receptor mutations in androgen-independent prostate cancer: Cancer and Leukemia Group B Study 9663. Journal of clinical oncology. 2003;21:2673-8.

96. Tran C, Ouk S, Clegg NJ, Chen Y, Watson PA, Arora V, et al. Development of a second-generation antiandrogen for treatment of advanced prostate cancer. Science. 2009;324:787-90.

97. Robinson D, Van Allen EM, Wu Y-M, Schultz N, Lonigro RJ, Mosquera J-M, et al. Integrative clinical genomics of advanced prostate cancer. Cell. 2015;161:1215-28.

98. Kuiper G, Faber P, Van Rooij H, Van der Korput J, Ris-Stalpers C, Klaassen P, et al. Structural organization of the human androgen receptor gene. Journal of Molecular Endocrinology. 1989;2:R1-R4.

99. Attard G, Swennenhuis JF, Olmos D, Reid AH, Vickers E, A'Hern R, et al. Characterization of ERG, AR and PTEN gene status in circulating tumor cells from patients with castration-resistant prostate cancer. Cancer research. 2009;69:2912-8.

100. Griffiths K. The regulation of prostatic growth. Molecular Biology of Prostate Cancer. 1998:9-21.

101. Harris WP, Mostaghel EA, Nelson PS, Montgomery B. Androgen deprivation

therapy: progress in understanding mechanisms of resistance and optimizing androgen depletion. Nature Reviews Urology. 2009;6:76-85.

102. Tsao CK, Galsky MD, Small AC, Yee T, Oh WK. Targeting the androgen receptor signalling axis in castration‐resistant prostate cancer (CRPC). BJU international. 2012;110:1580-8.

103. McDonnel TJ, Navone NM, Troncoso P, Pisters LL, Conti C, von Eschenbach AC, et al. Expression of bcl-2 oncoprotein and p53 protein accumulation in bone marrow metastases of androgen independent prostate cancer. The Journal of urology. 1997;157:569-74.

104. Gleave M, Tolcher A, Miyake H, Nelson C, Brown B, Beraldi E, et al. Progression to androgen independence is delayed by adjuvant treatment with antisense Bcl-2 oligodeoxynucleotides after castration in the LNCaP prostate tumor model. Clinical Cancer Research. 1999;5:2891-8.

105. Cohen MB, Rokhlin OW. Mechanisms of prostate cancer cell survival after inhibition of AR expression. Journal of cellular biochemistry. 2009;106:363-71.

106. Bitting RL, Armstrong AJ. Targeting the PI3K/Akt/mTOR pathway in castration-resistant prostate cancer. Endocrine-related cancer. 2013;20:R83-R99.

107. Bao Z, Malki MI, Forootan SS, Adamson J, Forootan FS, Chen D, et al. A Novel Cutaneous Fatty Acid–Binding Protein-Related Signaling Pathway Leading to Malignant Progression in Prostate Cancer Cells. Genes & cancer. 2013;4:297-314.

108. Randle P, Garland P, Hales C, Newsholme E. The glucose fatty-acid cycle its role in insulin sensitivity and the metabolic disturbances of diabetes mellitus. The Lancet. 1963;281:785-9.

109. Furuhashi M, Hotamisligil GS. Fatty acid-binding proteins: role in metabolic

diseases and potential as drug targets. Nature reviews Drug discovery. 2008;7:489-503.

110. Di Sebastiano K, Mourtzakis M. The role of dietary fat throughout the prostate cancer trajectory. Nutrients. 2014;6:6095-109.

111. McArthur MJ, Atshaves BP, Frolov A, Foxworth WD, Kier AB, Schroeder F. Cellular uptake and intracellular trafficking of long chain fatty acids. Journal of lipid research. 1999;40:1371-83.

112. Berg JM, Tymoczko JL, Stryer L. Biochemistry, ; W. H. Freeman: New York; 2002.

113. Chmurzyńska A. The multigene family of fatty acid-binding proteins (FABPs): function, structure and polymorphism. Journal of applied genetics. 2006;47:39-48.

114. Ockner RK, Manning JA, Poppenhausen RB, Ho WK. A binding protein for fatty acids in cytosol of intestinal mucosa, liver, myocardium, and other tissues. Science. 1972;177:56-8.

115. Smathers RL, Petersen DR. The human fatty acid-binding protein family: evolutionary divergences and functions. Human genomics. 2011;5:170-191.

116. Haunerland NH, Spener F. Fatty acid-binding proteins–insights from genetic manipulations. Progress in lipid research. 2004;43:328-49.

117. Crovetto CA, Córdoba OL. Structural and biochemical characterization and evolutionary relationships of the fatty acid-binding protein 10 (Fabp10) of hake (Merluccius hubbsi). Fish physiology and biochemistry. 2016;42:149-65.

118. Storch J, Thumser AE. The fatty acid transport function of fatty acid-binding proteins. Biochimica et Biophysica Acta (BBA)-Molecular and Cell Biology of Lipids. 2000;1486:28-44.

119. Storch J, McDermott L. Structural and functional analysis of fatty acid-binding proteins. Journal of lipid research. 2009;50:S126-S31.

120. Schachtrup C, Emmler T, Bleck B, Sandqvist A, Spener F. Functional analysis of peroxisome-proliferator-responsive element motifs in genes of fatty acid-binding proteins. Biochemical journal. 2004;382:239-45.

121. Tan N-S, Shaw NS, Vinckenbosch N, Liu P, Yasmin R, Desvergne B, et al. Selective cooperation between fatty acid binding proteins and peroxisome proliferator-activated receptors in regulating transcription. Molecular and cellular biology. 2002;22:5114-27.

122. Michalik L, Wahli W. PPARs mediate lipid signaling in inflammation and cancer. PPAR research. 2008;2008.

123. Forootan FS, Forootan SS, Malki MI, Chen D, Li G, Lin K, et al. The expression of C-FABP and PPARγ and their prognostic significance in prostate cancer. International journal of oncology. 2014;44:265-75.

124. Zimmerman A, Veerkamp J. New insights into the structure and function of fatty acid-binding proteins. Cellular and Molecular Life Sciences CMLS. 2002;59:1096-116.

125. Balendiran GK, Schnütgen F, Scapin G, Börchers T, Xhong N, Lim K, et al. Crystal structure and thermodynamic analysis of human brain fatty acid-binding protein. Journal of Biological Chemistry. 2000;275:27045-54.

126. Coe NR, Bernlohr DA. Physiological properties and functions of intracellular fatty acid-binding proteins. Biochimica et Biophysica Acta (BBA)-Lipids and Lipid Metabolism. 1998;1391:287-306.

127. Madsen P, Rasmussen HH, Leffers H, Honore B, Celis JE. Molecular cloning

and expression of a novel keratinocyte protein (psoriasis-associated fatty acid-binding protein [PA-FABP]) that is highly up-regulated in psoriatic skin and that shares similarity to fatty acid-binding proteins. The Journal of investigative dermatology. 1992;99:299-305.

128. Masouyé I, Saurat J-H, Siegenthaler G. Epidermal fatty-acid-binding protein in psoriasis, basal and squamous cell carcinomas: an immunohistological study. Dermatology. 1996;192:208-13.

129. Morgan EA, Forootan SS, Adamson J, Foster CS, Fujii H, Igarashi M, et al. Expression of cutaneous fatty acid-binding protein (C-FABP) in prostate cancer: potential prognostic marker and target for tumourigenicity-suppression. International journal of oncology. 2008;32:767-75.

130. Kawaguchi K, Kinameri A, Suzuki S, Senga S, Ke Y, Fujii H. The cancer-promoting gene fatty acid-binding protein 5 (FABP5) is epigenetically regulated during human prostate carcinogenesis. Biochemical Journal. 2016;473:449-61.

131. Jing C, Beesley C, Foster CS, Chen H, Rudland PS, West DC, et al. Human cutaneous fatty acid-binding protein induces metastasis by up-regulating the expression of vascular endothelial growth factor gene in rat Rama 37 model cells. Cancer research. 2001;61:4357-64.

132. Suojalehto H, Kinaret P, Kilpeläinen M, Toskala E, Ahonen N, Wolff H, et al. Level of fatty acid binding protein 5 (FABP5) is increased in sputum of allergic asthmatics and links to airway remodeling and inflammation. PloS one. 2015;10:e0127003.

133. Hu Z, Fan C, Livasy C, He X, Oh DS, Ewend MG, et al. A compact VEGF signature associated with distant metastases and poor outcomes. BMC medicine.

2009;7:9-23.

134. Forootan SS, Bao ZZ, Forootan FS, Kamalian L, Zhang Y, Bee A, et al. Atelocollagen-delivered siRNA targeting the FABP5 gene as an experimental therapy for prostate cancer in mouse xenografts. International journal of oncology. 2010;36:69-76.

135. Forootan FS, Forootan SS, Gou X, Yang J, Liu B, Chen D, et al. Fatty acid activated PPARγ promotes tumorigenicity of prostate cancer cells by up regulating VEGF via PPAR responsive elements of the promoter. Oncotarget. 2016;7:9322-9339.

136. Fang LY, Wong TY, Chiang WF, Chen YL. Fatty‐acid‐binding protein 5 promotes cell proliferation and invasion in oral squamous cell carcinoma. Journal of oral pathology & medicine. 2010;39:342-8.

137. Morgan E, Kannan-Thulasiraman P, Noy N. Involvement of fatty acid binding protein 5 and PPAR/in prostate cancer cell growth. PPAR research. 2010;2010.

138. Núñez NP, Liu H, Meadows GG. PPAR-γ ligands and amino acid deprivation promote apoptosis of melanoma, prostate, and breast cancer cells. Cancer letters. 2006;236:133-41.

139. Segawa Y, Yoshimura R, Hase T, Nakatani T, Wada S, Kawahito Y, et al. Expression of peroxisome proliferator‐activated receptor (PPAR) in human prostate cancer. The Prostate. 2002;51:108-16.

140. Nwankwo J, Robbins M. Peroxisome proliferator-activated receptor-γ expression in human malignant and normal brain, breast and prostate-derived cells. Prostaglandins, Leukotrienes and Essential Fatty Acids (PLEFA). 2001;64:241-5.

141. Chaffer CL, Thomas DM, Thompson EW, Williams ED. PPARγ-independent induction of growth arrest and apoptosis in prostate and bladder carcinoma. BMC

cancer. 2006;6:53-66.

142. Wolfrum C, Borrmann CM, Börchers T, Spener F. Fatty acids and hypolipidemic drugs regulate peroxisome proliferator-activated receptors α-and γ-mediated gene expression via liver fatty acid binding protein: a signaling path to the nucleus. Proceedings of the National Academy of Sciences. 2001;98:2323-8.

143. Kliewer SA, Umesono K, Noonan DJ, Heyman RA, Evans RM. Convergence of 9-cis retinoic acid and peroxisome proliferator signalling pathways through heterodimer formation of their receptors. Nature. 1992;358:771-774.

144. Seargent JM, Yates EA, Gill JH. GW9662, a potent antagonist of PPARγ, inhibits growth of breast tumour cells and promotes the anticancer effects of the PPARγ agonist rosiglitazone, independently of PPARγ activation. British journal of pharmacology. 2004;143:933-7.

145. Nakamura M, Chi Y-M, Yan W-M, Nakasugi Y, Yoshizawa T, Irino N, et al. Strong Antinociceptive Effect of Incarvillateine, a Novel Monoterpene Alkaloid from Incarvillea s inensis. Journal of natural products. 1999;62:1293-4.

146. Wang M-L, Yu G, Yi S-P, Zhang F-Y, Wang Z-T, Huang B, et al. Antinociceptive effects of incarvillateine, a monoterpene alkaloid from Incarvillea sinensis, and possible involvement of the adenosine system. Scientific reports. 2015;5:16107-16118.

147. Al-Jameel W, Gou X, Forootan SS, Al Fayi MS, Rudland PS, Forootan FS, et al. Inhibitor SBFI26 suppresses the malignant progression of castration-resistant PC3-M cells by competitively binding to oncogenic FABP5. Oncotarget. 2017;8:31041-31056.

148. Balcom E, Liu R-Z, Poon S, Godbout R. FABP5 (fatty acid binding protein 5

(psoriasis-associated)). Atlas of Genetics and Cytogenetics in Oncology and Haematology. 2015.

149. Hohoff C, Börchers T, Rüstow B, Spener F, van Tilbeurgh H. Expression, purification, and crystal structure determination of recombinant human epidermal-type fatty acid binding protein. Biochemistry. 1999;38:12229-39.

150. Al-Jameel W, Gou XJ, Jin X, Zhang J, Wei Q, Ai J, et al. Inactivated FABP5 suppresses malignant progression of prostate cancer cells through inhinbiting the activation of nuclear fatty acid receptor PPARγ by wild type FABP5. Int J Cancer. 2018;in the process of review.

151. Green DR, Kroemer G. The pathophysiology of mitochondrial cell death. science. 2004;305:626-9.

152. Caltabiano R, Leonardi R, Musumeci G, Bartoloni G, Rusu MC, Almeida LE, et al. Apoptosis in temporomandibular joint disc with internal derangement involves mitochondrial-dependent pathways. An in vivo study. Acta Odontologica Scandinavica. 2013;71:577-83.

153. Galluzzi L, Vitale I, Abrams J, Alnemri E, Baehrecke E, Blagosklonny M, et al. Molecular definitions of cell death subroutines: recommendations of the Nomenclature Committee on Cell Death 2012. Cell death and differentiation. 2012;19:107-120.

154. Loreto C, La Rocca G, Anzalone R, Caltabiano R, Vespasiani G, Castorina S, et al. The role of intrinsic pathway in apoptosis activation and progression in Peyronie's disease. BioMed research international. 2014;2014.

155. Al-Jameel WH. FABP5-Related Signalling Pathway used as Therapeutic Target for Castration-Resistance Prostate Cancer: University of Liverpool; 2017.

156. Kruger NJ. The Bradford method for protein quantitation. The protein protocols handbook: Springer; 2009. p. 17-24.

157. Schroeder F, Petrescu AD, Huang H, Atshaves BP, McIntosh AL, Martin GG, et al. Role of fatty acid binding proteins and long chain fatty acids in modulating nuclear receptors and gene transcription. Lipids. 2008;43:1-17.

158. Chandra V, Huang P, Hamuro Y, Raghuram S, Wang Y, Burris TP, et al. Structure of the intact PPAR-γ–RXR-α nuclear receptor complex on DNA. Nature. 2008;456:350-356.

159. Subbarayan V, Sabichi AL, Kim J, Llansa N, Logothetis CJ, Lippman SM, et al. Differential peroxisome proliferator-activated receptor-γ isoform expression and agonist effects in normal and malignant prostate cells. Cancer Epidemiology and Prevention Biomarkers. 2004;13:1710-6.

160. Elix C, Pal SK, Jones JO. The role of peroxisome proliferator-activated receptor gamma in prostate cancer. Asian J Androl. 2018;20:238-43.

161. Ahmad I, Mui E, Galbraith L, Patel R, Tan EH, Salji M, et al. Sleeping beauty screen reveals PPARg activation in metastatic prostate cancer. Proceedings of the National Academy of Sciences of the United States of America. 2016;113:8290-5.

162. Al-Jameel W, Gou X, Forootan SS, Al Fayi MS, Rudland PS, Forootan FS, et al. Inhibitor SBFI26 suppresses the malignant progression of castration-resistant PC3-M cells by competitively binding to oncogenic FABP5. Oncotarget. 2017;8:31041-56.

163. Bao Z, Malki MI, Forootan SS, Adamson J, Forootan FS, Chen D, et al. A novel cutaneous Fatty Acid-binding protein-related signaling pathway leading to malignant progression in prostate cancer cells. Genes Cancer. 2013;4:297-314.

164. Reed JC. Apoptosis-targeted therapies for cancer. Cancer cell. 2003;3:17-22.

165. Takahashi N, Okumura T, Motomura W, Fujimoto Y, Kawabata I, Kohgo Y. Activation of PPARγ inhibits cell growth and induces apoptosis in human gastric cancer cells. Febs Letters. 1999;455:135-9.

166. Kulkarni AA, Thatcher TH, Olsen KC, Maggirwar SB, Phipps RP, Sime PJ. PPAR-γ ligands repress TGFβ-induced myofibroblast differentiation by targeting the PI3K/Akt pathway: implications for therapy of fibrosis. PloS one. 2011;6:e15909.

167. Shiau C-W, Yang C-C, Kulp SK, Chen K-F, Chen C-S, Huang J-W, et al. Thiazolidenediones mediate apoptosis in prostate cancer cells in part through inhibition of Bcl-xL/Bcl-2 functions independently of PPARγ. Cancer research. 2005;65:1561-9.

168. Amaravadi R, Thompson CB. The survival kinases Akt and Pim as potential pharmacological targets. The Journal of clinical investigation. 2005;115:2618-24.

169. Sakamoto S, Kyprianou N. Targeting anoikis resistance in prostate cancer metastasis. Molecular aspects of medicine. 2010;31:205-14.

170. Franke TF, Yang S-I, Chan TO, Datta K, Kazlauskas A, Morrison DK, et al. The protein kinase encoded by the Akt proto-oncogene is a target of the PDGF-activated phosphatidylinositol 3-kinase. Cell. 1995;81:727-36.

171. Okano J-i, Gaslightwala I, Birnbaum MJ, Rustgi AK, Nakagawa H. Akt/protein kinase B isoforms are differentially regulated by epidermal growth factor stimulation. Journal of Biological Chemistry. 2000;275:30934-42.

172. Vivanco I, Sawyers CL. The phosphatidylinositol 3-kinase–AKT pathway in human cancer. Nature Reviews Cancer. 2002;2:489-501.

173. Alessi DR, Andjelkovic M, Caudwell B, Cron P, Morrice N, Cohen P, et al. Mechanism of activation of protein kinase B by insulin and IGF‐1. The EMBO

journal. 1996;15:6541-51.

174. del Peso L, González-García M, Page C, Herrera R, Nuñez G. Interleukin-3-induced phosphorylation of BAD through the protein kinase Akt. Science. 1997;278:687-9.

175. Datta SR, Dudek H, Tao X, Masters S, Fu H, Gotoh Y, et al. Akt phosphorylation of BAD couples survival signals to the cell-intrinsic death machinery. Cell. 1997;91:231-41.

176. Cardone MH, Roy N, Stennicke HR, Salvesen GS, Franke TF, Stanbridge E, et al. Regulation of cell death protease caspase-9 by phosphorylation. Science. 1998;282:1318-21.

177. Baldwin Jr AS. The NF-κB and IκB proteins: new discoveries and insights. Annual review of immunology. 1996;14:649-81.

178. Karin M, Ben-Neriah Y. Phosphorylation meets ubiquitination: the control of NF-κB activity. Annual review of immunology. 2000;18:621-63.

179. Gilmore TD. Introduction to NF-κB: players, pathways, perspectives. Oncogene. 2006;25:6680-6684.

180. Suh J, Payvandi F, Edelstein LC, Amenta PS, Zong WX, Gélinas C, et al. Mechanisms of constitutive NF‐κB activation in human prostate cancer cells. The Prostate. 2002;52:183-200.

181. Madrid LV, Mayo MW, Reuther JY, Baldwin AS. Akt stimulates the transactivation potential of the RelA/p65 subunit of NF-κB through utilization of the IκB kinase and activation of the mitogen activated protein kinase p38. Journal of Biological Chemistry. 2001.

182. May MJ, Ghosh S. Signal transduction through NF-κB. Immunology today.

1998;19:80-8.

183. Viatour P, Merville M-P, Bours V, Chariot A. Phosphorylation of NF-κB and IκB proteins: implications in cancer and inflammation. Trends in biochemical sciences. 2005;30:43-52.

184. Amiri KI, Richmond A. Role of nuclear factor-κ B in melanoma. Cancer and Metastasis Reviews. 2005;24:301-13.

185. Pomerantz JL, Baltimore D. Two pathways to NF-κB. Molecular cell. 2002;10:693-5.

186. Matsuzaki H, Tamatani M, Mitsuda N, Namikawa K, Kiyama H, Miyake S-i, et al. Activation of Akt kinase inhibits apoptosis and changes in Bcl-2 and Bax expression induced by nitric oxide in primary hippocampal neurons. Journal of neurochemistry. 1999;73:2037-46.

187. Shankar S, Srivastava RK. Involvement of Bcl-2 family members, phosphatidylinositol 3'-kinase/AKT and mitochondrial p53 in curcumin (diferulolylmethane)-induced apoptosis in prostate cancer. International journal of oncology. 2007;30:905-18.

188. Davies MA, Koul D, Dhesi H, Berman R, McDonnell TJ, McConkey D, et al. Regulation of Akt/PKB activity, cellular growth, and apoptosis in prostate carcinoma cells by MMAC/PTEN. Cancer Research. 1999;59:2551-6.

189. Thornberry NA, Lazebnik Y. Caspases: enemies within. Science. 1998;281:1312-6.

190. Cohen GM. Caspases: the executioners of apoptosis. Biochemical Journal. 1997;326:1-16.

191. Adams JM, Cory S. The Bcl-2 protein family: arbiters of cell survival. Science.

1998;281:1322-6.

192. Hockenbery DM, Oltvai ZN, Yin X-M, Milliman CL, Korsmeyer SJ. Bcl-2 functions in an antioxidant pathway to prevent apoptosis. Cell. 1993;75:241-51.

193. Revelos K, Petraki C, Gregorakis A, Scorilas A, Papanastasiou P, Koutsilieris M. Immunohistochemical expression of Bcl2 is an independent predictor of time-to-biochemical failure in patients with clinically localized prostate cancer following radical prostatectomy. Anticancer Res. 2005;25:3123-33.

194. Catz S, Johnson J. BCL-2 in prostate cancer: a minireview. Apoptosis. 2003;8:29-37.

195. Aziz MH, Nihal M, Fu VX, Jarrard DF, Ahmad N. Resveratrol-caused apoptosis of human prostate carcinoma LNCaP cells is mediated via modulation of phosphatidylinositol 3′-kinase/Akt pathway and Bcl-2 family proteins. Molecular cancer therapeutics. 2006;5:1335-41.

196. Cardone MH, Roy N, Stennicke HR, Salvesen GS, Franke TF, Stanbridge E, et al. Regulation of cell death protease caspase-9 by phosphorylation. Science. 1998;282:1318-21.

197. Chen GG, Lee JF, Wang SH, Chan UP, Ip PC, Lau WY. Apoptosis induced by activation of peroxisome-proliferator activated receptor-gamma is associated with Bcl-2 and Nf-kB in human colon cancer. Life sciences. 2002;70:2631-46.

198. Gupta S, Afaq F, Mukhtar H. Involvement of nuclear factor-kappa B, Bax and Bcl-2 in induction of cell cycle arrest and apoptosis by apigenin in human prostate carcinoma cells. Oncogene. 2002;21:3727-3738.

199. Wang Y-B, Qin J, Zheng X-Y, Bai Y, Yang K, Xie L-P. Diallyl trisulfide induces Bcl-2 and caspase-3-dependent apoptosis via downregulation of Akt

phosphorylation in human T24 bladder cancer cells. Phytomedicine. 2010;17:363-8.

200. Sinha S, Pal BC, Jagadeesh S, Banerjee PP, Bandyopadhaya A, Bhattacharya S. Mahanine inhibits growth and induces apoptosis in prostate cancer cells through the deactivation of Akt and activation of caspases. The Prostate. 2006;66:1257-65.

201. Yoo HG, Jung SN, Hwang YS, Park JS, Kim MH, Jeong M, et al. Involvement of NF-κB and caspases in silibinin-induced apoptosis of endothelial cells. International journal of molecular medicine. 2004;13:81-6.

202. Salakou S, Kardamakis D, Tsamandas AC, Zolota V, Apostolakis E, Tzelepi V, et al. Increased Bax/Bcl-2 ratio up-regulates caspase-3 and increases apoptosis in the thymus of patients with myasthenia gravis. In vivo. 2007;21:123-32.

203. Oltval ZN, Milliman CL, Korsmeyer SJ. Bcl-2 heterodimerizes in vivo with a conserved homolog, Bax, that accelerates programed cell death. cell. 1993;74:609-19.

204. Korsmeyer SJ, Shutter JR, Veis DJ, Merry DE, Oltvai ZN. Bcl-2/Bax: a rheostat that regulates an anti-oxidant pathway and cell death. Seminars in cancer biology; 1993. p. 327-32.

205. Cheng EH-Y, Kirsch DG, Clem RJ, Ravi R, Kastan MB, Bedi A, et al. Conversion of Bcl-2 to a Bax-like death effector by caspases. Science. 1997;278:1966-8.

206. Rossé T, Olivier R, Monney L, Rager M, Conus S, Fellay I, et al. Bcl-2 prolongs cell survival after Bax-induced release of cytochrome c. Nature. 1998;391:496-499.

207. Kirsch DG, Doseff A, Chau BN, Lim D-S, de Souza-Pinto NC, Hansford R, et al. Caspase-3-dependent cleavage of Bcl-2 promotes release of cytochrome c. Journal of Biological Chemistry. 1999;274:21155-61.

208. Huggins C, Stevens R, Hodges CV. Studies on prostatic cancer: II. The effects of castration on advanced carcinoma of the prostate gland. Archives of surgery. 1941;43:209-23.

209. Sharifi N, Gulley JL, Dahut WL. Androgen deprivation therapy for prostate cancer. Jama. 2005;294:238-44.

210. Chen Y, Clegg NJ, Scher HI. Anti-androgens and androgen-depleting therapies in prostate cancer: new agents for an established target. The lancet oncology. 2009;10:981-91.

211. Grasso CS, Wu Y-M, Robinson DR, Cao X, Dhanasekaran SM, Khan AP, et al. The mutational landscape of lethal castration-resistant prostate cancer. Nature. 2012;487:239-243.

212. Currie E, Schulze A, Zechner R, Walther TC, Farese Jr RV. Cellular fatty acid metabolism and cancer. Cell metabolism. 2013;18:153-61.

213. Pascual G, Avgustinova A, Mejetta S, Mart ń M, Castellanos A, Attolini CS-O, et al. Targeting metastasis-initiating cells through the fatty acid receptor CD36. Nature. 2017;541:41-45.

214. Adamson J, Morgan EA, Beesley C, Mei Y, Foster CS, Fujii H, et al. High-level expression of cutaneous fatty acid-binding protein in prostatic carcinomas and its effect on tumorigenicity. Oncogene. 2003;22:2739-2749.

215. Hertzel AV, Bernlohr DA. The mammalian fatty acid-binding protein multigene family: molecular and genetic insights into function. Trends in Endocrinology & Metabolism. 2000;11:175-80.

216. Schoonjans K, Staels B, Auwerx J. Role of the peroxisome proliferator-activated receptor (PPAR) in mediating the effects of fibrates and fatty acids on gene

expression. Journal of lipid research. 1996;37:907-25.

217. Papadopoulou N, Charalampopoulos I, Anagnostopoulou V, Konstantinidis G, Föller M, Gravanis A, et al. Membrane androgen receptor activation triggers down-regulation of PI-3K/Akt/NF-kappaB activity and induces apoptotic responses via Bad, FasL and caspase-3 in DU145 prostate cancer cells. Molecular cancer. 2008;7:88-101.

218. Misra UK, Deedwania R, Pizzo SV. Activation and cross-talk between Akt, NF-κB, and unfolded protein response signaling in 1-LN prostate cancer cells consequent to ligation of cell surface-associated GRP78. Journal of Biological Chemistry. 2006;281:13694-707.

219. Deep G, Gangar SC, Oberlies NH, Kroll DJ, Agarwal R. Isosilybin A induces apoptosis in human prostate cancer cells via targeting Akt, NF‐κB, and androgen receptor signaling. Molecular carcinogenesis. 2010;49:902-12.

Appendixes

8.1. Equipments

AccuWeigh, WA, USA

Portable Lab Scale

Bandelin, Germany

Sonicator

BD) FACSCanto , UK

FACSCanto II Flow Cytometer

BD Microlance 3, Ireland

Needle

Syringes

BD Plastics, Sunderland, UK

Syringes

Beckman coulter, UK

Microcentrifuge

Becton Dikinson, USA

Falcon 2059 tube

Berthold detection system, Germany

Sirius Luminometer

BioTek, USA

Multiskan MS (plate reader)

Borolabs, Basingstoke, UK

CO2 incubator Model TC2323

Jenway, Genova, UK

Spectrophotometer

Generier bio-one, UK

Tissue culture pipettes (5-50 ml) Universal tube

Grant Instruments, UK

H2O bath

Leica, Germany

Superior Adhesive slide

Leitz Labovert, Luton, UK

Light microscope

Merck Millipore, UK

Immobilon, Transfer membrane

Merck Millipore, UK

D-Tube dialyzer

Nalgene, UK

Cryobox DNA

New Brunswick Scientific, USA

CO2 Shaking incubator

Nunc, Denmark

Cell culture filter cap flasks

Cell culture plates

Cryogenic vial

QIAGEN, Crawley, UK

Qiagen tip

QIA Shredder spin column

SLS Ltd., Nottingham, UK

Haemocytometer

Magnificent stirrer

Starlab, Milton Keynes, UK

Microtubes

Pipette tips

Surgipath, UK

Microslide

Tissue cassette

Whatman, England, UK

Whatman filter paper

Weber scientific International, NJ, USA

Haemocytometer slide

8.2. Reagents

8.2.1. Reagents for general molecular biology

Absolute ethanol	BDH, England, UK
Ampicillin	Invitrogen, CA, USA
Agarose	Genflow, Fradley, UK
Bromophenol blue	Sigma, USA
DH5α *E. coli* bacteria	Invitrogen, CA, USA
DNA marker III	Roche, England, UK
E. coli DH5α cells	InvivoGen, USA

Glucose	Sigma, USA
Glycerol	Sigma, USA
IPTG	Sigma, USA
Isopropanol	BDH, England, UK
LB agar	Sigma, USA
LB broth	Sigma, USA
Ligation enzyme buffer	New England BioLabs
Magnesium chloride	Sigma, USA
Magnesium sulphate	Sigma, USA

MOPS	Sigma, USA
pBluescript II SK vector	InvivoGen, USA
Potassium acetate	Sigma, USA
Potassium chloride	Sigma, USA
pQE-32 vector	InvivoGen, USA
QIAGEN Ni-NTA Fast Start Kit	QIAGEN, CA, USA
QIAGEN Plasmid mini-preparation kit	QIAGEN, CA, USA
Restriction enzyme buffers	New England BioLabs

Restriction enzymes	New England BioLabs
SDS	Sigma, USA
T4 DNA ligase	New England BioLabs
Tryptone	Sigma, USA
Wizard DNA Clean-Up System	Promega, WI, USA
Xylene	GENTA, Tockwith, UK
Yeast extract	Fisher scientific, Loughborough, UK

8.2.2. Reagents for cell culture

DMSO	Sigma, USA

Fetal calf serum	Biosera, East Sussex, UK
L-Glutamine	Lonza, Belgium
Penicillin/Streptomycin	Lonza, Belgium
Phosphate buffered saline	Gibco, Invitrogen, Paisley, UK
RPMI 1640	Gibco, Invitrogen, Paisley, UK
Trypsin	Gibco, Invitrogen, Paisley, UK
Versene	Gibco, Invitrogen, Paisley, UK

8.2.3. Reagents for western blot

Mini-PROTEAN® TGX Stain-Free™ Precast Gels	Bio-Rad GmbH, Munchen, Germany
Bradford reagent	Sigma, USA
CelLytic-M	Sigma, USA
Commassie brilliant blue	Bio-Rad GmbH, Munchen, Germany
Immobilon ECL Ultra Western HRP substrate	Merck Millipore, UK
Glycine	Melford, UK
Methanol	Fisher scientific, Loughborough, UK
Ponceau solution	Sigma, USA

PVDF membrane	Merck Millipore, UK
Tris base ultrapure	Melford, UK
Tween-20	Sigma, USA
β-mercaptoethanol	Sigma, USA
2×sample loading buffer	Bio-Rad GmbH, Munchen, Germany
25×running buffer	Bio-Rad GmbH, Munchen, Germany

8.2.4. Reagents for flow cytometry

Annexin V-FITC Apoptosis Detection Kit	Sigma, USA

8.2.5. Reagents for cell nuclear extraction

Nuclear extraction kit	Abcam, UK
DTT	Sigma, USA

8.2.6. Reagents for NFκB transcription factor assay

NFκB p65 transcription factor assay kit	Abcam, UK

8.3. Buffers

8.3.1. Buffers for western blot

Transfer buffer (pH 8.3)

Glycine 14.4g (192mM)

Tris base 3.03g (25mM)

Methanol 20% (v/v)

Fill dH_2O to 1Lit

pH is adjusted with HCl and NaOH

10 × TBS buffer (pH 7.6)
Sodium chloride 87.66g (1500mM)

Tris base 60.58g (500mM)

Fill dH_2O to 1 Lit

pH is adjusted with HCl and NaOH

1 ×TBS-Tween 1%

10 × TBS buffer 100ml

Tween-20 1ml

Fill dH_2O to 1 Lit

TBS-T-milk 5%

Dried skimmed milk 5g

1 ×TBS-T buffer 100ml

8.3.2. Buffers for cell culture

Routine cell culture medium

RPMI medium 1640 500ml

Fetal calf serum (FCS) 10% (v/v)

Penicillin-Streptomycin (5000 U/ml) 5ml

L-Glutamine (20mM) 5ml

Trypsin/Versene solution (2.5%)

1 × Versene 100ml

Trypsin 2.5ml

Freezing medium

Routine cell culture medium 92.5% (v/v)

DMSO 7.5% (v/v)

PBS

PBS tablet 1

dH_2O 500ml

Autoclave

8.3.3. Buffers for molecular biology

LB medium

LB broth 20g

dH_2O 1 Lit

Autoclave

LB agar

LB agar 35g

dH2O 1 Lit

Autoclave

RF1 buffer (pH 5.8)

KCl 7.456g (100mM)

$MgCl_2.4H_2O$ 9.9g (50mM)

$CaCl_2$ 1.5g (10mM)

K-acetate 2.94g (30mM)

Glycerol (v/v) 150ml (15%)

Fill dH_2O to 1 Litre

pH was adjusted

Sterilized by filtration

RF2 buffer (pH 6.8)

MOPS 2.1g (10mM)

$CaCl_2$ 11g (75mM)

KCl 0.745g (10mM)

Glycerol (v/v) 150ml (15%)

dH_2O up to 1 Lit

pH was adjusted

Sterilized by autoclave

Glucose 20%

Glucose 20g

dH_2O 10ml

Sterilized by filtration

SOB medium (pH 7)

NaCl 0.5g

Tryptone 20g

Yeast extracts 5g

KCl 0.186g

dH_2O up to 1 Lit

pH was adjusted

Sterilized by autoclave

SOC medium

SOB medium 4.85ml

Mg2+ salt solution (2M) 50µl

Glucose 20% 150µl

Stock medium for bacteria

Glycerol 5ml

LB medium 4ml

Bacteria culture 3ml

100mM IPTG

IPTG 238mg

Sterile distilled H_2O 10ml

Filter sterilized

10 × TBE stock solution

Boric acid 55g (890mM)

Tris base 108g (890mM)

EDTA 0.5M, pH 8 40ml (20mM)

Fill dH_2O to 1 Lit

pH was adjusted

Sterilized by autoclave

6 ×DNA loading buffer

Bromophenol blue 0.5% 0.5ml

Xylene cyanol FF 0.5ml

Glycerol in sterile dH_2O (60%) 1ml

8.3.4. Cell line authentication

UNIVERSITY OF LIVERPOOL Institute *of* Translational Medicine	**Cell Line Authentication Facility** Academic lead: Dr Lakis Liloglou WH Duncan Building, W. Derby Str, L7 8TX Tel 0151 7949121 Email: T.Liloglou@liv.ac.uk

Certificate of cell line authenticity

Customer	Asmaa Al-Bayati
Organisation	University of Liverpool
Tested Cell line	PNT 2
Authentication method	GenePrint® 10, Promega Corporation
Database(s) used for comparison	Cellosaurus
Authentication undertaken by	Andy Birss
Date	24/7/2018

	Alleles		Match
TH01	6	9.3	√
D21S11	29	33.2	√
D5S818	12	13	√
D13S317	8	13	√
D7S820	11	11	√
D16S539	9	9	√
CSF1PO	11	13	√
AMEL	X	Y	√
vWA	17	17	√
TPOX	8	9	√

Comments (optional):
Matched with Cellosaurus database

Operator

Andy Birss/Pat Gerard
Research Technicians

Academic Lead

Dr Lakis Liloglou
Senior Lecturer

UNIVERSITY OF LIVERPOOL
Institute *of* Translational Medicine

Cell Line Authentication Facility
Academic lead: Dr Lakis Liloglou
WH Duncan Building, W. Derby Str, L7 8TX
Tel 0151 7949121 Email: T.Liloglou@liv.ac.uk

Certificate of cell line authenticity

Customer	Asmaa Al-Bayati (Prof Ke)
Organisation	UoL ITM DMCCM
Tested Cell line	22RV1
Authentication method	GenePrint® 10, Promega Corporation
Database(s) used for comparison	DSMZ, ATCC
Authentication undertaken by	Pat Gerard/Andy Birss
Date	08/05/18

	Alleles		Match
TH01	6	9.3	√
D21S11	29	30	X
D5S818	11	13	√
D13S317	9	12	√
D7S820	9	10 11	√
D16S539	11	12	X
CSF1PO	10	11 12	√
AMEL	X	Y	√
vWA	15	21	√
TPOX	8	8	√

Comments (optional):
DSMZ 90% match
ATCC 94% match

Operator

Pat Gerard/Andy Birss
Research Technician

Academic Lead

Dr Lakis Liloglou
Senior Lecturer

UNIVERSITY OF LIVERPOOL
Institute *of* Translational Medicine

Cell Line Authentication Facility
Academic lead: Dr Lakis Liloglou
WH Duncan Building, W. Derby Str, L7 8TX
Tel 0151 7949121 Email: T.Liloglou@liv.ac.uk

Certificate of cell line authenticity

Customer	Asmaa Al-Bayati (Prof Ke)
Organisation	UoL ITM DMCCM
Tested Cell line	PC3
Authentication method	GenePrint® 10, Promega Corporation
Database(s) used for comparison	DSMZ, ATCC
Authentication undertaken by	Pat Gerard/Andy Birss
Date	05/05/18

	Alleles		Match
TH01	6	7	√
D21S11	29	31.2	√
D5S818	13	13	√
D13S317	11	11	√
D7S820	8	11	√
D16S539	11	11	√
CSF1PO	11	11	√
AMEL	X		√
vWA	17	17	√
TPOX	8	9	√

Comments (optional):
DSMZ 100% match
ATCC 100& match

Operator

Pat Gerard/Andy Birss
Research Technician

Academic Lead

Dr Lakis Liloglou
Senior Lecturer